The role of Cyclin O in ER stress signalling

Alexander Balsiger

TESI DOCTORAL UPF / 2014

DIRECTOR DE LA TESI

Dr. Gabriel Gil Gómez

Programa de Recerca en Càncer – IMIM Hospital del Mar

To my father

ACKNOWLEDGEMENT

Many people contributed to this work and made it possible for me to finally reach the end of this long journey.

Above all, I would like to thank especially Dr. Gabriel Gil Gómez for letting me do this project and for his critical suggestions, for his patience and his trust in me.

Many thanks to my labmates who accompanied me during all those years. Marta, Marc, Kathi, Laura, Lara, and Mercè - I really enjoyed your support! Special thanks to Marta and her brilliant cheerfulness and sense of humour. Marc, I really liked working with you as your team spirit and the conversations over lunch motivated me a lot!

I would like to thank as well all the people from the Cancer department of the IMIM. I spent a really nice time during and in between experiments and could always find people having a moment for questions, to find a good protocol or an antibody when it was needed.

Last, but not least, special thanks to my father who supported me. Your patience is very much appreciated!

ABSTRACT

We recently identified a novel cyclin called Cyclin O which is able to bind and activate Cdk1 and Cdk2 in response to intrinsic apoptotic stimuli like DNA damage or ER stress. Cyclin O has been shown to be involved in the unfolded protein response (UPR) as an activator of PERK signalling. The aim of this thesis has been to study the molecular role of Cyclin O in response to ER stress. We have found that expression of Cyclin O is upregulated upon ER stress by pathways of the UPR that signal through eIF2α phosphorylation and CHOP expression. Furthermore, we have observed that Cyclin O activates the MAPK pathways independently of IRE1α signalling. This effect is most likely mediated by Cdk1 and Cdk2-dependent phosphorylation and consequent activation of MEKK4, which leads to the activation of JNK and p38. We have also found employing phosphoproteomics technology that many proteins involved in protein folding and translation depend on Cyclin O.

RESUMEN

En nuestro laboratorio hemos identificado recientemente un nuevo miembro de la familia de las ciclinas, la Ciclina O, la cuál puede unirse y activar a Cdk1 y Cdk2 en respuesta a estímulos apoptóticos tales como el daño genético o el estrés del retículo endoplásmico. También hemos demostrado que la Ciclina O participa en la respuesta celular desencadenada por el acúmulo de proteínas mal plegadas (UPR) actuando a través de la activación de la señalización de la ruta de PERK. El objetivo de esta tesis ha sido el estudio molecular de la participación de la Ciclina O en la respuesta al estrés del retículo. Nuestros resultados indican que los niveles de expresión de la Ciclina O incrementan en respuesta al estrés del retículo a través de rutas de la UPR que señalizan a través de la fosforilación de eIF2α y de la expresión de CHOP. Además hemos observado que en respuesta al estrés reticular la Ciclina O activa la ruta de las MAPK de manera independiente de la señalización a través de IRE1α. Este efecto posiblemente tiene lugar a través de la fosforilación y consecuente activación de MEKK4 dependiente de Cdk1 y Cdk2. Esto conlleva la activación de las kinasas de stress

JNK y p38. Asimismo, mediante experimentos de fosfoproteómica hemos demostrado que un gran número de proteínas involucradas en los procesos bioquímicos de traducción y plegado dependen de la expresión de la Ciclina O.

ABBREVIATIONS

ASK-1: Apoptosis Signal-Regulating kinase 1
Apaf-1: Apoptosis Protease-Activating Factor-1
ATF4: Activating Transcription Factor 4
Bak: Bcl-2 homologous antagonist killer
Bax: Bcl-2 associated X
Bcl-2: B-cell lymphoma-2
Bim: BCL2-interacting mediator of cell death
BiP/GRP78: Binding immunoglobulin Protein/ Glucose-Regulated Protein
BrdU: Bromodeoxyuridine
BSA: Bovine Serum Albumin
Cdk: Cyclin-dependent kinases
CHOP: CAAT/enhancer-binding-protein-Homologous Protein
DAPI: 4',6-diamino-2-phenylindole dihydrochloride
DDR: DNA Damage Response
DISC: Death-Inducing Signalling Complex
DMEM: Dulbecco's Modified Eagle's Medium
DR5: Death Receptor 5
dsRNA: double-stranded RNA
DTT: Ditriothreitol
ECL: Enhanced Chemiluminescence
EDTA: Ethylenediaminetetraacetic Acid
eIF: eukaryotic Initiation Factor
E**R:** Endoplasmic Reticulum
ERAD: ER Associated Degradation
FACS: Fluorescent Activated Cell Sorting
FITC: Fluorescein Isothiocyanate
GADD134: Growth Arrest and DNA-damage-inducible protein-34
GCN2: General Control Non-derepressible-2
GSK3β: Glycogen Synthase Kinase-3
GST: Glutathione-S-Transferase
HA: Hemagglutinin
HEK: Human Embryonic Kidney
HEPES: 4-(2-hydroxyethyl)-1-piperazineethanesulfonic acid
HRI: Heme-Regulated Inhibitor
HRP: Horse Radish Peroxidase
IF: Immunofluorescence
IPTG: Isopropyl-beta-D-thiogalactopyranoside
IRE1: Inositol-Requiring transmembrane kinase/Endonuclease 1
JNK: Jun N-terminal Kinase

KD: Kinase Dead
mCyclin O: mouse Cyclin O
MEFs: Mouse Embryonic Fibroblasts
mCyclin O: mouse Cyclin O
MAPK: Mitogene Activated Protein Kinase
MOI: Multiplicity Of Infection
MOMP: Mitochondrial Outer Membrane Permeabilization
MW: Molecular Weight
ORF: Open Reading Frame
PBS: Phosphate Buffered Saline
PCR: Polymerase Chain Reaction
PERK: PKR-like Endoplasmic Reticulum Kinase
PI: Propidium Iodide
PKR: Protein Kinase RNA
qRT-PCR: quantitative Reverse Transcriptase-Polymerase Chain Reaction
RIPA: Radio-Immunoprecipitation Assay
ROS: Reactive Oxigen Species
RT: Room Temperature
RT-PCR: Reverse Transcriptase-Polymerase Chain Reaction
SDS: Sodium Dodecyl Sulfate
SDS-PAGE: Sodium Dodecyl Sulfate Polyacrilamide Gel Electrophoresis
SEM: Standard Error of the Mean
shRNA: short hairpin RNA
TRB3: Tribbles Related Protein 3
Tris: Tris-hydroxymethyl-aminomethane
UPR: Unfolded Protein Response
UV: Ultraviolet
WB: Western Blot
WT: Wild Type
XBP1: X-box Binding Protein 1

INTRODUCTION

Introduction

1. The integrated stress response

1.1 Control of mRNA translation

Initiation of mRNA translation is the key step in regulating protein translation[1]. It starts with the formation of the 43S preinitiation complex (PIC) which is composed of various eukaryotic initiation factors (eIF), the 40S ribosomal subunit, and the ternary complex (TC) consisting of initiator methionyl-tRNA and the GTP-bound form of eIF2 (Figure 1). The mRNA is capped at its 5´ end by various types of eIF4 proteins and the poly(A)-binding protein tethered to the poly(A) tail which results in the circular "closed loop" structure of the mRNA. Once attached near the cap, the PIC scans the mRNA along the 5´ untranslated region until recognition of the initiation codon triggers hydrolysis of eIF2-associated GTP, a process catalysed by the GTPase-activating factor eIF5. Subsequent release of eIF2·GDP and other eIFs present in the PIC is followed by joining of the 60S ribosomal subunit to form the 80S initiation complex ready to begin the elongation phase of protein synthesis. eIF2·GDP must be recycled to eIF2·GTP for renewed TC assembly, a reaction catalyzed by the guanine nucleotide exchange factor eIF2B. eIF2 is composed of three subunits α, β, and γ. eIF2γ binds directly to both GTP and Met-tRNA and it appears that the α and β subunits each increase the affinity of the eIF2 complex for Met-tRNA by ~100 fold[2]. Various stress signals lead to the phosphorylation of eIF2α at residue serine 51. This phosphorylation

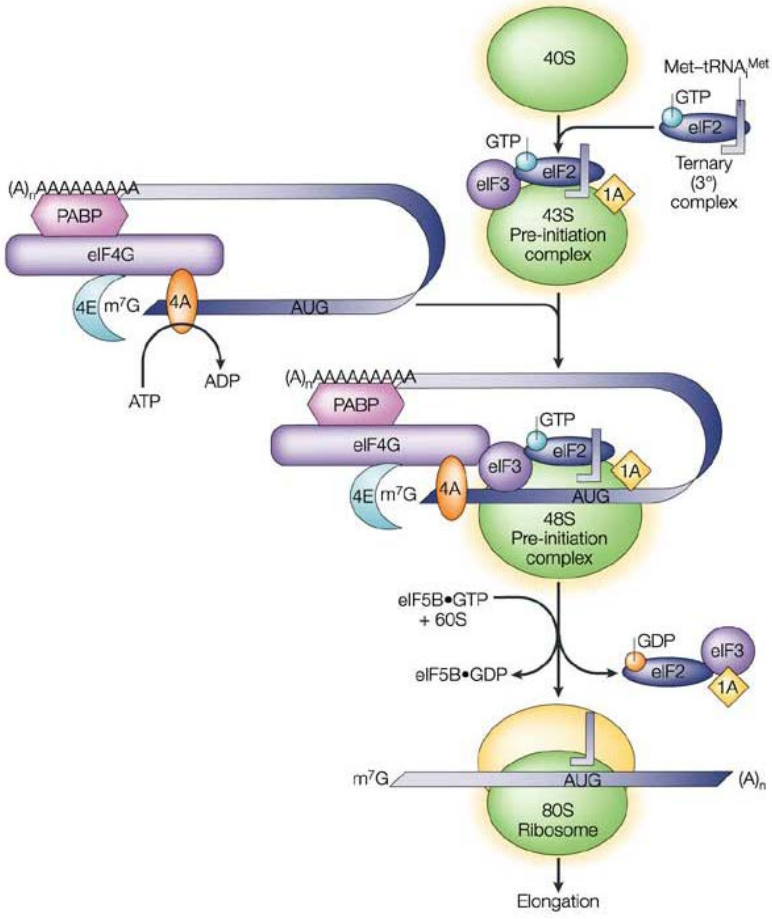

Figure 1. Initiation of translation. Eukaryotic translation involves assembly of the 80S ribosome at the mRNA. This process is mediated by initiation factors (eIFs). (Adapted from Klann *et al.*, 2004)

increases the affinity of eIF2B for the eIF2 complex leading to a subsequent impairment of dissociation[3] of eIF2B from the eIF2 complex. Sequestering eIF2B to the eIF2 complex blocks the GDP-GTP exchange reaction and, as a consequence, the TC is not formed and protein translation is inhibited. However, phosphorylation of eIF2α enhances specific translation of stress-related proteins like the transcription factor ATF4 which in turn is responsible for inducing

genes involved in damage control. This specific translation of ATF4 is mediated by two short inhibitory open reading frames (ORF) located upstream of the ATF4 start codon[4]. In an unstressed cell where the availability for TC is not limited translation initiation takes place at the upstream ORFs. In response to stress the lack of TC allows scanning ribosomes to pass the upstream ORFs and initiate translation at the ATF4 start codon. An important proapoptotic transcription factor induced by ATF4 is C/EBP homologous protein (CHOP) which is (like ATF4) preferentially translated when eIF2α is phosphorylated. CHOP represses the antiapoptotic protein BCL-2[5] and induces the prodeath proteins Bim and PUMA[6,7]. Another important gene target of ATF4 is GADD34 which is the regulatory subunit of Protein Phosphatase 1 (PP1). PP1 dephosphorylates eIF2α allowing the resumption of general translation and the expression of other ATF4 targets[8].

1.2 eIF2α kinases

Phosphorylation of eIF2α is mediated by four distinct serine/threonine protein kinases: General Control Non-Derepressible-2 (GCN2), Heme-Regulated Inhibitor (HRI), Protein Kinase R (PKR), and PKR-like Endoplasmic Reticulum Kinase (PERK). These kinases share homology in their catalytic domains, but their effector domains are different and subjected to distinctive regulatory mechanisms (Figure 2). The four kinases respond to a large variety of different stress signals and converge in the phosphorylation of eIF2α, which activates or represses a large number of genes through ATF4 (Figure 3). It is this diversity of

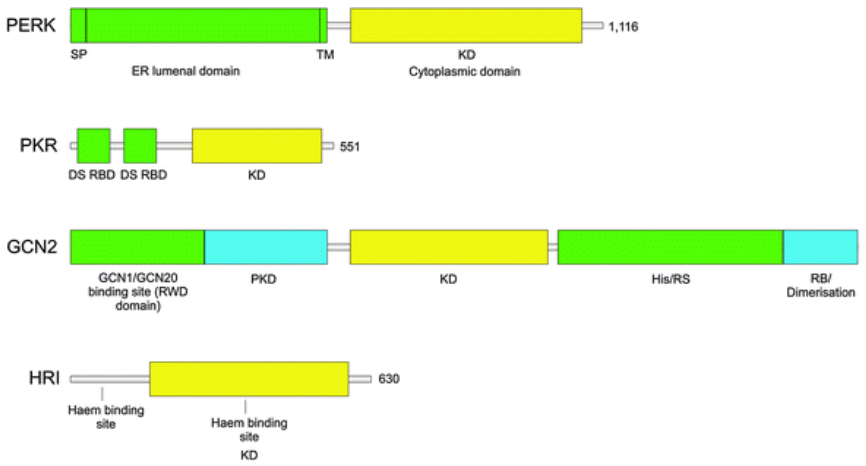

Figure 2. The four mammalian eIF2α kinases. Domain organization of the mammalian eIF2α kinases. *SP* signal peptide, *TM* transmembrane domain, *KD* kinase domain, *DS RBD* double-stranded RNA binding domain, *PKD* pseudokinase domain, *His/Rs* histidyl-tRNA synthetase-related domain, *RB* ribosome binding. Domains involved in sensing stress signals/activation are in green. Kinase domains are in yellow. Other domains are coloured blue. Domains are drawn to scale. Adapted from Donelly *et al*., 2013)

outputs coupled with the variety of signals which can activate the eIF2α kinases that led to the coining of the term "integrated stress response" (ISR)[9].

1.2.1 PERK

PERK is an endoplasmic reticulum (ER) transmembrane protein. The C-terminus is cytosolic and contains the kinase domain and autophosphorylation sites whereas the N-terminus lies inside of the ER lumen and contains the region responsible for homodimerization and binding of the ER chaperone Immunoglobulin Binding Protein (BiP)[10]. In its inactive state PERK is bound by BiP. Accumulation of misfolded proteins in the ER, a phenomenon called ER stress, causes BiP to dissociate from PERK allowing for dimerization and

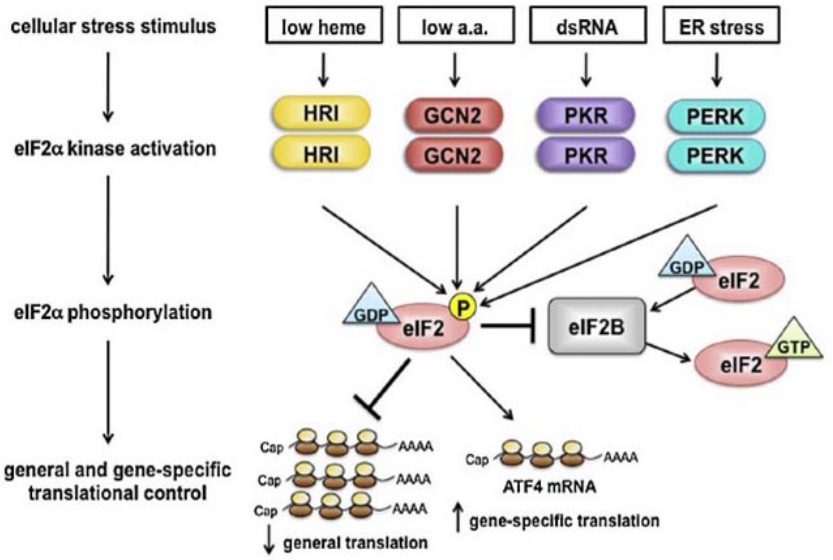

Figure 3. Integrated Stress Response. Various stimuli activate the eIF2α kinases leading to phosphorylation of eIF2α at serine 51, a key step in controlling general and gene-specific translation during cellular stress. (Adapted from Trinh *et al.*, 2013)

autophosphorylation leading to activation of PERK[11]. Apart from eIF2α, another direct substrate of PERK is nuclear factor (erythroid-derived 2)-like two (Nrf2), a transcription factor that upregulates expression of antioxidant and detoxifying enzymes that aim to restore redox homeostasis[12]. A consequence of ER stress is the accumulation of reactive oxygen species (ROS) that promotes a state of oxidative stress. PERK signaling, via activation of the Nrf2 and ATF4 transcription factors, coordinates the convergence of ER stress with oxidative stress signalling. While early activation of PERK is a cytoprotective prosurvival response, prolonged activation has been suggested to represent the terminal, proapoptotic phase of ER-stress[13,14].

1.2.2 PKR

PKR was initially discovered as a kinase that phosphorylates eIF2α in response to viral infection, thereby blocking the translation of viral mRNAs and promoting apoptosis in response to viral infection. However, PKR also plays a more general role in cellular physiology. It can be activated in response to oxidative[15] and ER stress[16,17]. PKR is localized in the cytosol and the nucleus. Its regulatory N-terminal region contains a double-stranded RNA (dsRNA) binding domain. In response to binding of viral dsRNA dimerization is induced, which in turn leads to autophosphorylation mediated by the C-terminal kinase domain resulting in a complex capable of phosphorylating eIF2α[18]. An important regulator of PKR in response to cellular stresses in the absence of dsRNA is PACT (Protein Activator) which becomes phosphorylated in response to various insults and associates with and activates PKR. PACT has been shown to be the link between stress signals such as ER stress[19], serum starvation, and arsenite exposure. Activation of PKR leads to apoptosis by inducing expression of CHOP in response to ER stress[20]. PKR signaling is not always proapoptotic in nature. In response to certain stress stimuli and in certain cell types PKR may also function to promote cellular survival through its activation of NF-κB signaling[21].

1.2.3 GCN2

GCN2 is primarily a sensor of amino acid availability and regulates changes of gene expression in response to amino acid deprivation[22].

GCN2 is loosely associated with the ribosome[23] and harbors a histidyl-tRNA synthetase (HisRS)-related domain, which binds uncharged transfer RNAs (tRNAs) with higher affinity than it does charged tRNAs. Uncharged tRNAs accumulate in response to starvation for essential amino acids and activation of GCN2 is thought to occur through the binding of uncharged transfer RNAs (tRNAs) to the HisRS domain of the protein[24]. As with other eIF2α kinases, dimerization and subsequent autophosphorylation appears to be key for activation of GCN2. In addition to amino acid starvation, GCN2 can also be activated by viral infection via direct binding of the genomic RNA of Sindbis Virus to the HisRs domain[25]. GCN2 activation has also shown to be a consequence of glucose deprivation and compromised GCN2 signaling severely hampered tumor growth *in vivo*[26]. Furthermore, conditions of hypoxia[27] and UV-irradiation[28] seemed to activate GCN2 as well.

1.2.4 HRI

HRI coordinates the synthesis of globin chains with the availability of heme in reticulocytes and promotes survival of erythroid precursor cells when iron levels are low. There are two binding sites for heme in the HRI protein. Once synthesized, HRI is bound by heme at its N-terminus, which triggers intermolecular autophosphorylation stabilizing the HRI–HRI dimer competent for sensing intracellular heme concentrations. At high levels of heme the HRI dimer is bound by additional heme and further phosphorylation leading to activation is inhibited. When heme levels are low, HRI is activated by autophosphorylation and

proceeds to phosphorylate eIF2α[29,30]. It has been demonstrated that HRI in reticulocytes and fetal liver nucleated erythroid progenitors is activated independently of heme by oxidative stress induced by arsenite, heat shock, and osmotic stress but not by endoplasmic reticulum stress or nutrient starvation[31]. However, a recent report indicates that HRI signaling may also be involved in ER homeostasis in the liver [32].

2. The unfolded protein response

Many different perturbations can alter the function of the ER, leading to the accumulation of unfolded or misfolded proteins inside the ER, a condition referred to as ER stress. As depicted in figure 4, ER stress initiates a series of adaptive mechanisms collectively called the unfolded protein response (UPR). Activation of the UPR aims to restore protein-folding homeostasis (proteostasis), and, if cell damage is sufficiently severe, UPR signalling results in apoptosis. There are three sensors that respond to ER stress: Inositol-Requiring Enzyme 1 (IRE1), PERK (see introduction chapter 1.2.1), and Activating Transcription Factor 6 (ATF6). All of these sensors are ER transmembrane proteins (Figure 5) and are maintained in an inactive state by binding of their ER-lumenal domain to the chaperone BiP. Upon accumulation of unfolded proteins, BiP dissociates from ATF6, IRE1 and PERK to act as a chaperone for misfolded proteins and to allow the activation of one or more of these sensors.

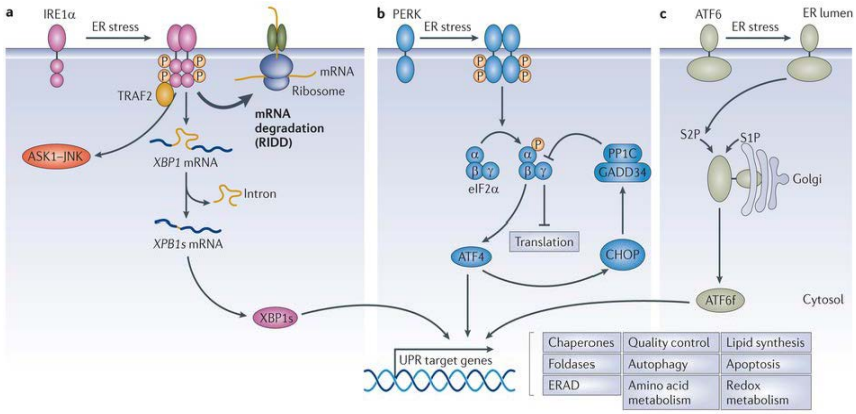

Figure 4. The unfolded protein response. ER stress induces an adaptive response known as the unfolded protein response. Three major stress sensors control UPR-dependent responses: IRE1α (**a**), PERK (**b**), and ATF6 (**c**). These ER transmembrane proteins transduce signals to the cytosol and nucleus to restore protein-folding capacity through various pathways. (Adapted from Hetz *et al.*, 2013)

2.1 IRE1α

Mammalian cells have two paralogs of IRE1, IRE1α and IRE1β, sharing structural similarity but different functions. IRE1α is expressed ubiquitiously whereas expression of IRE1β is restricted to epithelial cells of the gastrointestinal tract[33]. Activation of IRE1 occurs through its dimerization, oligomerization and trans-autophosphorylation, which leads to a conformational change that activates its RNase domain (Figure 6). Active IRE1β functions to attenuate protein translation by site-specific cleavage of 28S ribosomal RNA[34]. Activated IRE1α excises a 26-nucleotide intron of the mRNA that encodes the transcription factor X-box binding protein 1 (XBP1) shifting the coding reading frame and leading to the translation of the active form known as XBP1s (spliced)[35]. Target genes of XBP1s are involved in protein folding, ER-

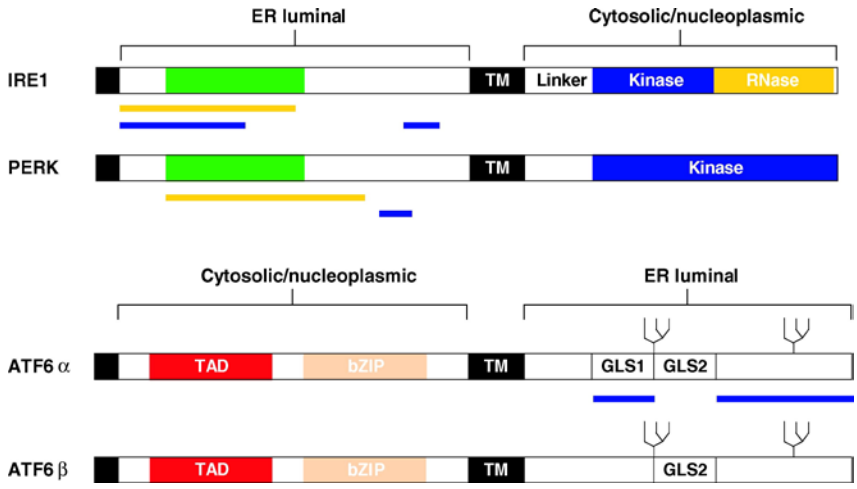

Figure 5. The mammalian ER stress sensors. Primary structure of the mammalian ER stress sensors: IRE1, PERK, and ATF6. Yellow bars represent regions sufficient for signal transduction or oligomerization. Blue bars represent regions interacting with BiP. The black boxes represent the signal peptides, and the green boxes depict the region of homology between IRE1 and PERK. *bZIP*, basic leucine zipper; *GLS1* and *GLS2*, Golgi localization sequences 1 and 2; *TAD*, transcriptional activation domain; *TM*, transmembrane domain. Drawings are not to scale. (Adapted from Schroder *et al.*, 2005)

associated protein degradation, protein translocation to the ER, and protein secretion[36,37]. The XBP1u (unspliced) protein does not act directly as a transcription factor, but rather functions as negative feedback regulator of XBP1s by sequestering the protein from the nucleus and promoting its degradation by the proteasome, which seems to be important at the recovery phase of ER stress[38]. IRE1α RNase activity also degrades a subset of mRNAs through a process known as regulated IRE1-dependent decay (RIDD) of mRNA[39]. The pool of mRNAs degraded by RIDD activity depends on the cell type and includes mRNAs that encode proteins of the secretory pathway. RIDD of mRNAs may depend on the tendency of the

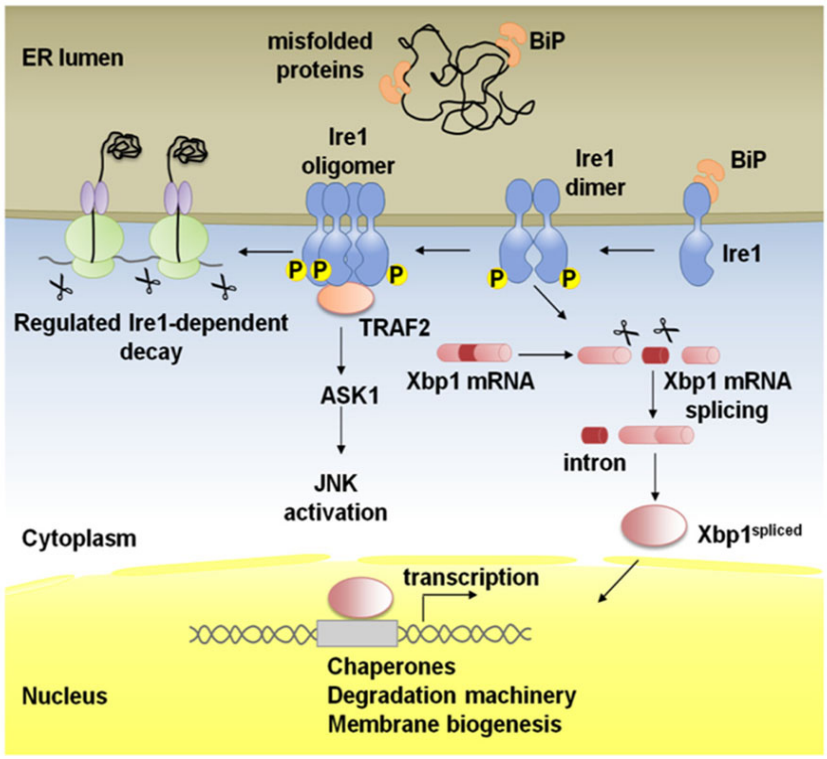

Figure 6. IRE1α signalling. Binding immunoglobulin protein (BiP) binds Ire1α luminal domain and maintains it in a monomeric inactive form. In stressed cells, BiP is recruited to misfolded proteins and Ire1 α is activated following conformational changes induced by dimerization of monomers in the plane of the membrane and trans-autophosphorylation. Higher order oligomers, which might form upon additional stress stimuli, reinforce Ire1α RNase activity. Activated Ire1α mediates the splicing of Xbp1 mRNA. Splicing of the intron from the Xbp1 transcript results in a frame-shift and the production of a potent transcription factor, Xbp1-spliced, that regulates many UPR target genes to promote protein folding in the ER lumen, ER-associated degradation (ERAD) of misfolded proteins and ER biogenesis. Ire1α can also act by alternative pathways; phosphorylated Ire1α associates with TRAF2 and activates the JNK pathway via ASK1. In the regulated Ire1α dependent decay (RIDD) pathway, Ire1α degrades mRNAs localized to the ER membrane through its RNase activity leading to a reduction in the amount of proteins imported into the ER lumen. Adapted from Coelho *et al*., 2014)

encoded protein to misfold and on the presence of a conserved nucleotide sequence accompanied by a defined secondary structure[40]. Interestingly, IRE1α controls its own expression by cleaving its own mRNA[41]. Among the regulators of IRE1α, proapoptotic proteins BAX and BAK play a role independently of their proapoptotic function at the mitochondria[42]. Under stress conditions, BAX and BAK interact with the cytosolic region of IRE1α which is essential for its activation. ER stress induced apoptosis may activate NF-κB. Canonical activation of NF-κB involves proteasomal degradation of its inhibitor IκB which is mediated by phosphorylation of IκB through the kinase complex IKK. IRE1α recruits the adapter protein TNF receptor-associated factor 2 (TRAF2) to form a complex with IKK, which leads to phosphorylation of IκB and activation of NF-κB[43] (Figure 7). Another important function of IRE1α is the induction of mitogen-activated protein kinases (MAPKs) sinalling (see introduction chapter 3).

2.2 ATF6α

Two isoforms of ATF6 have been described, ATF6α and ATF6β. ATF6α harbours a transcription factor domain in its N-term. During ER stress conditions dissociation of BiP from the ER luminal C-terminus exposes a Golgi localization sequence, which leads to transportation of ATF6α to the Golgi apparatus where it is cleaved by intramembrane proteases[44]. The resulting N-terminal fragment p50ATF6α translocates to the nucleus where it promotes transcription of UPR genes such as BiP[45], CHOP[46], and XBP1[47],

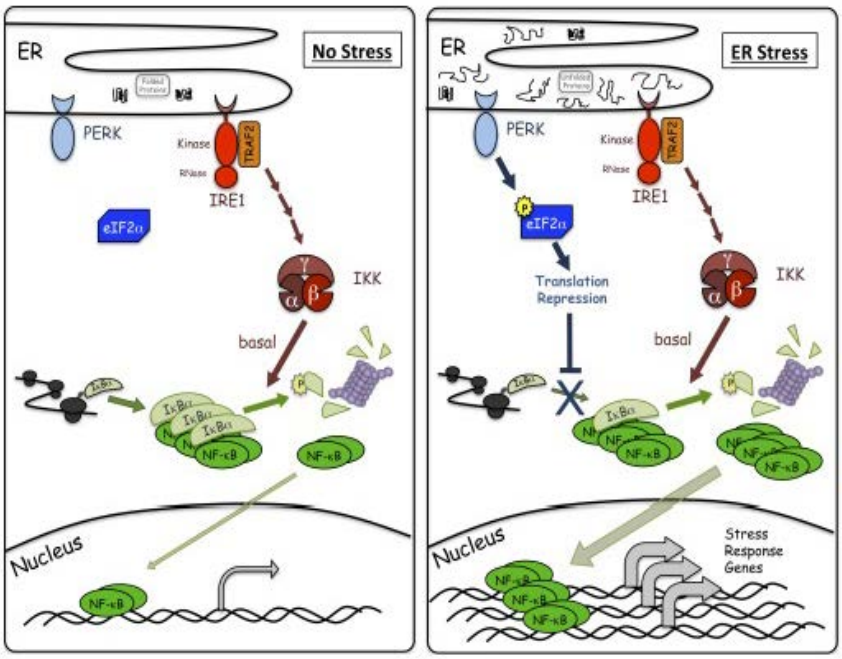

Figure 7. IRE1-mediated activation of NF-kB during ER stress. Under unstressed conditions, IκBα is being synthesized and inhibits NF-kB. IRE1, through TRAF2, is maintaining basal IKK activity leading to phosphorylation and proteosomal degradation of a subset of IκBα, which maintains basal NF-kB activity. However, most of the NF-kB is sequestered by IκBα. During ER stress, PERK phosphorylation of eIF2a leads to translation repression and prevents synthesis of new IκBα, which contributes to a decrease in IκBα levels and corresponding increase in free NF-kB levels. Additionally, basal IKK activity is responsible for phosphorylating and degrading the existing IκBα, including IκBα bound to NF-kB, causing a more dramatic decrease in IκBα levels resulting in an even greater amount of free NF-kB Free NF-kB can then translocate to the nucleus to assist in transcriptional activation of stress response genes. (Adapted from Tam *et al.*, 2012)

amongst others. The activation process of ATF6β is similar to the one of ATF6α yielding the N-terminal fragment p60ATF6β which seems to act as a transcriptional repressor opposing the action of p50ATF6α[48]. ATF6α is considered a very potent, but only transiently active transcription factor, as the increase in its

transcriptional activity raises its own degradation by the proteasome[49].

Recently a new family of ATF6 homologs has been identified that are modulated by ER stress in specific cell types. All of these ATF6-related transcription factors are processed at the Golgi in a similar way as ATF6[50]. OASIS (also known as CREBL1), for example, is expressed in astrocytes[51] and CREBH is expressed exclusively in the liver[52]. The role of these proteins in the UPR is still poorly characterized and more studies are required.

2.3 Cross talk between the different UPR branches

ER stress sensors use different mechanisms and effectors to activate the UPR, but at some points the three pathways communicate. One example is the close relationship between the IRE1α and ATF6α pathways. XBP1u targets the active form of ATF6α to the proteasome[53] while ATF6α on the other hand also controls the transcription of XBP1. Additionally, activated ATF6α heterodimerizes with XBP1s to induce ER-associated protein degradation[54]. The PERK pathway is also linked to IRE1α and ATF6. A dominant negative form of PERK was shown to activate ATF6 and XBP1[55]. In another study, PERK was shown to facilitate the synthesis and trafficking of ATF6 from the ER to the Golgi[56]. All these studies show that individual branches of the UPR are connected in ways that permit generating integrated responses to stress. The three ER stress sensors contribute to either adaptation or death, but it remains unknown how each branch contributes to the

final biological effect. A number of studies have attempted to resolve this issue. For instance, IRE1α and ATF6α activities are attenuated by persistent ER stress, while PERK signaling is not[14]. Indeed, sustained PERK signaling impairs cell proliferation and promotes apoptosis. By contrast, signaling via IRE1α for an equivalent period of time enhances cell proliferation without promoting cell death[13] suggesting that the differential activation of PERK and IRE1α may determine cell fate following ER stress.

3. MAPKs and ER stress

3.1 MAPKs

The evolutionarily conserved MAPKs are Ser/Thr protein kinases. They include, amongst others, extracellular signal-regulated kinases 1 and 2 (ERK1/2), c-Jun amino (N)-terminal kinases (JNKs), and the p38 family. They are activated through a three-tier kinase signalling cascade[57] (Figure 8). The MAPK subgroups are defined in part by the dual threonine/tyrosine motif in their activation loop, phosphorylation of which is required for their activation: ERK1/2 (Thr-Glu-Tyr), JNK (Thr-Pro-Tyr), and p38 (Thr-Gly-Tyr). These Thr-X-Tyr motifs are phosphorylated by specific MAP kinase kinases (MAP2Ks), which are in turn phosphorylated by a number of MAP kinase kinase kinases (MAP3Ks). The biological output of MAPK signalling depends on a variety of factors including the subcellular localisation of the MAPK, which is determined by scaffold proteins deciding the repertoire of substrates available, the

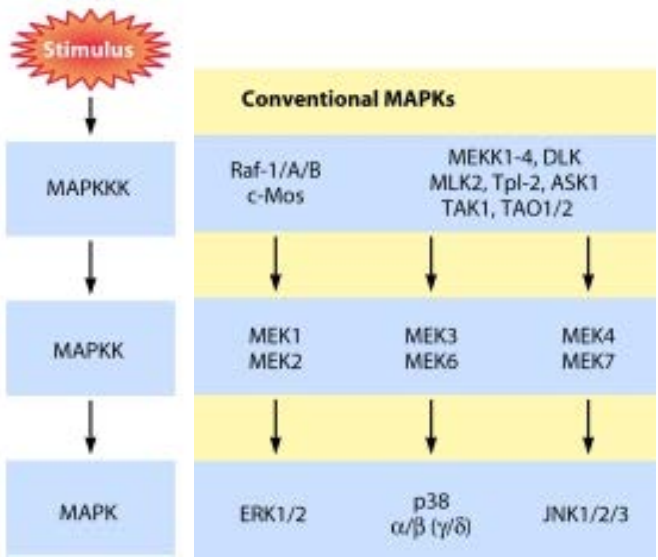

Figure 8. The stress MAP kinases. Mitogens, cytokines, oxidants, ER stress, and other cellular stresses promote the activation of different MAPK pathways. All the MAPKs and MAPKKs shown here have been reported to be envolved in UPR signalling. MEK4 is also known to activate p38. (Adapted from Cargnello *et al.*, 2011)

strength and duration of MAPK activation, and signalling inputs provided by other pathways. ERK1/2 were originally identified as cell growth inducing kinases activated in response to a huge variety of mitogenic growth factors. Nowadays, it is known that the canonical MAPKs (ERK1/2, JNK, and p38) play an extensive role in stress signalling induced by many environmental stresses and they are activated in response to ER stress, each with different kinetics and with different roles. ERK1/2 activation promotes cell survival, but the importance of this protective role in ER stress is still unclear.

3.2 Cell fate mediated by MAPKs in ER stress

ER stress induces an increase in both JNK and p38 phosphorylation and activation, suggesting that these MAPKs have a role in the response to ER stress [58,59].

3.2.1 IRE1α activates JNK to promote cell death

In a variety of cell lines, ER stress has been found to induce JNK activation and this is thought to initiate a proapoptotic response. While ER stress promotes the oligomerization of IRE1α and its activation, IRE1α activation can be enforced through its overexpression, in the absence of ER stress, which is sufficient to activate JNK in cells and this requires the active IRE1α kinase domain but not the endoribonuclease domain. Following ER stress, IRE1α oligomerizes, activating its kinase domain, which then interacts with TRAF2 via its C-terminal TRAF domain promoting the clustering of the N-terminal effector domain of TRAF2 [60]. More recently, the IRE1α-TRAF2 dependent activation of JNK following ER stress was found to require the MAP3K Apoptosis Signal-regulating Kinase 1 (ASK1) (Figure 9A) and cells from ASK1−/− mice showed a reduction in ER stress-induced JNK activation and were more resistant to ER stress-induced apoptosis [61]. Interaction with IRE1α-TRAF2 promotes ASK1 oligomerization[62] and induces a conformational change to promote intermolecular autophosphorylation of Thr845 within the ASK1 activation loop. ASK1 has been shown to phosphorylate and activate MEK4/MEK7 and MEK3/MEK6, the upstream kinases for JNK and p38 respectively[63]. Aside from activation by TRAF2,

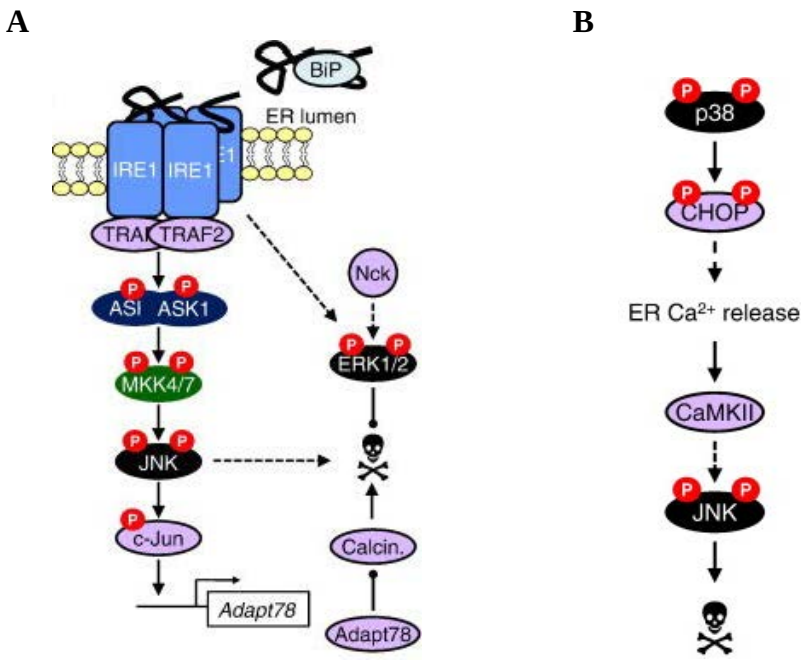

Figure 9. **A** ER stress promotes the IRE1-dependent activation of JNK and ERK1/2. IRE1-dependent oligomerisation of TRAF2 activates ASK1/MKK4,7/JNK signalling, which can promote survival through c-Jun-dependent expression of Adapt78 and inhibition of calcineurin or may promote cell death. IRE1 activation also promotes activation of prosurvival ERK1/2 signalling by promoting the dissociation of Nck from IRE1, though the mechanism for ERK1/2 activation has not been identified. **B** CHOP is regulated by p38-dependent phosphorylation although it is unclear what role this phosphorylation has in response to ER stress. CHOP promotes ER Ca^{2+} release, subsequent activation of CaMKII and the ASK1/MKK4/JNK signalling cascade (depicted in A), leading to cell death. Adapted from Darling *et al., 2014)*

ASK1 is regulated by interaction with a network of kinases and phosphatases in addition to binding proteins such as 14-3-3[64]. Phosphorylation of ASK1 on Ser83 by the prosurvival protein kinases PIM1 or the Ak mouse thymoma oncogene (Akt, also known as protein kinase B) decreases ASK1 activity leading to a reduction in JNK activation and reduced sensitivity to stress-

induced apoptosis [65,66]. ASK1 is inactivated by dephosphorylation of Thr845 and this may occur through protein phosphatase 5 activity, which binds to ASK1 in response to oxidative stress[67]. Furthermore, ASK1 dephosphorylation on Ser967 is required for dissociation from 14-3-3 and activation in response to stress[68]. It is currently unclear how this network of ASK1 regulators and binding proteins are coordinated in response to ER stress to promote ASK1 activation and subsequent JNK activation. Intriguingly, whilst in most cases the IRE1α-dependent activation of JNK is considered to be proapoptotic[61,65,66] inhibition of JNK2 activation in a human lymphoblast cell line following ER stress promoted apoptosis in these cells [69]. Thus, activation of JNK2 following ER stress might be prosurvival.

3.2.2 IRE1α-dependent c-Jun activation inhibits ER stress-induced death

The transactivation domain of the transcription factor and proto-oncogene c-Jun is phosphorylated by JNK and this promotes activation of the transcription factor c-Jun[70]. Phosphorylation of both JNK and c-Jun increases following ER stress, and c-Jun is required for the transcription of Adapt78 in response to ER stress[71]. Adapt78 is an inhibitor of the proapoptotic Ca^{2+}-responsive protein phosphatase Calcineurin (Figure 9B) and so can act to decrease Calcineurin activity following ER stress. ER stress promotes the cleavage and activation of an ER-associated caspase, Caspase-12 in rodents or Caspase-4 in human cells. This can contribute to ER stress-induced apoptosis[72,73]. Expression of c-Jun was shown to

reduce Caspase-12 cleavage and protect cells against thapsigargin-induced cell death, although it is unclear whether the increased expression of Adapt78 and Calcineurin inhibition has a role in this response[71]. In addition, Calcineurin is activated by caspase-dependent cleavage and inhibition of Calcineurin can attenuate thapsigargin-induced apoptosis[74], which suggests that Calcineurin can promote ER stress-induced cell death, but may act downstream of Caspase 12. Therefore, while JNK activation is implicated in promoting ER stress-induced apoptosis, it can also act to reduce ER stress-induced apoptosis through Adapt78 transcription and Calcineurin inhibition

3.2.3 IRE1α-dependent ERK1/2 activation promotes survival

ERK1/2 activation is partially IRE1α-dependent in ER stressed cells. Depletion of the adaptor protein Nck from the system resulted in a reduction in ER stress-induced ERK1/2 activation. Nck was found to associate at the ER membrane with the cytosolic domain of IRE1α via its SH3 domains. At the ER membrane Nck inhibited ERK1/2 activation, whereas dissociation of Nck from the ER membrane following ER stress promoted the increased activation of ERK1/2 and correlated in vivo with increased cell proliferation and reduced apoptosis[75]. Thus while ER localised Nck interacts with inactive IRE1α leading to inhibition of ERK1/2 activation, dissociation of Nck from active IRE1α and the ER membrane promotes the cytosolic localization of Nck and IRE1α-dependent ERK1/2 activation (Figure 9A). This suggests that activation of IRE1α promotes a conformational change within the cytosolic

domains to promote both Nck dissociation from IRE1α and the subsequent activation of ERK1/2. In gastric cancer cells, inhibition of ERK1/2 signalling promoted ER stress-induced apoptosis, perhaps through a reduction in BiP levels. ERK1/2 inhibition attenuated the ER stress-induced increase in BiP mRNA and protein levels and the reduction in BiP levels was sufficient to promote ER stress-induced apoptosis[76]. Thus, signalling through the IRE1α axis of the UPR can promote activation of ERK1/2, which has a prosurvival role following ER stress.

3.2.4 Phosphorylation and activation of CHOP by p38

CHOP contains two serines within a favourable sequence context for MAPK phosphorylation. Mutation of Ser78 or Ser81 to alanine reduced the proportion of stress-induced CHOP phosphorylation while the double mutation abolished phosphorylation. These sites were found to be phosphorylated by p38 increasing the activity of the CHOP transactivation domain[77] (Figure 9B) and p38-dependent phosphorylation of CHOP was required for maximal cell death in response to CHOP overexpression in HeLa cells[78]. It seems likely that p38-dependent phosphorylation of CHOP alters both the activity of the transactivation domain and subsequently its affinity for binding partners, leading to an altered gene expression profile.

3.2.5 JNK is a downstream effector of the CHOP-CaMKII pathway

CHOP expression can promote the ER stress-induced release of Ca^{2+} due to hyperoxidation of the ER. In macrophages, the ER

stress-induced release of Ca^{2+} from the ER lumen results in the transient activation of Ca^{2+}/calmodulin-dependent protein kinase II (CaMKII)[79]. This protein is then able to autophosphorylate and is further activated by ER stress-induced ROS production[80] leading to sustained CaMKII activation, which can induce apoptosis through promotion of JNK signalling by activating ASK1[81] and subsequently MKK4 (Figure 9A). *In vivo*, the knockout of CaMKII in mice reduced ER stress-induced apoptosis showing that ER stress-induced CaMKII activation is required for cell death. Therefore, in addition to activation by the IRE1α/TRAF2/ASK1 pathway, JNK is also activated in response to CaMKII signalling. However, it is unclear whether the PERK/eIF2α/CHOP axis of the UPR has a role in the ER stress-induced Ca^{2+} release and CaMKII activation.

3.2.6 p38 phosphorylates ATF6 increasing its transcriptional activity

Analysis of ATF6 showed that it can undergo phosphorylation and was a substrate for p38 *in vitro*. Furthermore, transfection of primary myocardial cells with ATF6 and p38α promoted the transactivation activity of ATF6[82]. Sustained p38 activation resulted in increased ATF6 phosphorylation and promoted the activity of the transactivation domain of ATF6 at the BiP promoter. Interestingly, following thapsigargin treatment, induction of BiP expression occurred independently of p38 activation. On the other hand, p38 signalling was required for induction of BiP transcription in response to the ER stress inducer and proline analogue azetidine[83].

This suggests variation in the use of p38 depending on the ER stress inducer.

4. Apoptosis

There are two main apoptotic pathways: the extrinsic and the intrinsic pathway. The intrinsic pathway is generated by various stressors, including DNA damage, endoplasmic reticulum stress, loss of adhesion, growth factor withdrawal, and others. The extrinsic pathway, on the other hand, is triggered when a specific cell surface receptor binds to its cognate protein ligand. The two pathways differ in their upstream events, but the executioner phase is similar in both and involves activation of effector caspases.

4.1 Intrinsic apoptosis

Intrinsic cell death signals generally converge within the cell at the outer membrane of the mitochondria resulting in the loss of mitochondrial membrane integrity through an event called mitochondrial outer membrane permeabilization (MOMP) which is controlled by Bcl-2 proteins (Figure 10). As a consequence of MOMP cytochrome c is released from the mitochondrial intermembrane space into the cytoplasm where it binds to Apoptosis Protease-Activating Factor 1 (APAF-1) and procaspase-9, generating a complex known as the apoptosome. Within the apoptosome caspase-9 is activated and processes effector caspases-3, -6 and -7 which in turn cleave many cellular components eventually leading to cell death. The Bcl-2 family of proteins

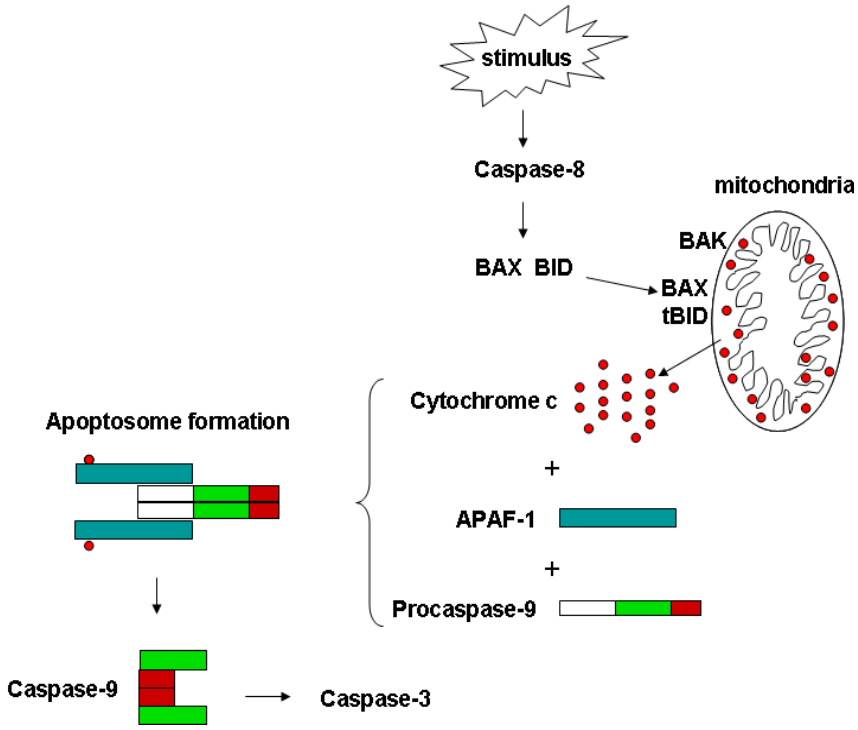

Figure 10. Intrinsic apoptosis. Events occurring at the mitochondria during intrinsic apoptosis are controlled by proteins of the Bcl-2 family, which leads to Cytochrome c release and apoptosome formation. Subsequently, effector caspases (Caspase-9 and Caspase-3) are activated.

regulates MOMP. The members of this family are characterized by having at least one Bcl-2 homology (BH) domain and are divided into three groups (Figure 11). The antiapoptotic Bcl-2-like proteins contain BH1, BH2, BH3 and BH4 domains. The proapoptotic Bcl-2-like proteins have BH1, BH2 and BH3 domains and the most important ones are BAX (Bcl-2 associated X) and BAK (Bcl-2 homologous antagonist killer). The third Bcl-2-like subfamily is represented by proapoptotic BH3-only proteins which only contain the short BH3 domain. The exact mechanism by which MOMP is

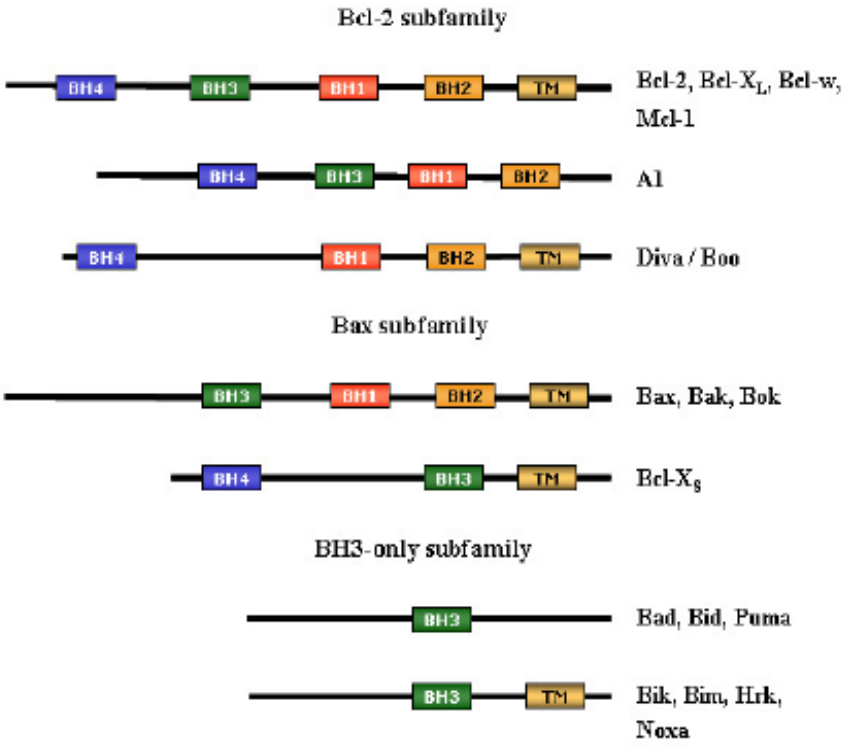

Figure 11. The Bcl-2 family. The Bcl-2 family can be classified in three groups: Bcl-2 subfamily (antiapoptotic), all encompassing multiple BH domains; Bax subfamily (proapoptotic), multidomain containing; and BH3-only subfamily (proapoptotic), including only a single BH3 domain. (Adapted from Roset *et al.*, 2007)

controlled via Bcl-2 proteins is still under debate but there are some generally accepted observations. BH3-only proteins carry out their proapoptotic function by two mechanisms: binding and neutralization of the prosurvival BCL-2 subfamily[84–86] and direct activation of the proapoptotic effectors BAX and BAK[87–90]. In healthy cells, BAK resides on the mitochondria and BAX is primarily in the cytoplasm, but death signals promote the accumulation of BAX on the mitochondria leading to oligomerization of BAX and BAK and pore formation, which

eventually results in MOMP. This transition can be driven by BH3-only proteins such as BIM or BID. In the case of BID proteolytic cleavage by caspase-8 is required to convert BID into tBID (truncated) which is then translocated from the cytoplasm to the mitochondria. Caspase-8 was the prototypical apical caspase for extrinsic apoptosis but has recently gained much attention in intrinsic apoptosis where it has shown to be important in genotoxic stress signalling[91] and ER stress[92,93] acting upstream of the mitochondria.

4.2 ER stress-induced apoptosis

At high levels of stress signalling, there is evidence that IRE1α contributes to a promiscuous degradation of mRNAs through RIDD. Although RIDD may help to defend cells against ER stress by degrading ER-associated mRNAs and thus limiting new protein translation, it may also be a mechanism of apoptosis in the setting of severe ER stress. In experiments in which IRE1α activity was manipulated towards RIDD, in an insulin-producing pancreatic beta cell line, ER stress-induced apoptosis was enhanced[94] (Figure 12). Moreover, similar findings were observed with induced overexpression of IRE1α, which is a way to activate IRE1α RNase activity through transphosphorylation in the absence of ER stress. Other possible links between IRE1α and ER stress-induced apoptosis may involve interaction of IRE1α with proteins implicated in apoptosis signalling. For example, co-immunoprecipitation experiments imply that mammalian IRE1α binds Bak and Bax, proteins involved in the mitochondrial pathway

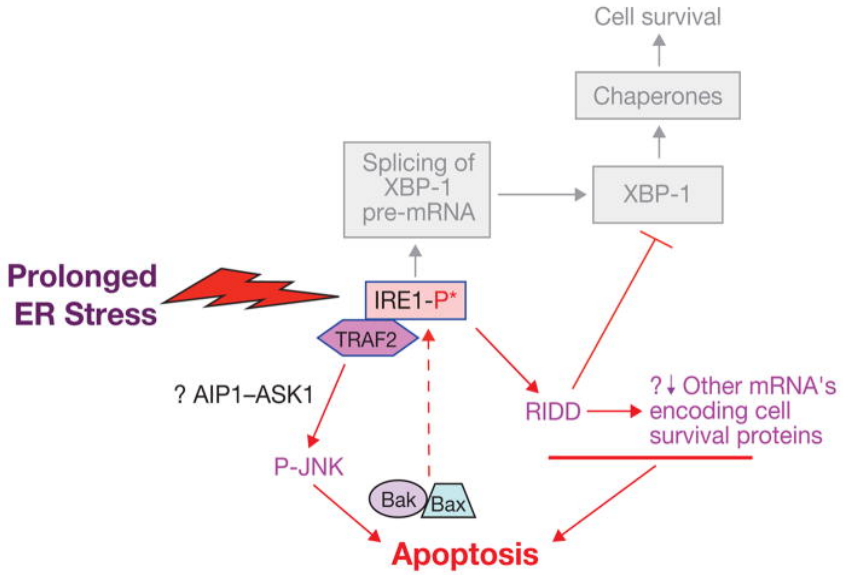

Figure 12. Prolonged activation of IRE1 leads to phosphorylation of JNK and apoptosis. The pro-apoptotic IRE1/TRAF2/JNK pathway can be activated by prolonged ER stress. Signal transduction between IRE1/TRAF2 and phosphorylation of JNK is mediated by the MAP3K ASK1 and its activator, AIP1. JNK-induced apoptosis may involve the proapoptotic Bcl-2 family members, Bax and Bak, which in turn, can amplify the IRE1 signal. Prolonged IRE1-mediated activation of the RIDD pathway may promote apoptosis by degrading mRNAs encoding essential cell-survival proteins, including XPB1 itself. Adapted from Tabas *et al*. 2011)

of apoptosis (Figure 12). This interaction seems to be important for IRE1α activation[42]. Phosphorylated, activated mammalian IRE1α also interacts with the adaptor protein TRAF2 and promotes a cascade of phosphorylation events that ultimately activates JNK[60]. Given the links between sustained JNK activity and cell death, JNK activity may link IRE1α-mediated ER stress signalling to cell death in certain settings. One study suggests that ER-localized Bim and Puma selectively activate the TRAF2/JNK axis of IRE1 signalling, biasing the response away from XBP-1 activation in favour of

JNK[95]. A key player in ER stress apoptosis signalling is CHOP which can be induced by all branches of the UPR but is predominantly upregulated by the PERK/eIF2α/ATF4 axis. Overexpression of CHOP has been reported to lead to cell cycle arrest and/or apoptosis. Cells lacking C/EBβ, the major dimerization partner of CHOP, are resistant to ER stress-induced apoptosis, suggesting that CHOP works as a transcriptional factor that regulates genes involved in either survival or death[96]. As a transcription factor, CHOP has been shown to regulate numerous pro- and antiapoptotic genes (Figure 13). A widely accepted mechanism of CHOP-induced apoptosis is the suppression of the prosurvival protein Bcl-2. Under ER stress, CHOP down-regulates the expression of Bcl-2 but not Bcl-X, sensitizing cells to apoptosis[5,97] (Figure 13). BAX is also up-regulated during ER stress as CHOP-deficient mice have less apoptotic cell death and lower Caspase-3 activation related to reduced BAX levels. Recent studies have shown that Bcl-2-associated athanogene 5 (Bag5) is over-expressed in prostate cancer and inhibits ER stress-induced apoptosis. Bag5 over-expression resulted not only in a decreased CHOP but also in a decreased BAX and an increased Bcl-2 gene expression[98]. CHOP has also been reported to regulate the expression of BH3-only proteins by interacting with FOXO3A and cJUN leading to its phosphorylation[6,99].

TRB3 is an intracellular pseudokinase that modulates the activity of several signal transduction cascades. TRB3 gene expression is highly regulated in many cell types. Amino acid starvation,

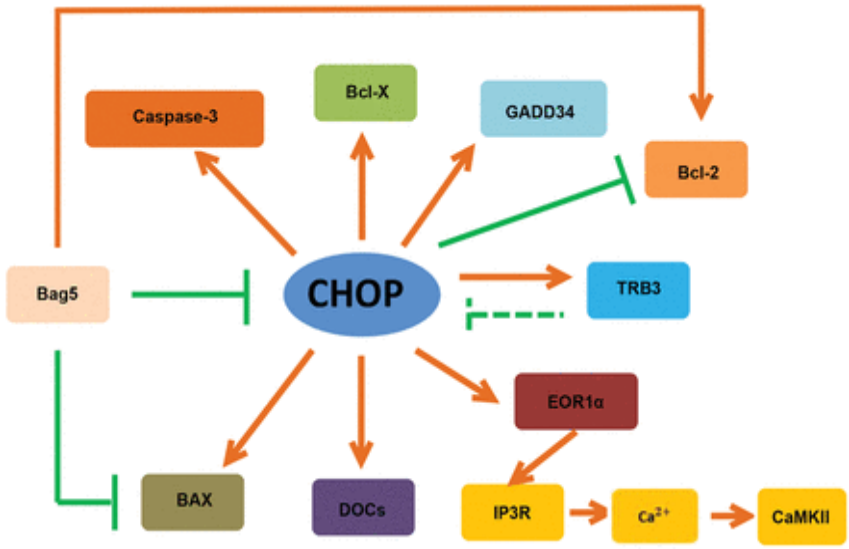

Figure 13. CHOP in ER stress induced apoptosis. Adapted from Li *et al.*, 2014

hypoxia, and ER stress promote TRB3 expression in non-cardiac cells. During ER stress, TRB3 is up-regulated by ATF4/CHOP[100]. Excess expression of TRB3 downregulates its own expression by negative feedback via the repression of ATF4/CHOP transcriptional activity[101]. CHOP expression increases in diabetic mouse kidneys and in podocytes treated with ROS and free fatty acid (FFA). In podocytes, transfection of CHOP increases TRB3 expression, and ROS augments the recruitment of CHOP to the proximal TRB3 promoter[102]..

ER stress has shown to upregulate transcription of death receptor 5 (DR5)[93], a signal transducer originally found in the context of extrinsic apoptosis[103]. DR5 recruits and activates Caspase-8 in the late phase of persistent ER stress. CHOP has been shown to induce

transcription of DR5. At early time points however DR5 mRNA is degraded by the RNase activity of IRE1α, which suggests that IRE1α counteracts apoptosis by mediating RIDD of DR5 at the early phase of ER stress and thus allowing for adaptation. Hence, CHOP and RIDD exert opposing effects on DR5 to control Caspase-8 activation and apoptosis.

Han *et al.* identified increased protein synthesis as one mechanism by which ATF4 and CHOP mediate cell death in response to ER stress[104]. They demonstrate a function of CHOP as a transcription factor that interacts with ATF4 to bind promoter regions of genes encoding proteins that increase protein synthesis. As a consequence of increased protein synthesis ROS are generated which is a powerful signal to induce apoptosis in response to ER stress (Figure 14). The fact that ATF4 and CHOP increase protein synthesis might appear paradox since ATF4 and CHOP mRNAs are preferentially translated when eIF2α is phosphorylated and phospho-eIF2α is known to disallow global protein synthesis. The idea is that eIF2α phosphorylation needs to be finely tuned to ensure proteostasis in the ER. Immediately after an insult, eIF2α is transiently phosphorylated to acutely and transiently attenuate protein synthesis. Subsequently, induction of ATF4 and CHOP and their downstream gene targets functions to restore protein synthesis. But, if protein synthesis increases before restoration of proteostasis, ROS are produced which leads to apoptosis.

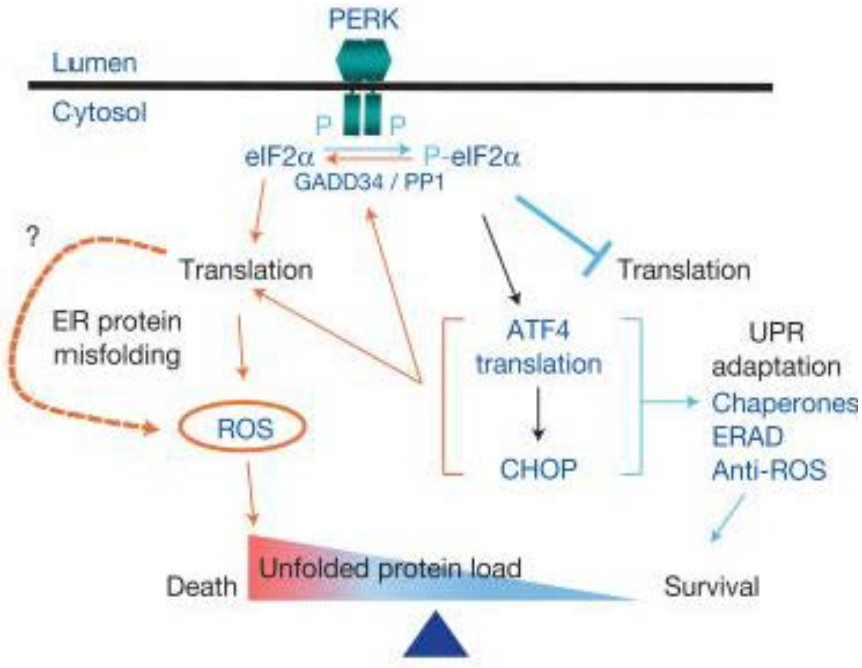

Figure 14. Mechanism of ATF4- and CHOP-mediated cell death. Upon ER stress, eIF2α phosphorylation by PERK promotes preferential translation of ATF4 for subsequent induction of CHOP. ATF4 and CHOP act together to upregulate target genes encoding functions in protein synthesis to restore general mRNA translation. If the adaptive UPR effectively reduces the unfolded protein load, restoration of protein synthesis promotes cell survival. However, if protein synthesis increases before restoration of proteostasis, ROS are produced as a signal to promote cell death. Blue colour indicates pro-survival pathways and red colour indicates pro-death pathways. (Adapted from Han *et al.*, 2012)

4.3 Cyclin O

The role of cyclin-dependent kinases (Cdk) in regulating cell-cycle progression has been well characterized and constitutes a standard issue in textbooks of cell biology. Over a decade ago, Cdks were discovered to play an additional role in intrinsic apoptosis. In thymocytes, activation of Cdk2 regulates apoptosis during antigen-mediated negative selection[105]. Furthermore, chemical inhibition of

Cdk2 in thymocytes treated with dexamethasone or γ-irradiation reduces cell-death [106,107]. In addition, these reports demonstrate that Cdk2 activity within apoptosis signalling is positioned upstream of Caspase-8 activation and MOMP. *De novo* protein synthesis is required in intrinsic apoptosis of thymocytes since cycloheximide blocks Cdk2 activity and subsequently prevents cells from dying. Interestingly, degradation of the Cdk2 inhibitor p27 parallels the increase in Cdk2 activity during apoptosis but inhibition of *de novo* protein synthesis by cycloheximide does not prevent degradation of p27. These findings along with data showing that the classical Cdk2 binding partners, Cyclin A and Cyclin E, are not involved in mediating Cdk2 activation during intrinsic apoptosis strongly suggests that activation of Cdk2 depends on the synthesis of a factor that had not been discovered yet. Recently, a novel protein termed Cyclin O has been identified[108]. Overexpression of Cyclin O induces cell death while downregulation of Cyclin O levels protects cells from DNA damage- and glucocorticoid-induced apoptosis. Moreover, γ-irradiation and ER stress[109] induce Cyclin O mRNA production. Active Cyclin O-Cdk2 complexes were isolated from cells expressing recombinant Cyclin O. The Cyclin O locus encodes four transcripts by use of two alternative promoters and alternative splicing sites (Figure 15): Cyclin Oα, Cyclin Oβ, Cyclin Oε and Cyclin Oδ/γ. However, in this thesis the focus is exclusively on Cyclin Oα (and will be henceforth called Cyclin O).

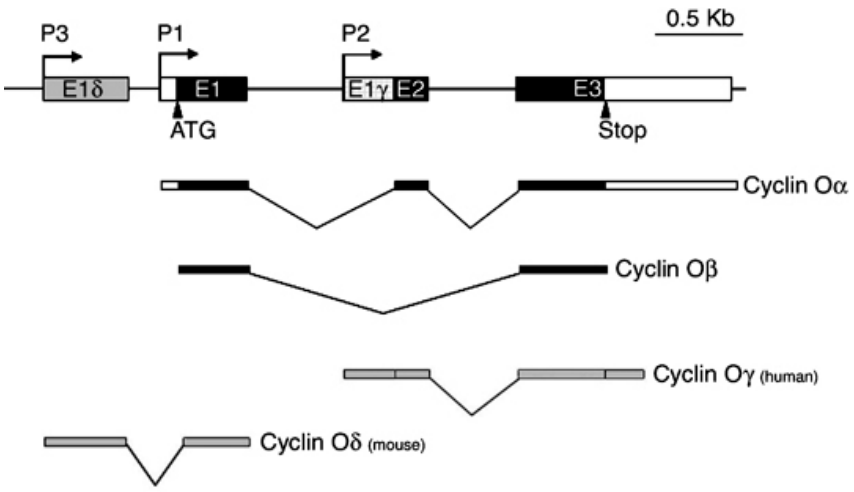

Figure 15. Cyclin O locus and expression. The Cyclin O locus encodes four transcripts that arise from the use of three alternative promoters: P1 (human/mouse Cyclin Oα and the alternatively spliced product human/mouse Cyclin Oβ), P2 (human Cyclin Oγ) and P3 (mouse Cyclin Oδ). Black boxes indicate coding regions. White boxes represent 5' and 3' non-coding regions. Grey boxes denote non-coding transcripts. (Adapted from Roig *et al.*, 2009)

5. Erythropoiesis

RBC are the most abundant cell type in the body and function primarily to transport oxygen and carbon dioxide. Mature RBCs in the bloodstream of mammals lack the nucleus and have the shape of a biconcave disc. The development of RBCs is regulated by a variety of growth factors, transcription factors, and microRNAs (Figure 10A). It starts with the hematopoetic stem cell (HSC) in the bone marrow where growth factors like interleukin-3 (IL-3) and granulocyte macrophage colony-stimulating factor (GM-CSF) activate transcription factors like GATA binding protein 2 (GATA2) and GATA1, which drives the HSCs into lineage-committed, definitive erythroid progenitors, termed burst-forming

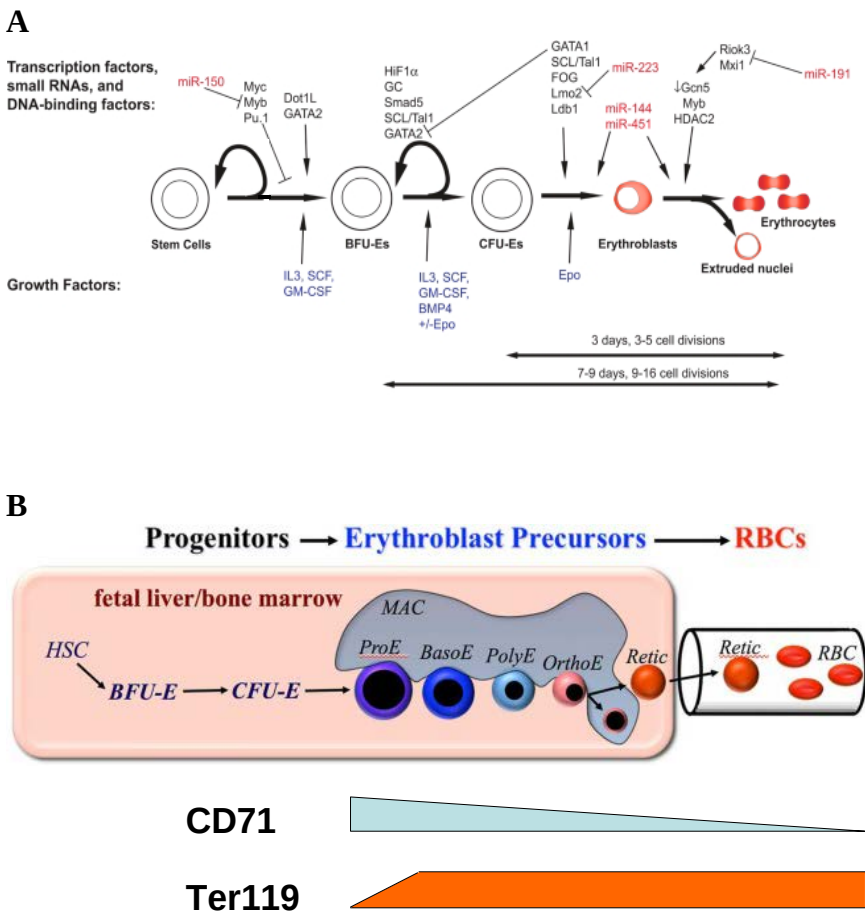

Figure 10. Erythropoiesis (A) Adapted from Hattangadi *et al.* 2011 **(B)** Adapted from Palis *et al.* 2014

unit erythroid (BFU-E) and colony-forming unit erythroid (CFU-E). These progenitors are defined by their ability to form colonies of mature erythroid cells in semisolid media. HSCs and BFU-Es still have the capacity for self renewal. BFU-E-derived colonies require 7 and 14 days in mouse and human systems, respectively, to form mature colonies typically containing more than a thousand erythroid cells. In contrast, the more mature CFU-E progenitors require only

2 and 7 days in mouse and human systems, respectively, to form mature colonies that consist of only 16–32 cells. Thus, CFU-E are only 4–5 cell divisions upstream of mature RBCs and the first 2-3 rounds of cell division depend exquisitely on the cytokine erythropoietin (EPO). The final 1-2 terminal cell divisions are no longer dependent on EPO but on adhesion to the extracellular fibronectin matrix mediated by expression of integrin receptors on the erythroid progenitors. The development downstream of CFU-E goes through several morphologically distinguishable stages of erythroblast maturation (Figure 10B): from proerythroblast to basophilic, polychromatophilic, and orthochromatic forms. The typical markers expressed on erythroblasts and later stages are Ter119 which remains present throughout the whole development and CD71 which progressively decreases. Erythroblasts mature in the bone marrow within erythroblastic islands, composed of erythroblasts physically attached to central macrophage cells[110]. In mammals, the end result of precursor maturation is enucleation, which results in the formation of two cell types: reticulocytes that contain most of the cytoplasm and hemoglobin, as well as the proteins needed to form a unique cytoskeletal network[111,] 1979; Koury et al., 1989;[112,113] and pyrenocytes (“extruded nuclei”) that contain the condensed nucleus surrounded by a lipid bilayer and a thin rim of cytoplasm[114]. Pyrenocytes are rapidly ingested by macrophages[115] because they flip phosphotidylserine onto their cell surface, providing the classical ingestion signal for macrophages. As the reticulocyte leaves the bone marrow into the bloodstream its further maturation results in approximately 20% loss of plasma

membrane surface area, reduced cell volume, increased association of the cytoskeleton to the outer plasma membrane, and the loss of all residual cytoplasmic organelles, including mitochondria and ribosomes[116,117]. Organelle clearance occurs through both autophagy and exocytosis[118]. The membrane changes convert the multilobulated reticulocyte into a biconcave disc with improved viscoelasticity, the final RBC. The unique cytoskeletal network ensures that mature RBCs can passively deform during their repeated passage through capillary networks yet maintaining their biconcave shape. With progressing age, surface area and volume become reduced whereas hemoglobin content remains unaltered, which results in increased RBC density. Senescent RBCs are cleared by splenic macrophages that recognize, among other changes, clustered cytoskeletal proteins on the RBC surface[119].

OBJECTIVES

Our group has identified a novel cyclin called Cyclin O as an activator of Cdks in response to cellular stress that activates intrinsic apoptosis. Here, we address specifically the role of Cyclin O in ER stress with the following objectives:

1. The function of Cyclin O in the Integrated Stress Response, especially in regard to the PERK/eIF2α signalling pathway.

2. The role of Cyclin O in MAPK signalling.

3. The characterization of Cyclin O knockout mice.

MATERIALS AND METHODS

MATERIALS AND METHODS

1. Antibodies

Protein	Antibody	Source	Supplier	Technique
PERK	H-300	Rabbit polyclonal	Santa Cruz	WB
PKR	Ab47509	Rabbit polyclonal	Abcam	WB
Caspase-8	H-134	Rabbit polyclonal	Santa Cruz	WB
Caspase-8	9429	Rabbit polyclonal	Cell signaling	WB
Pyruvate kinase		Goat polyclonal	Chemicon	WB
CHOP	F-168	Rabbit polyclonal	Santa Cruz	WB
Lamin B1	16048	Rabbit polyclonal	Abcam	WB
phospho-p38	9211	Rabbit polyclonal	Cell signaling	WB
p38	C-20	Goat polyclonal	Santa Cruz	WB
phospho-JNK	G-7	Mouse monoclonal	Santa Cruz	WB
JNK	C-17	Rabbit polyclonal	Santa Cruz	WB
MEKK4	M7194	Mouse monoclonal	Sigma	IF
hCyclin O	C5	Rabbit polyclonal	Home made	IF
phospho-MEK6	B-9	Mouse monoclonal	Santa Cruz	WB
MEK6		Rabbit monolyclonal	E. Perdigero	WB
Flag	7425	Rabbit polyclonal	Sigma	IP
HA	12CA5	Mouse monoclonal	Clone lab	IP
myc	9E10	Mouse monoclonal		IP
CD4-FITC	GK1.5	Rat monoclonal	eBioscience	FACS
B220-FITC	RA3-6B2	Rat monoclonal	eBioscience	FACS
CD71-FITC	01594D	Rat monoclonal	Pharmingen	FACS
CD45-FITC	30-F11	Rat monoclonal	eBioscience	FACS
NK1.1-FITC	PK136	Rat monoclonal	eBioscience	FACS
Ter119-FITC	TER-119	Rat monoclonal	eBioscience	FACS
CD8a-PE	53-6.7	Rat monoclonal	eBioscience	FACS
Ter119-PE	TER-119	Rat monoclonal	eBioscience	FACS
IgM-PE	11/41	Rat monoclonal	eBioscience	FACS
CD41-PE	eBIOMWReg30	Rat monoclonal	eBioscience	FACS
Gr-1-PE	RB6-8C5	Rat monoclonal	eBioscience	FACS
NKp46-PE	29A1.4	Rat monoclonal	eBioscience	FACS
Foxp3-PE	FJK-16s	Rat monoclonal	eBioscience	FACS
CD3e-PECy5	145-2C11	Rat monoclonal	eBioscience	FACS
CD44-PECy5	IM7	Rat monoclonal	eBioscience	FACS
CD41-PECy7	eBIOMWReg30	Rat monoclonal	eBioscience	FACS
CD11b-APC	M1/70	Rat monoclonal	eBioscience	FACS
CD24-APC	M1/69	Rat monoclonal	eBioscience	FACS
TCRβ-APC	H57-597	Rat monoclonal	eBioscience	FACS
CD31-APC	390	Rat monoclonal	eBioscience	FACS
CD69-APC	H1.2F3	Rat monoclonal	eBioscience	FACS
CD25-APC	PC61.5	Rat monoclonal	eBioscience	FACS
CD49b-APC	DX5	Rat monoclonal	eBioscience	FACS
CD62L-APC	MEL-14	Rat monoclonal	eBioscience	FACS
TCRγδ-APC	eBIOGL3	Rat monoclonal	eBioscience	FACS

Table 1. Primary antibodies used.

Protein	Antibody	Source	Supplier	Technique
Anti-mouse Fc	Alexa Fluor 555	Goat monoclonal	Invitrogen	IF
Anti-rabbit Fc	Alexa Fluor 488	donkey monoclonal	Invitrogen	IF
Anti-mouse HRP	NA931V	sheep monoclonal	GE healthcare	WB
Anti-rabbit HRP				WB

Table 2. Secondary antibodies used.

2. Quantitative RT-PCR

RNA was obtained using Trizol reagent (Invitrogen) following the manufacturer's instructions. Quantitative RT-PCR (qRT-PCR) was performed with QuantiTect SybrGreen reagent (Qiagen) using 100 ng of RNA per reaction in a final volume of 10 µl. Samples were analysed in triplicate and the data was analysed using SDS2.1 software (Applied Biosystems). PCR cycles are described below. All qRT-PCR results derive from three independent experiments.

Primers used for Cyclin O: 5'-CGCTTGCAAGCAGGTAGAGG-3' and 5'-CTACCTCGTGAGGACTTCG-3'.

Primers used for HPRT: 5'-GGCCAGACTTTGTTGGATTTG-3' and 5'-TGCGCTCATCTTAGGCTTTGT-3'.

One-step quantitative RT-PCR:

50ºC 30 min
95ºC 15 min

95ºC 15 sec
55ºC 30 sec 40 cycles
72ºC 30 sec

72ºC 10 min

3. Cell culture, transfection, and lentivirus infection

All cell lines were grown in Dulbecco's modified Eagle's medium DMEM (Sigma) supplemented with antibiotics and 10% fetal calf serum (Biological Industries). Cells were maintained at 37 ºC with a humid atmosphere of 5% of CO_2.

Mouse fibroblasts were grown in medium supplemented with non-essential amino acids (Sigma) and 50 μM β-mercaptoethanol. The mouse T-cell lymphoma cell line WEHI7.2 was grown in low glucose (1 g/L) RPMI medium. WEHI7.2 cells stably expressing shRNA against GFP or Cyclin O were previously generated in our laboratory.

HEK 293T cells were transfected with pcDNAmychCycOα, pcDNAHAmMEKK4αKD, and pcDNAI-Flag-MTK1(K/R) by preparing a solution containing NaCl (150 mM), plasmid DNA (11.25 μg/10 cm dish) and PEI (1 mg/ml). After incubating the transfection solution 15 min at RT it was added drop-wise to the cells. 24 hours post transfection, cells were harvested. For lentiviral production we used the pLVTHM vector (Tronolab) carrying short hairpin inserts directed against Cyclin O (pLVTHMsiEx3 expressing sh#1 and pLVTHMsiC5 expressing sh#2) or a scrambled sequence (pLVTHMscrambled). Furthermore, pWPI vectors (Tronolab) were used for expression of wild type Cyclin O (pWPI-mCy5α-myc) and Cdk binding-deficient Cyclin O (pWPILinkBK190A). Lentivirus were produced by cotransfecting HEK-293T with helper vectors pMD2G (envelope vector, 10%) and

pPAX2 (packaging vector, 40%) together with pLVTHM (50%) using the PEI method. 48 and 72 hours post transfection supernatants were collected, pooled, sterile filtrated, and used undiluted for infection of fibroblasts.

4. DNA constructs

The constructs pcDNAmychCycOα, pGEXTevCyclinOα, pLVTHMsiEx3, pLVTHMsiC5, pLVTHMscrambled, pWPI-mCy5α-myc, and pWPILinkBK190A were generated previously in our laboratory. The vectors pcDNAHAmMEKK4αKD, pMALcMEK6, and pcDNAI-Flag-MTK1(K/R) were kindly provided by Addagene, A. Ne, and M. Takekawa respectively. Table 3 gives an overview of the constructs used.

Plasmid	Expression
pcDNAmychCycOα	myc-Cyclin O
pGEXTevCyclinOα	GST-Tev-Cyclin O
pLVTHMsiEx3	sh1 (lentivirus)
pLVTHMsiC5	sh2 (lentivirus)
pLVTHMscrambled	shscrambled (lentivirus)
pWPI-mCy5α-myc	myc-Cyclin O (lentivirus)
pWPILinkBK190A	myc-Cyclin O K190A (lentivirus)
pcDNAHAmMEKK4αKD	HA-murineMEKK4 (kinase death)
pcDNAI-Flag-MTK1(K/R)	HA-humanMEKK4 (kinase death)
pMALcMEK6	MBP-MEK6

Table 3. DNA constructs used

5. Immunofluorescence

Cells were grown overnight on coverslips and incubated with 0.1 μM thapsigargin prior to fixation with 4% paraformaldehyde for 20 minutes at RT. After washing with PBS, cells were incubated with

ammonium chloride (50 mM) for 30 minutes. Permeabilization of the cells was performed with 0.1 % Triton X-100 for 10 minutes at RT. Nonspecific binding sites were blocked with 2% BSA. Incubation with primary antibody was carried out overnight and incubation with secondary antibodies lasted 1 hour. Finally, cells were mounted with DAPI containing mounting medium Vectashield® (Vector laboratories) prior to analysis by confocal microscopy (Leica TCS SPE).

6. Western Blot

Cells were incubated with 0.1 μM thapsigargin or left untreated. Then, cells were washed with cold PBS, scraped and frozen at -80 ºC. Pellets where extracted with lysis buffer (10 mM Tris-HCl pH 7.4, 1% NP-40, 1% sodium deoxycolate and 0.15 M NaCl) to which protease and phosphatase inhibitors were added (2 μg/ml aprotinin, 2 μg/ml leupeptin, 2 μg/ml antipain, 20 μg/ml soybean trypsin inhibitor, 1 mM DTT, 1 M NaF, 0.5 M β-glycerophosphate, 0.1 M sodium pyrophosphate, 1 mM Pefablock™ and 20 mM sodium ortovanadate) and the protein concentration was determined by the Bradford assay (BioRad). Equal amounts of protein from total cellular extracts were loaded on each lane, resolved by SDS-Polyacrylamide Gel Electrophoresis (SDS-PAGE) and transferred onto a nitrocellulose membrane (Protran). Membranes were blocked either with 5% non-fat milk overnight at 4 ºC or with 3% BSA overnight at 4 ºC for detection of phosphorylated proteins. Primary antibodies were diluted in 2% BSA and were incubated either for 2 hours at RT or overnight at 4 ºC for detection of phosphorylated

proteins. After extensive washing, membranes were incubated for 1 hour with the secondary HRP-conjugated antibody. Membranes where then blotted using either the standard Pierce™ ECL chemiluminiscent substrate (Thermo Scientific) or the Immobilion™ Western substrate (Millipore).

7. Subcellular fractionation

Subcellular extracts were obtained by using a differential detergent fractionation procedure[120]. After irradiation with 10 Gy or incubation with 0.1 μM thapsigargin cells were trypsinized, washed, and resuspended in digitonin buffer (pH 6.8, 0.015% digitonin, 5 mM EDTA, 300 mM sucrose, 100 mM NaCl, 10 mM PIPES, 3 mM $MgCl_2$) for 10 min at 4 ºC. After centrifugation, supernatant (cytosolic fraction) was removed and the pellet resuspended in triton buffer (pH 7.4, 0.5 % TX-100, 3 mM EDTA, 300 mM sucrose, 100 mM NaCl, 10 mM PIPES, 3 mM $MgCl_2$) for 30 min at 4 ºC. After centrifugation, supernatant (membrane/organelle fraction, not used) was removed and the pellet resuspended in RIPA buffer (10 mM Tris-HCl pH 7.4, 1% NP-40, 0.1% SDS, 1% sodium deoxycholate and 0.15 M NaCl) for 10 min at 4 ºC. After centrifugation, supernatant (nuclear fraction) was removed.

8. Production of recombinant proteins in *E. coli*

For the production of recombinant fusion proteins we used the *Escherichia coli* (E. coli) strain BL21 (DE3) transformed either with pGEXTevCyclinOα expressing GST-Tev-Cyclin O or with pMALcMEK6 expressing MEK6-MBP. 10 mL of LB medium plus

antibiotic were inoculated with bacteria carrying the plasmid of interest and incubated at 37 ºC overnight with constant agitation at 200 rpm. The following morning, the saturated culture was diluted 1:1000 and incubated at 37 ºC until OD_{600nm} reached 1.0. Protein expression was induced by adding IPTG (Isopropyl-beta-D-thiogalactopyranoside) 1 mM to the media. The culture was incubated at 30 ºC during four hours with constant agitation at 200 rpm. Cells were harvested by centrifuging at 3500 rpm for 10 minutes. The bacteria pellet was frozen at -80 ºC and then resuspended with 1/40 (of the initial culture volume) of NTEN (20 mM Tris-HCl pH 8, 150 mM NaCl, 1 mM EDTA, 0.5% NP40, 1 mM DTT, 2 μg/ml aprotinin, 2 μg/ml leupeptin, 2 μg/ml antipain, 20 μg/ml soybean trypsin inhibitor, 1 mM Pefablock™) and lysed by sonication (3 times 15 sec at an amplitude set to 40% with 0,5 sec ON/0,5 sec OFF). To obtain a clear lysate, the extract was centrifuged at 10.000 rpm for 10 minutes at 4 ºC and the pellet was discarded. The supernatant was aliquoted and stored at -80 ºC.

9. Pull-down

Cell extracts from M6 cells as well as from wild type and PERK-/- fibroblast were obtained with lysis buffer (50 mM Tris HCl pH 7.4, 0.5% NP-40, 20 mM EDTA, 0.15 M NaCl) to which protease and phosphatase inhibitors were added (2 μg/ml aprotinin, 2 μg/ml leupeptin, 2 μg/ml antipain, 20 μg/ml soybean trypsin inhibitor, 1 mM DTT, 1 mM NaF, 1 mM β-glycerophosphate, 1 mM sodium orthophosphate, 1 mM Pefablock™ and 200 mM sodium ortovanadate). Protein concentration was determined using the

Bradford reagent. Extracts were then precleared by incubation with sepharose beads. 0.5 mg of cell extracts were incubated overnight at 4 ºC with 3 µg of GST only or GST-Tev-Cyclin O fusion protein bound to 20 µl of glutathione-sepharose beads. Then, beads were washed with lysis buffer and boiled in 40 µl of Laemmli buffer 2X. 10 µl were loaded for SDS-PAGE and subsequent western blotting. Prior to adding Laemmli buffer to the samples used for PKR, cleavage with TEV (Tobacco Etch Virus) protease was performed, taking advantage of the Tev cleavage site in the GST-Tev-Cylin O fusion protein, and supernatants were processed for western blotting.

10. Immunoprecipitation and kinase assay

Fibroblasts and transfected HEK 293T cells were incubated with 0.1 µM thapsigargin or left untreated prior to resuspension in lysis buffer (50 mM Tris-HCl pH 7.5, 150 mM NaCl, 20mM EDTA, 0.5% NP-40, 1 mM DTT, 2 µg/ml aprotinin, 2 µg/ml leupeptin, 2 µg/ml antipain, 20 µg/ml soybean trypsin inhibitor, 1 mM Pefablock^{TM}, 1 mM sodium orthophosphate, 0.2 mM sodium ortovanadate, 1 mM sodium fluoride and 1mM β-glycerophosphate). 1.2 µg of commercial antibody, 200 µl of hybridoma supernatant (α-HA and α-myc antibodies), or 2 µl of crude serum (α-cyclin O antibodies) were used per immunoprecipitation and antibodies were bound to 20 µl protein G-sepharose beads. Beads were washed extensively and finally resuspended in 20 µl (for Histone H1) or 30 µl (for MEKK4 and MEK6) of Hot Mix (50mM Tris-HCl pH=7.5, 10mM MgCl2, 20µM

ATP, 10μCi [γ−32P] dATP, 1mM DTT) supplemented with the substrate: 2 μg of soluble substrate calf thymus Histone H1; 2 μg of MBP-MEK6 bound to 20 μl of amylose beads; immunoprecipitated HA-mMEKK4 bound to 20 μl of protein G-sepharose beads coated with α-HA antibody; immunoprecipitated Flag-hMEKK4 bound to 20 μl of protein G-sepharose beads coated with α-Flag antibody. The equivalent of one 10 cm dish of HEK 293T cells transfected with plasmids expressing HA-tagged MEKK4 was used per kinase reaction. Kinase reactions were performed during 30 minutes at 30ºC and then stopped by adding 30 μl of Laemmli buffer 2x (for Histone H1) or 20 μl of Laemmli Buffer 4x (for MEKK4 and MEK6). 40 μl of the reaction were loaded on a SDS-PAGE. Gels were coomassie stained, dried and subjected to autoradiography.

11. FACS: measurement of apoptosis by DNA content

Fibroblasts or thymocytes were incubated with 0.1 μM thapsigargin or left untreated prior to resuspension in hypotonic staining solution (0.1% sodium citrate, 0.1% TritonX-100, 10 μg/ml RNAase A, 50 μg/ml propidium iodide) at a final density of 10^6 cells/ml and subsequent incubation at 4 ºC for at least 24 hours. Samples were analysed by flow cytometry using a FACScan™ flow cytometer (Beckton Dickinson) and the CellQuest™ software (Beckton Dickinson) for acquisition. Data analysis was performed using the FlowJo software (Tree Star Inc.).

12. FACS: analysis of hematopoietic cells

Thymus, bone marrow, and spleen were squashed through a 70 μm nylon cell strainer BD Falcon™ (Becton, Dickinson and Company). Bone marrow was obtained by cutting and flushing femur and tibia. Freshly drawn blood was anticoagulated with EDTA. Cells from thymus, blood, bone marrow, and spleen were subsequently lysed with red blood cell lysing buffer (Sigma). Cells were washed and resuspended at 10^7 cells/ml in 100 μl of antibody solution. After 20 min of incubation at RT cells were washed and fixed in 0.5% paraformaldehyde overnight at 4 ºC. The next day FACS analysis was carried out on a FACScanto™ flow cytometer (BDbioscience) using the FACSDiva™ software (BDbioscience) for acquisition and analysis.

13. Generation of Cyclin O knockout mice

Design and construction of a Cyclin O-targeting vector, ES cell transfection and identification of correctly targeted cell clones were done by KOMP (Knock-Out Mouse Project). In Figure.M1 is shown the strategy used to target the Cyclin O gene. The Cyclin O ORF was replaced by homologous recombination by the LacZ coding sequence preserving the Cyclin O regulatory elements of the promoter. The inserted sequence also includes a floxed neomycin resistance cassette that could be removed later on by intercrossing with transgenic mice expressing the Cre recombinase.

Three ES targeted clones were purchased and injected into into C57Bl/6N blastocysts and these implanted into foster mothers. Six alive male chimaeras were obtained from two of the clones

(Table.M1). The ES microinjection into pre-implantation stage mouse embryos and the generation of chimeras were done at the Transgenesis Unit of CNIO (Madrid).

All six male chimaeras were bred to C57Bl/6N females and the offspring screened for germ line transmission by PCR. All the chimaeras transmitted the knockout allele and then we established two lines: AC4/ALO and AD9/ALN that showed identical phenotype. Animals were kept under pathogen-free conditions and all procedures were approved by the Animal Care Committee.

To obtain the definitive KO line, the heterozygous mice were crossed to Cre-deleter mice (Schwenk et al., 1995) to remove the floxed neo cassette (Figure.M1). After getting Cre-mediated excision of the neo marker, the transgene was segregated from the targeted allele by crossings with wild type C57Bl/6N mice.

Since all this process takes a long time, we intercrossed the Cyclin O null, neo-containing alleles to obtain the cellular models used in this work.

14. Genotyping

For the purpose of genotyping we have designed primers for PCR that allowed us to distinguish WT and KO alleles based on unique amplification products (Table.M2). Primer sequences are shown in the Table.M3 and PCR conditions in Table.M4. Genomic DNA used for genotyping was isolated from tail biopsies and extracted by proteinase K digestion over night at 55ºC in tail buffer (10mM Tris ph:8, 100mM NaCl, 10mM EDTA pH:8, 0,5% SDS). The next day,

the DNA was isolated by isopropanol precipitation and rehydrated with TE solution (10mM Tris·Cl pH8 and 1mM EDTA).

RESULTS

RESULTS

1. ER stress

Our group demonstrated earlier that Cyclin O is necessary for radiation induced apoptosis[108]. The model that was used employed the WEHI7.2 cell line originally derived from a mouse T-cell lymphoma[121] carrying short hairpin RNA constucts directed against Cyclin O. Recently, we obtained evidence that Cyclin O plays a role in response to ER stress[109]. In addition, we developed new experimental models thanks to the availability of Cyclin O knockout mice.

1.1 Apoptosis induced by ER stress depends on Cyclin O

First, we addressed the essential question whether Cyclin O is necessary for ER stress-induced apoptosis using our new experimental tools. Immortalized fibroblasts were generated from Cyclin O knockout and wild type mice by stable transfection with the large T-Antigen. Induction of ER stress with thapsigargin served as the apoptotic stimulus to assess the potential of these cells to undergo cell death. Cells were harvested after treatment and their DNA content was analyzed by flow cytometry (see materials and methods). Cyclin O knockout cells showed a lower percentage of apoptotic cells compared with the wild type cells (Figure 1A). Similar results were obtained using thymocytes isolated from Cyclin O knockout mice and subjected to thapsigargin treatment (Figure 1B). Cyclin O deficient thymocytes showed a reduced percentage of apoptotic cells and heterozygous cells displayed an

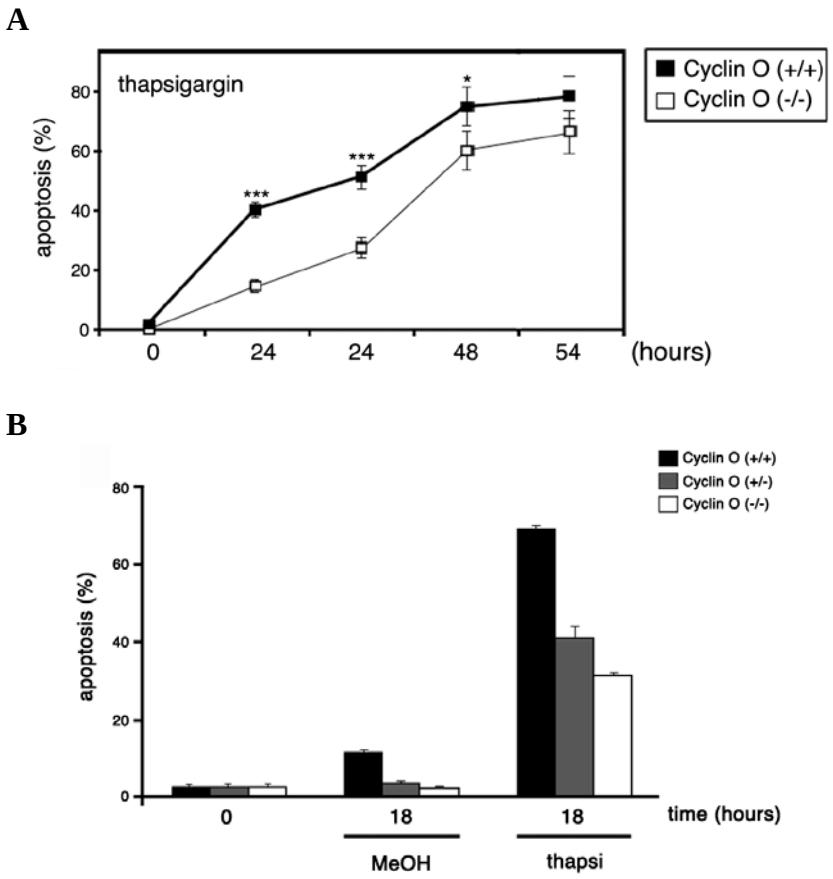

Figure 1. Apoptosis induced by ER stress depends on Cyclin O. Wild type and Cyclin O (-/-) fibroblasts **(A)** as well as *ex vivo* thymocytes **(B)** were incubated with thapsigargin. Apoptosis was measured at indicated time points using FACS analysis.

intermediate phenotype. Taken together, these experiments suggest that Cyclin O is necessary for ER stress-induced apoptosis.

1.2 ER stress induces Cyclin O-associated Cdk activity

Previously, our group demonstrated that Cyclin O mRNA levels rise in ER stressed cells[109]. In order to prove that this finding is connected to the Cdk-associated function of Cyclin O we performed

a kinase assay with immunoprecipitated endogenous Cyclin O and purified calf thymus Histone H1 as a substrate (Figure 2). Unfortunately, we have not been able to measure Cyclin O-associated kinase activity in fibroblasts due to the low expression levels of Cyclin O. Instead, we used WEHI 7.2 cells expressing short hairpin RNA constructs directed against Cyclin O or GFP (control) treated with thapsigargin. Control cells showed a time-dependent increase in Cyclin O-associated kinase activity whereas cells carrying short hairpin constructs against Cyclin O showed a blunted response. These results indicate that ER stress induces Cyclin O-associated Cdk activity.

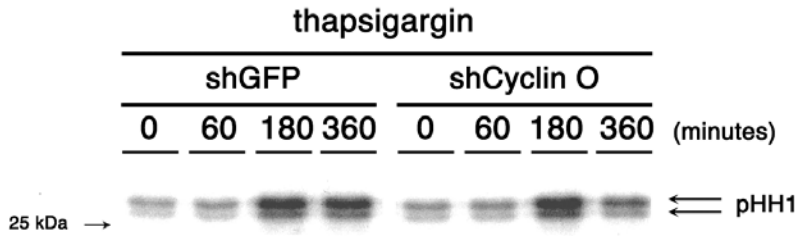

Figure 2. ER stress induces Cyclin O-associated Cdk activity. WEHI 7.2 cells were stably transfected with short hairpin constructs against Cyclin O and GFP (control), treated with thapsigargin and harvested at indicated time points. Endogenous Cyclin O was immunoprecipitated from extracts in order to assess Cyclin O-associated Cdk activity in a kinase assay employing Histone H1 (HH1) and radioactive [γ-^{32}P]ATP as a substrate. Depicted is the autoradiogram of the kinase assay.

1.3 ER stress-induced expression of Cyclin O depends on eIF2α and CHOP

Previous results concerning the biochemical positioning of Cyclin O during ER stress-induced apoptosis indicated that Cyclin O acts upstream of PERK to induce the eIF2α-dependent stress response pathway. In this context, we wanted to know how the expression levels of Cyclin O change in an ER stressed cell. Knockin fibroblasts were used that carry a point mutation in the eIF2α locus which converts serine 51 to an alanine residue. No phosphorylation of eIF2α at ser51 can occur and therefore PERK-dependent signalling is blocked. Incubation with thapsigargin led to a robust induction of Cyclin O mRNA levels in wild type cells whereas S51A knockin fibroblasts failed to elevate it (Figure 3A). These results show that the induction of Cyclin O in response to ER stress is dependent on the PERK/eIF2α axis. We set out to further investigate whether Cyclin O is under the control of the transcription factors that are specifically synthesised downstream of eIF2α in response to ER stress. We decided to use CHOP knockout fibroblasts to measure Cyclin O levels in response to thapsigargin treatment. CHOP knockout cells were incapable to induce Cyclin O levels indicating that this transcription factor is essential for the induction of Cyclin O in response to ER stress (Figure 3B).

These results, together with the previous finding that Cyclin O acts upstream of PERK, allowed us to come to the conclusion that there is a positive feedback loop emanating from CHOP and acting on Cyclin O.

A

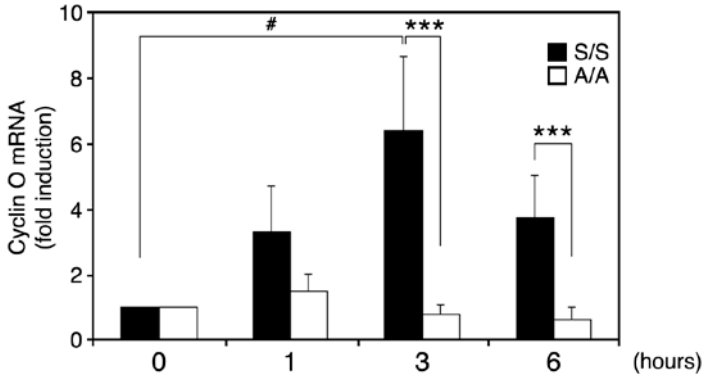

B

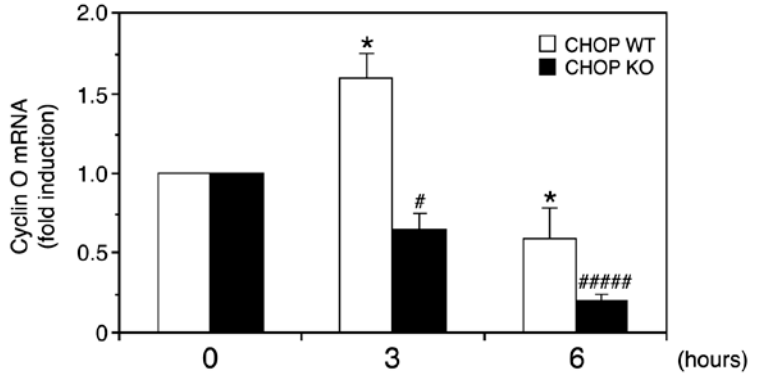

Figure 3. ER stress induced expression of Cyclin O depends on eIF2α and CHOP

(A) Wild type eIF2α (S/S) and phosphorylation deficient eIF2α (A/A) fibroblasts carrying a serine 51 to alanine mutation were incubated with thapsigargin. The levels of Cyclin O mRNA were measured at the indicated time points by quantitative RT-PCR. **(B)** Wild type and CHOP deficient fibroblasts were processed as in A.

1.4 Cyclin O binds to PERK and PKR *in vitro*

As a complementary approach to characterize the molecular mechanism by which Cyclin O activates PERK we hypothesized that Cyclin O may interact directly with it. PERK is an ER transmembrane protein exposing its BiP binding domain to the lumen of the ER, whereas its kinase domain is located in the cytoplasm. Previous results in regard to the subcellular localisation of Cyclin O indicate that most of it is in the cytoplasm and a fraction of the Cyclin O pool is located to the ER and probably associated with the cytosolic side of the ER membrane[109]. Pull-down experiments were performed using recombinant GST-Cyclin O fusion protein or GST alone as a negative control in combination with extracts from M6 cells. M6 human colon adenocarcinoma cells were used because they are secretory cells that have a high amount of ER and therefore high levels of endogenous PERK. We detected PERK in pulldowns of GST-Cyclin O protein (Figure 4A) but not when GST alone was used. The occurrence of multiple closely migrating bands led us to wonder whether those might be postranslationally modified forms of PERK. To check whether they correspond to phosphorylations, we performed phosphatase treatment in hope the bands would collapse into one single band. The pattern of the phosphatase treated sample looked similar to the untreated one ruling out that phosphorylation was a cause for the occurrence of multiple closely migrating bands. We took advantage of this pull-down assay to assess whether Cyclin O binds to PKR. PKR is another eIF2α kinase that can be activated in response to ER stress and we cannot exclude the possibility that Cyclin O exerts its

function in eIF2α signaling not only through PERK but also through PKR. Indeed, we were able to pull down PKR together with Cyclin O in extracts of wild type fibroblasts but not when PKR-/- cells were used as a negative control (Figure 4B). Taken together, these results demonstrate that Cyclin O interacts directly with PERK and PKR *in vitro*.

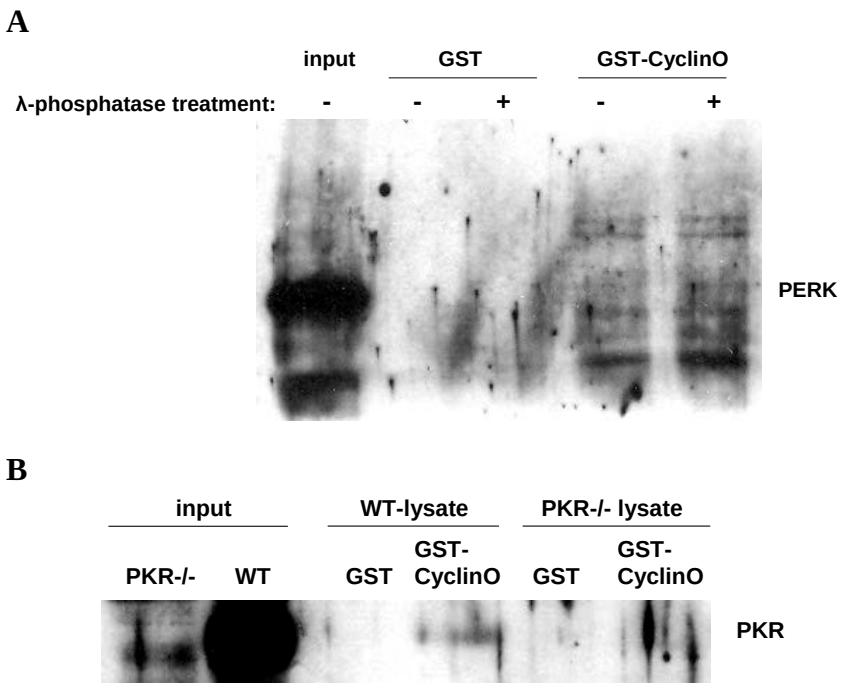

Figure 4. Cyclin O binds to PERK and PKR *in vitro*. (A) Recombinant GST-Cyclin O or GST alone were used as a bait to pull down PERK from extracts of M6 cells. Subsequently, PERK was detected by western blotting. Where indicated λ-phosphatase treatment was performed to yield dephosphorylated proteins. Input represents 25% of the whole cell lysate that was used in the pull-down samples.
(B) Recombinant GST-Cyclin O or GST alone served to pull down PKR from wild type and PKR-/- cell lysate. Immunoblotting was employed to detect PKR. Input is 25% of the lysate used for the pull-down samples.

1.5 Crosstalk between ER stress pathway and the DNA damage response

Previously, our group demonstrated that Cyclin O plays a role in radiation induced apoptosis[108]. Given the fact that Cyclin O is involved in both ER stress and DNA damage response (DDR) we wondered whether there might be crosstalk between those two pathways. Using the S51A knockin fibroblasts we performed experiments using either γ-radiation to induce the DDR or thapsigargin to activate the ER stress pathway. Western blotting of Procaspase-8 cleavage served as an indicator of a Cyclin O downstream effector response[107] and CHOP expression levels were detected to monitor the ER stress pathway. In addition, cells were subjected to subcellular fractionation to obtain cytosol-enriched extracts for detection of Caspase-8 and nuclear extract for CHOP. In irradiated cells we observed, as expected, high levels of the p43 Caspase-8 cleavage product in WT and S51A knockin fibroblasts (Figure 5A). In addition CHOP levels were induced in an eIF2α-dependent manner due to the fact that no CHOP protein could be detected in the S51A knockin fibroblasts. When thapsigargin was used to induce ER stress (Figure 5B) CHOP levels increase in an eIF2α-dependent fashion, but no cleavage of Procaspase-8 could be detected. Taken together, we conclude that the ER stress pathway contributes to the DDR via CHOP activation but not vice versa: there is no activation of the DDR during ER stress, at keast not in our experimental system. This finding contradicts some reports claiming that Caspase-8 is activated during ER stress by CHOP-induced expression of DR5[93].

A

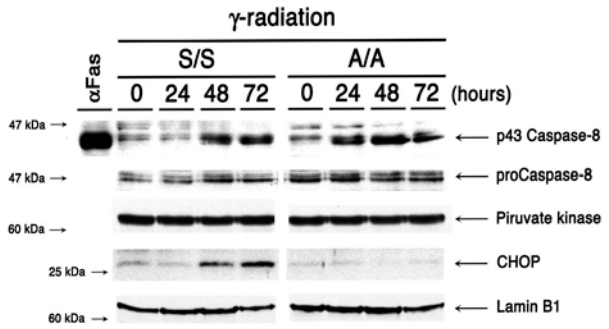

B

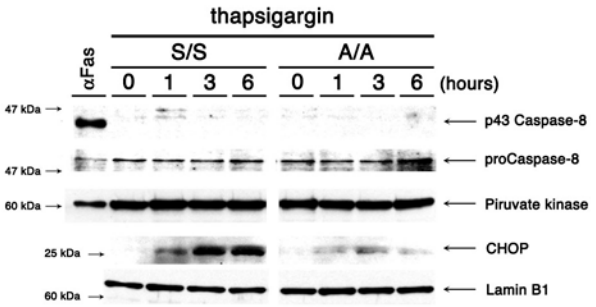

Figure 5. Crosstalk between ER stress pathway and the DNA damage response.
(A) Wild type eIF2α (S/S) and phosphorylation deficient eIF2α (A/A) fibroblasts were irradiated and harvested at the indicated time points. Prior to western blotting cells were fractionated and cytoplasmic extract served for detection of Caspase-8 and pyruvate kinase (loading control) whereas nuclear extracts were used for CHOP and Lamin B1 (loading control). In addition, thymocytes were stimulated with an agonistic α-Fas antibody which targets the Fas receptor of the TNF receptor superfamily. Activation of Fas leads to a robust induction of extrinsic apoptosis and therefore to a highly efficient cleavage of Procaspase-8 which served here as a positive control. **(B)** Thapsigargin was employed to induce ER stress and cells were processed in the same way as in (A).

1.6 Activation of p38 and JNK depends on Cyclin O

Based on earlier findings there was indication that Cyclin O was somehow related to SAPK signalling. We were curious to gain deeper insights into the involvement of Cyclin O in the SAPK signalling in response to ER stress response. Therefore, we used Cyclin O deficient fibroblasts to look at SAPK activation in response to thapsigargin treatment. We performed western blotting of phosphorylated p38 and JNK (isoforms p54 and p46) after thapsigargin treatment as shown in Figure 6. Phosphorylation of both p38 and JNK was clearly reduced in Cyclin O knockout fibroblasts in comparison to wild type cells. These results indicate that activation of SAPK signalling depends partially on Cyclin O.

1.7 MEKK4 is activated by ER stress in a Cyclin O-dependent manner

Recent evidence found in *drosophila*[122] showed that Cdk5 phosphorylates the MAP3K dMEKK1 (mammalian MEKK4) when cells undergo ER stress. This finding caught our attention because Cyclin O is known to form active complexes with Cdk1 and Cdk2[108] and in some *in vitro* conditions with Cdk5[123]. We therefore hypothesized that perhaps Cyclin O-Cdk5 complexes phosphorylating MEKK4 could constitute an apical step in Cyclin O-dependent SAPK signalling. It is well described in the literature that in mammals the apical MAP3K activated by ER stress is ASK1 (ref). However, in our model MEKK4 might be an additional MAP3K activated by ER stress. To proof this we incubated wild type and Cyclin O deficient fibroblasts with thapsigargin and

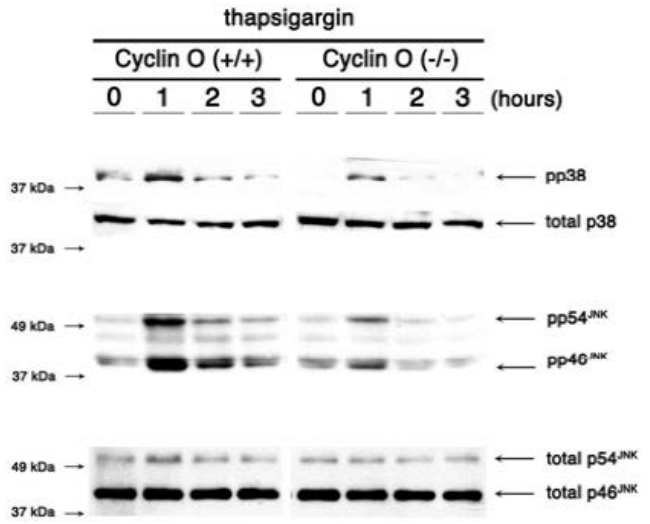

Figure 6. Activation of p38 and JNK depends on Cyclin O. Wild type and Cyclin O knockout fibroblasts were incubated with thapsigargin and collected at the indicated time points. Subsequently, lysates were probed with antibodies specific for the phosphorylated forms of p38 and JNK by western blotting.

immunoprecipitated endogenous MEKK4 in order to perform a kinase assay using MEK6 as a substrate (Figure 7). Phosphorylation of MEK6 was monitored by western blotting. At 2h MEKK4 is activated in a time-dependent manner in response to ER stress. This activation is detectable in wild type cells but not in Cyclin O -/- cells. We can therefore conclude that MEKK4 is activated by ER stress and that this activation depends on Cyclin O. These results indicate that there is an alternative pathway employing MEKK4 as the MAP3K in addition to the described ASK1-dependent pathway.

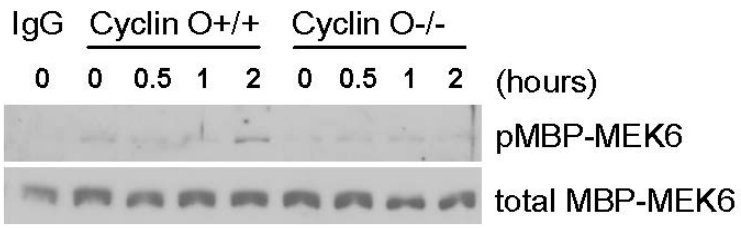

Figure 7. MEKK4 is activated by ER stress in a Cyclin O-dependent manner. Wild type and Cyclin O deficient fibroblasts were subjected to treatment with thapsigargin and harvested at the indicated time points to perform a kinase assay with immunoprecipitated endogenous MEKK4 and recombinant MBP-MEK6 as a substrate. Phosphorylated and total MBP-MEK6 were detected on a western blot.

1.8 Activation of p38 can occur in the absence of IRE1α in a Cyclin O-dependent fashion

To gather additional proof of this alternative pathway we asked the basic question whether activation of the SAPKs in response to ER stress can occur in the absence of IRE1α, the upstream kinase of ASK1, indicating that an alternative pathway exists that does not depend on the IRE1α/ASK1 axis. Fibroblasts deficient for IRE1α were subjected to thapsigargin treatment and western blotting of phosphorylated p38 revealed that IRE1α-/- cells are still capable of activating SAPK signalling indicative for the presence of an IRE1α independent pathway (Figure 8A). To demonstrate that Cyclin O is part of this pathway we employed two different short hairpin constructs to downregulate the Cyclin O protein levels in IRE1α-/- cells. As depicted in figure 8B, the additional decrease of p38 phosphorylation caused by reduced Cyclin O levels in IRE1α-/-

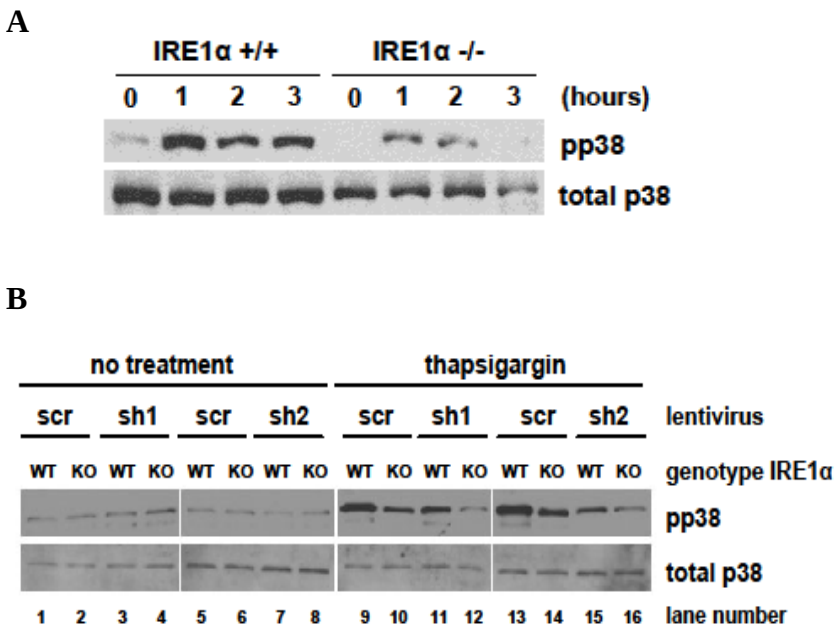

Figure 8. Activation of p38 can occur in absence of IRE1α in a Cyclin O-dependent fashion. (A) Wild type and IRE1α knockout fibroblasts were subjected to treatment with thapsigargin and processed for immunoblotting of p38 at the indicated time points. **(B)** The same cells as in A were infected with scrambled control (scr) or short hairpin RNAs (shRNAs) directed against Cyclin O (sh1 and sh2). Cells were either left untreated or were incubated for 1 hour with thapsigargin. Then, cells were harvested and analysed by western blotting for p38.

cells indicates that Cyclin O is part of the IRE1α independent pathway (compare lanes 10 with 12 and lanes 14 with 16).

1.9 Cyclin O colocalizes with MEKK4

Based on the results indicating Cyclin O-dependent activation of MEKK4 (Figure MEKK4/MEK6) we hypothezised that Cyclin O might control MEKK4 activation by direct interaction. As a first approach, we employed confocal immunofluorescence microscopy. RWP1 cells are derived from a human pancreas adenocarcinoma

and were used because they have a prominent ER in agreement with their secretory properties. RWP1 cells were stimulated with thapsigargin and double labelling of Cyclin O and MEKK4 revealed a clear colocalization with increased intensities after 3 hours of treatment (Figure 9), in agreement with increased levels of Cyclin O in response to thapsigargin.

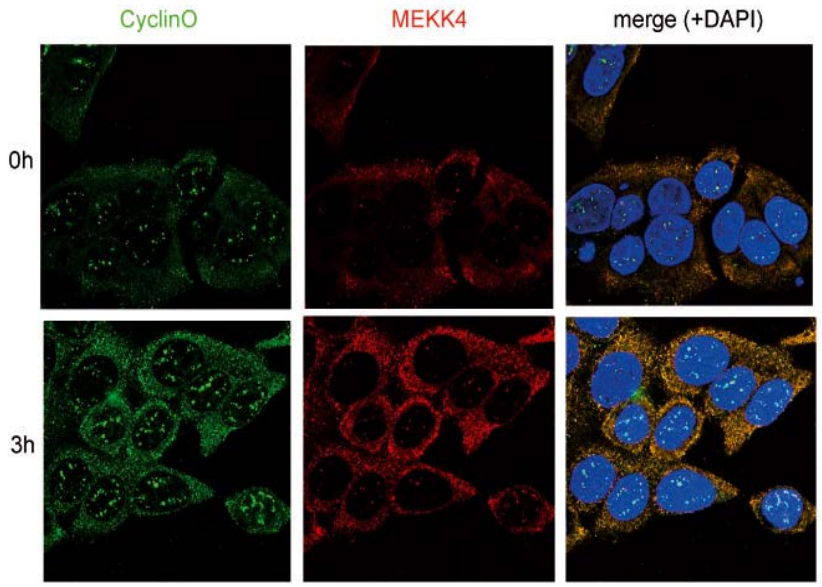

Figure 9. Cyclin O colocalizes with MEKK4. Confocal microscopy of thapsigargin-stimulated RWP1 cells. Fluorochrome labelled secondary antibodies were used to show colocalization of Cyclin O and MEKK4. In addition, merged pictures include DAPI staining to visualize the nucleus.

1.10 Cyclin O complexes phosphorylate MEKK4 through Cdk1 and Cdk2 *in vitro*

In order to check *in vitro* that Cyclin O complexes can phosphorylate MEKK4 we used lysates of HEK 293T cells transfected with plasmids expressing myc-tagged Cyclin O as a source of active Cyclin O complexes[108]. As substrates we used immunoprecipitated HA-tagged murine MEKK4 and Flag-tagged human MEKK4 from transiently transfected HEK293T cells. As a positive control for the Cyclin O complexes we used purified calf thymus Histone H1 as a substrate. First, we performed test experiments comparing wild type MEKK4 with a kinase death (KD) mutant of MEKK4 because the physiological activation of MEKK4 requires autophosphorylation[124] which would interfere with our assay. The test experiments clearly indicated that wild type MEKK4 is not a suitable substrate because there is a high degree of autophosphorylation as there is no difference between the negative and positive controls (Figure 10A). Human and mouse MEKK4KD were successfully phosphorylated by Cyclin O complexes (Figure 10B). To identify the Cdk responsible for the phosphorylation of MEKK4 together with Cyclin O we immunoprecipitated Cdk1, Cdk2, Cdk5, and Cyclin B1 (as a source for Cyclin B1-Cdk1 complexes) from myc-Cyclin O transiently transfected 293T extracts to carry out the kinase assay (Figure 11). We used Cyclin B1 antibodies to obtain Cdk1 complexes because our α-Cdk1 antibody did not work in HEK 293T cells. Cdk1 and Cdk2 were positively identified to phosphorylate MEKK4 (Figure 11A). We were not able to immunoprecipitate Cdk5 activity from HEK 293T

cells probably due to the low abundance of Cdk5 in these cells. With use of brain lysates we were able to establish a functional kinase assay for Cdk5 due to the high abundance of active complexes of Cdk5 in neuronal tissue (Figure 11B). Cdk5 immunoprecipitates were able to phosphorylate Histone H1 but not MEKK4. Therefore, we conclude that in mammals the kinase phosphorylating MEKK4 is not Cdk5 (as it is in *drosophila*) but Cdk1 and Cdk2.

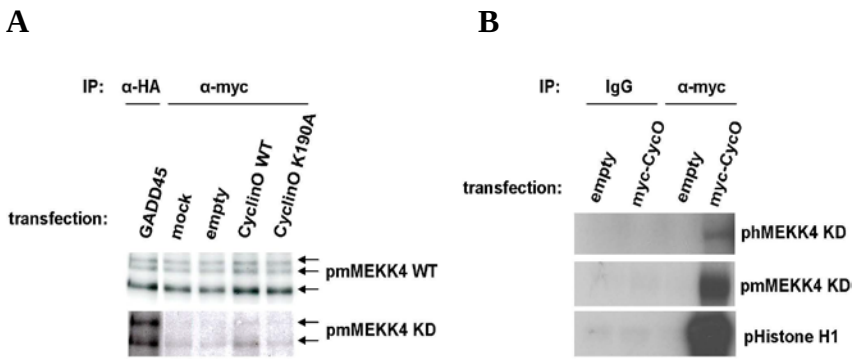

Figure 10. Cyclin O complexes phosphorylate MEKK4 *in vitro*. Depicted are autoradiograms of kinase assays carried out in presence of radioactive [γ-^{32}P]ATP. **(A)** Extracts of HEK 293T cells transfected with plasmids expressing myc-tagged Cyclin O were used to immunoprecipitate Cyclin O complexes. Subsequently, a kinase assay was performed with immunoprecipitated mMEKK4KD or mMEKK4WT as the substrate. GADD45 is a known activator of MEKK4 and served here as a positive control. Cyclin O K190A, a mutant that cannot form complexes with Cdks, was used as a negative control. **(B)** Human MEKK4KD, mouse MEKK4KD, or purified Histone H1 were used as a substrate for kinase assay.

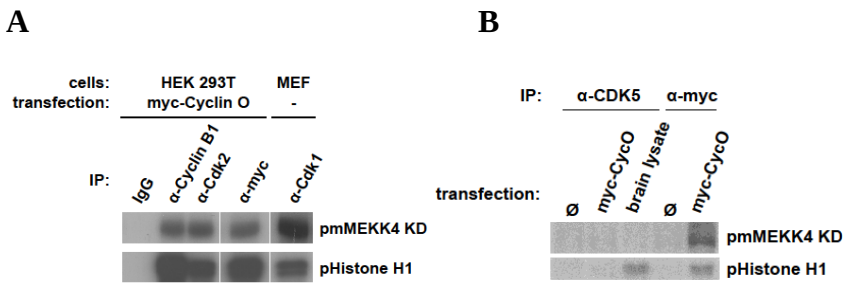

Figure 11. Cyclin O complexes phosphorylate MEKK4 through Cdk1 and Cdk2 *in vitro*. (A) Lysates of myc-Cyclin O transfected HEK 293T cells were immunoprecipitated for Cdk2 and Cyclin B1 and lysates of fibroblasts were used to immunoprecipitate Cdk1 to perform kinase assays. **(B)** Brain lysate was used in case of Cdk5 (right panel).

1.11 Mapping the phosphorylation site in MEKK4 with mass spectrometry

To gain further insight into the molecular mechanism of MEKK4 activation by Cyclin O complexes we employed mass spectrometry (MS) to identify phosphorylation sites in MEKK4. Similarly to the kinase assay mentioned above we immunoprecipitated separately Cyclin O complexes from Cyclin O transfected 293T lysates and MEKK4KD. As a negative control we used purified total IgG from normal mice with the same lysates. The immunoprecipitates were then mixed with murine myc-MEKK4 KD to perform the kinase reaction now using non-radioactive ATP. Subsequently, we gel-purified MEKK4 (Figure 12A) and sent the samples to the proteomics facility where they were digested with trypsin prior to MS analysis. The detected trypsin peptides covered in total 65.5 % of the MEKK4 sequence (61.8% in the sample phosphorylated with Cyclin O complexes and 59% in the control IP) which is a good

A

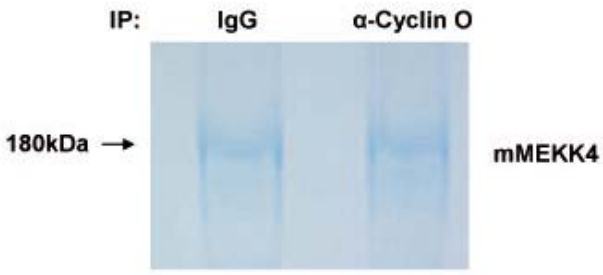

B

1 3 5 7 9 11 13
peptide sequence: MNTPSQSPHKDLGK

Modifications	IgG (control)	α-Cyclin O	phosphoRS Site Probabilities
none	1,489E8	1,622E8	
M1(Oxidation)	1,903E8	1,753E8	
S7(Phosp)	8,956E7	0,000E0	T(3): 0.0; S(5): 0.3; S(7): 99.7
M1(Oxidation); S5(Phosp)	8,538E7	1,445E8	T(3): 0.0; S(5): 50.0; S(7): 50.0
M1(Oxidation); T3(Phosp); S7(Phosp)	0,000E0	5,652E6	T(3): 99.9; S(5): 7.5; S(7): 92.6

Figure 12. Mapping the phosphorylation site in MEKK4 by mass spectrometry. (A) Coomassie blue staining of samples run in an acrylamide gel. The depicted bands were cut out and analysed by MS. **(B)** MS read-out of trypsin peptide MNTPSQSPHKDLGK. The first column depicts the types of posttranslational modifications that were detected; the second and third columns show the peak intensities/abundance of the peptide with the corresponding modifications; the fourth column indicates the confidence of the modification in percentage. Highlighted in red is the threonine that corresponds to Thr112 in the mouse MEKK4 sequence.

result taking into account that MEKK4 is quite a large protein (179kDa). As a potential phosphorylation motif we chose to look for serine-proline (SP) and threonine-proline (TP), which are the minimal consensus sequences for Cdk phosphorylation sites. In one trypsin peptide we found a single residue that was phosphorylated

in the Cyclin O sample but not in the IgG control sample and it corresponded to a TP motif: threonine 112 (Figure 12B).

2 Searching for new Cyclin O targets using microarray and phosphoproteomics technology

The fact that CHOP is activated upon DDR and under the control of Cyclin O during ER stress motivated us to look for gene targets of Cyclin O in response to γ-radiation in anticipation to find similar targets as in the proteomics experiments mentioned above. Also, previous evidence obtained in our laboratory suggested the need of *de novo* transcription and translation downstream of Cyclin O[107]. To identify genes whose expression changes as a consequence of Cyclin O signalling in response to γ-radiation, we used microarray technology. WEHI 7.2 cells stably transfected with short hairpin constructs either against Cyclin O or against GFP (control) were irradiated and processed for RNA extraction and subsequent microarray analysis six hours after irradiation. By comparing the gene expression profiles we found in total 159 genes changed in a Cyclin O dependent fashion of which 84 genes were upregulated and 75 genes downregulated. Of the downregulated ones we could identify 50 genes to be involved in RNA- and ribosome-related functions like rRNA and tRNA metabolic processes, ribosome/nucleoprotein biogenesis and assembly, and RNA processing. In addition, several genes could be identified as typical targets of the SAPK p38 which caught our attention because in the proteomics experiments we found indication for the involvement of SAPK in Cyclin O signalling too.

As a non-hypothesis driven approach to find downstream targets of Cyclin O we decided to use proteomics. Moreover, we chose to employ phosphoproteomics technology to find direct or indirect phosphorylation targets of Cyclin O. Cyclin O KO fibroblasts were infected with lentiviruses encoding for wild type Cyclin O or Cyclin O K190A which is a point mutant that cannot form complexes with Cdks. The cell extracts were digested with trypsin and one part of the sample was directly subjected to MS analysis whereas the other part was purified on TiO_2 columns for enrichment of phosphopeptides prior to MS analysis (Figure 13). This procedure allowed us to analyse both the total proteome and the phosphoproteome. We compared the wild type sample with the negative control sample (Cyclin O K190A) in order to find proteins and phosphoproteins that were differentially abundant. Only proteins with a statitistically significant p-value of $p<0.05$ were considered relevant. 106 proteins were overexpressed and 27 proteins were reduced in the total proteome (Figure 14A). The analysis of the phosphoproteome revealed 22 phosphorylated proteins of higher abundance and 31 proteins of lower abundance. (Figure 14B). In the total proteome an increase of many chaperones and other ER-resident proteins was detected which is consistent with our finding that Cyclin O plays a role in the ER stress response (Figure 15A and Table 1). Proteins that fall into the category of protein translation machinery including initiation factors, elongation factors, ribosomal proteins, and proteins involved in RNA metabolism were increased in general. Furthermore, metabolic

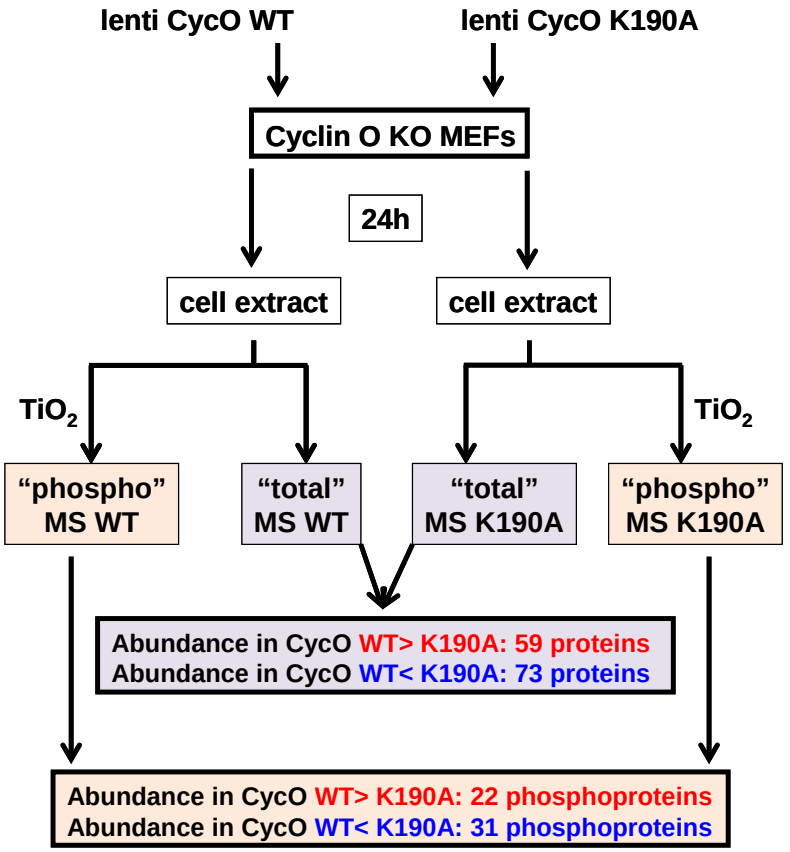

Figure 13. Scheme of the proteomics analysis performed to find new phosphorylation targets of Cyclin O.

enzymes, chromatin associated factors, and transcriptional regulators were also more expressed. In addition, we detected cytoskeletal proteins and integrin signalling related ones, most of which were lower expressed. Noteworthy, eIF2α and Cdk1 were overexpressed and PP1α was reduced. PP1α is the catalytic subunit of the phosphatase complex that dephosphorylates Ser51 of eIF2α. Cdk1 is one of the Cdks that forms active complexes with Cyclin O. Another protein that caught our attention is RAP1B as it is involved in SAPK signalling. The same functional groups of proteins of the

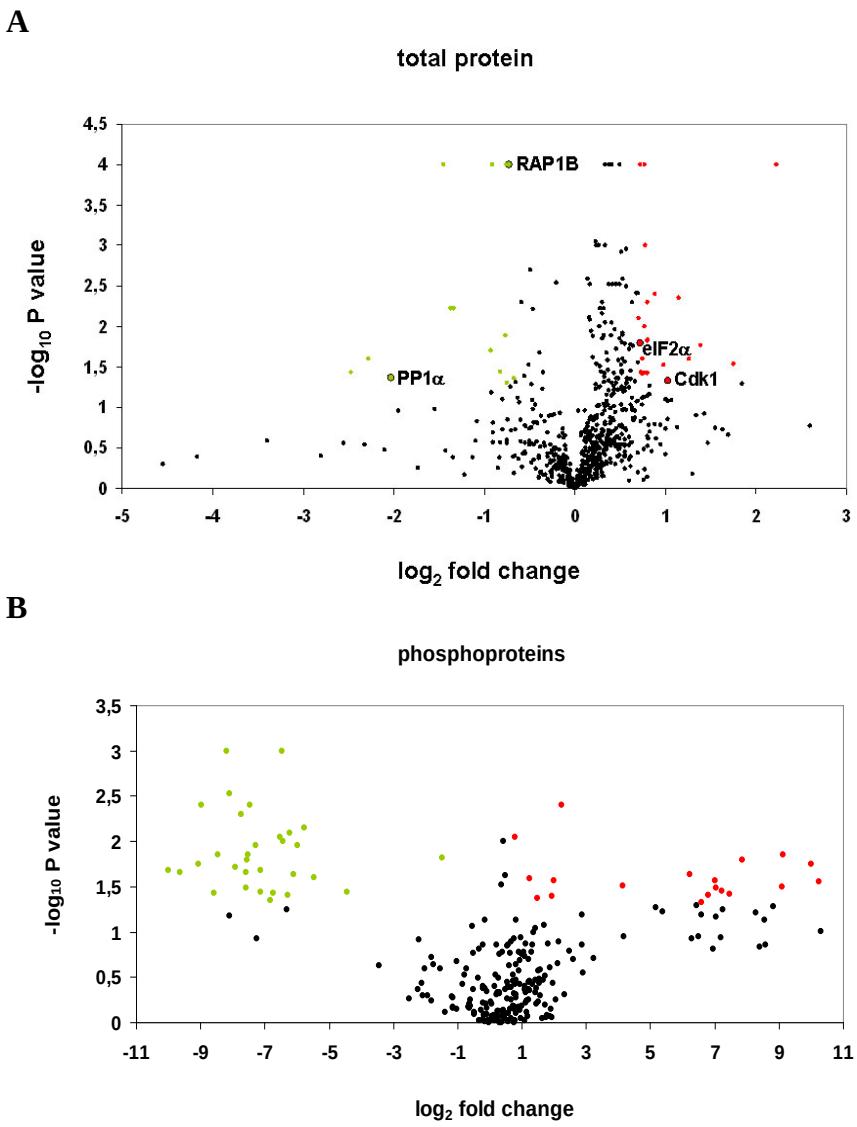

Figure 14. Searching for new Cyclin O phosphorylation targets using phosphoproteomics. Vulcano plots of total protein **(A)** and phosphoprotein **(B)**. Cyclin O -/- fibroblasts were infected with lentiviruses encoding wild type Cyclin O or a binding deficient mutant Cyclin O K190A as a negative control. Coloured data points are of statistical significance ($p<0.05$). For the total protein the threshold for the fold change has been set to $-0,7 > \log_2$ fold change$> 0,7$. For the phosphoprotein the threshold has been set to $-1 > \log_2$ fold change> 1.

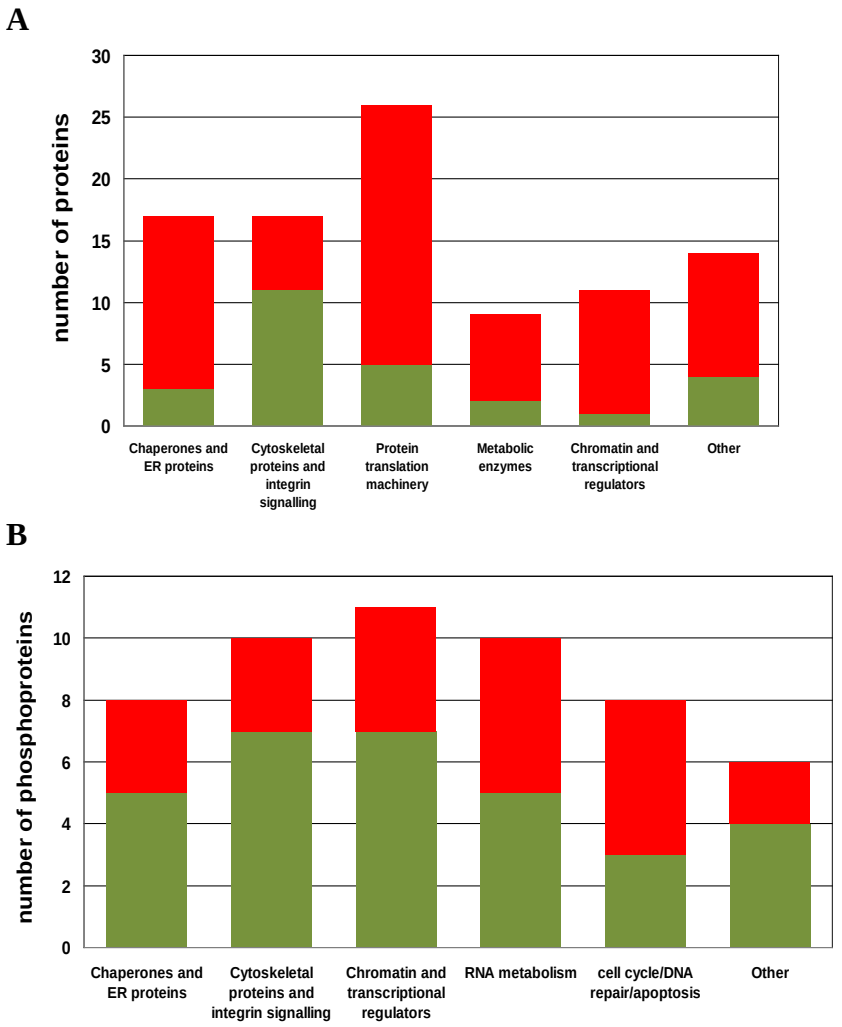

Figure 15. Searching for new Cyclin O phosphorylation targets using phosphoproteomics. Cyclin O knockout fibroblasts were infected with lentiviruses either expressing wild type Cyclin O or Cyclin O K190A (negative control). 36 hours post infection cells were lysed and the extracts were used either directly for MS analysis of the total proteome **(A)** or for enrichment of phosphoproteins to analyse the phosphoproteome **(B)**. Depicted in red are proteins of higher abundance and in green of lower abundance.

phosphoproteome (Figure 15B and Table 2). All chaperones and ER-proteins that were differentially phosphorylated are related to membrane-trafficking, which might suggest that Cyclin O regulates

changes in vesicle transport following ER stress. Most of the proteins in the category cell cycle/DNA repair/apoptosis are related to the cohesins. Cohesins are involved in the tethering of sister chromatids and play an important role in DNA damage induced cell cycle arrest.

Short name	protein	p value	log2 fold change
Chaperones and ER proteins:			
TXNL1	Thioredoxin-like protein 1	0,017	1,39
PPIase	Peptidyl-prolyl cis-trans isomerase-like 1	0,030	0,98
BIN1	Myc box-dependent-interacting protein 1	0,026	0,7
HSP 90-alpha	Heat shock protein HSP 90-alpha	0,013	0,58
HSP 84	Heat shock protein HSP 90-beta (Heat shock 84 kDa)	0,003	0,57
14-3-3 gamma	14-3-3 protein gamma	0,026	0,53
HSC70	Heat shock cognate 71 kDa protein	0,026	0,53
SERCA2	Sarcoplasmic/endoplasmic reticulum calcium ATPase 2	0,044	-0,67
Cytoskeletal proteins and integrin signalling:			
MAP-4	Microtubule-associated protein 4 (MAP-4)	0,038	0,8
4.1G	Band 4.1-like protein 2	0,015	0,8
VCL	Vinculin (Metavinculin)	0,008	0,71
ACTBL2	Beta-actin-like protein 2 (Kappa-actin)	0,044	0,7
MYL9	Myosin regulatory light polypeptide 9	0,019	0,64
TPM1	Tropomyosin alpha-1/3 chain	0,050	0,58
RAP1B	Ras-related protein Rap-1b	0,000	-0,73
CD29	Integrin beta-1 (CD antigen CD29)	0,000	-0,91
ACTG	Actin, cytoplasmic 2	0,006	-1,34
COF1	Cofilin-1 (Cofilin, non-muscle isoform)	0,000	-1,45
CTNA1	Catenin alpha-1	0,043	-2,03

Protein translation machinnery:			
eIF4A-1	Eukaryotic initiation factor 4A-I	0,000	2,23
EF-1-beta	Elongation factor 1-beta	0,004	0,88
eIF3gamma	Eukaryotic translation initiation factor 3 subunit gamma	0,038	0,77
eIF2alpha	Eukaryotic translation initiation factor 2 subunit alpha	0,016	0,72
SR-beta	Signal recognition particle receptor subunit beta	0,038	0,5
eIF3e	Eukaryotic translation initiation factor 3 subunit e	0,041	-0,56
eIF5A1	Eukaryotic translation initiation factor 5A-1	0,049	-0,65
Ribosomal proteins:			
L12	39S ribosomal protein L12, mitochondrial (L12mt) (MRP-L12)	0,010	0,77
L27	60S ribosomal protein L27	0,000	0,72
L17	60S ribosomal protein L17	0,021	0,52
L3	60S ribosomal protein L3 (J1 protein)	0,009	0,51
L23	60S ribosomal protein L23	0,042	0,5
Metabolic enzymes:			
CYB5	Cytochrome b5	0,039	0,75
QCR2	Cytochrome b-c1 complex subunit 2	0,003	0,68
NDUA8	NADH dehydrogenase [ubiquinone] 1 alpha subcomplex subunit 8	0,047	0,53
KAR	Estradiol 17-beta-dehydrogenase 12	0,000	0,52
CUBP	Adenosylhomocysteinase (AdoHcyase)	0,001	0,51
GANAB	Neutral alpha-glucosidase AB	0,013	0,5
PRDX6	Peroxiredoxin-6	0,030	-0,51
Fp	Succinate dehydrogenase [ubiquinone] flavoprotein subunit	0,036	-0,82
Chromatin and transcriptional regulators:			
HMG-1	High mobility group protein	0,025	1,26
NP1L1	Nucleosome assembly protein 1-like 1	0,005	0,8
H1.3	Histone H1.3	0,037	0,73
BAF57	SWI/SNF-related matrix-associated actin-dependent regulator of chromatin subfamily E member 1	0,011	0,63

HP1 gamma	Chromobox protein homolog 3	0,000	0,62
NSF1C	NSFL1 cofactor p47	0,013	0,57
THOC4	THO complex subunit 4	0,000	0,55
CN166	UPF0568 protein C14orf166 homolog	0,049	0,5
H3.3	Histone H3.3	0,025	-2,28
RNA metabolism:			
PAI-RBP1	Plasminogen activator inhibitor 1 RNA-binding protein	0,029	1,75
G3BP-1	Ras GTPase-activating protein-binding protein 1	0,003	0,62
FA-1	NHP2-like protein 1 (Fertilization antigen 1)	0,000	0,55
CTBP	Poly(rC)-binding protein 2 (Alpha-CP2)	0,035	0,53
hnRNP A/B	Heterogeneous nuclear ribonucleoprotein A/B	0,005	-0,59
PTB	Polypyrimidine tract-binding protein 1	0,000	-0,76
Others:			
CATB	Cathepsin B (EC 3.4.22.1) (Cathepsin B1)	0,004	1,15
Cdk1	Cyclin-dependent kinase 1 (CDK1)	0,047	1,03
BAP 32	Prohibitin (B-cell receptor-associated protein 32)	0,015	0,8
RTN4	Reticulon-4 (Neurite outgrowth inhibitor)	0,001	0,78
BUB3	Mitotic checkpoint protein BUB3	0,000	0,77
VIP36	Vesicular integral-membrane protein VIP36	0,025	0,75
PSA6	Proteasome subunit alpha type-6	0,044	0,67
CD147	Basigin (Basic immunoglobulin superfamily)	0,038	0,62
PKCI-1	Histidine triad nucleotide-binding protein 1	0,009	0,6
CO1A1	Collagen alpha-1(I) chain	0,001	0,52
NPM	Nucleophosmin	0,050	-0,75
GBB2	Guanine nucleotide-binding protein subunit beta-2	0,013	-0,77
PP-1A	Serine/threonine-protein phosphatase PP1-alpha	0,020	-0,93
MPCP	Phosphate carrier protein, mitochondrial	0,006	-1,37

Table 1. Searching for new Cyclin O targets using proteomics. List of proteins with increased (red) or decreased (green) expression. The threshold is set to $-0,5 > \log_2$ fold change $< 0,5$.

short name	protein	p value	log2 fold change
Chaperones and ER proteins:			
MYOF	Myoferlin (Fer-1-like protein 3)	0,016	7,8443
Toca-1	Formin-binding protein 1-like	0,035	7,2336
SDPR	Serum deprivation-response protein (Cavin-2)	0,026	1,2248
WIPI-2	WD repeat domain phosphoinositide-interacting protein 2	0,001	-6,4695
SPTB2	Spectrin beta chain, non-erythrocytic 1 (Beta-II spectrin)	0,045	-6,8204
FAM21	WASH complex subunit FAM21	0,016	-7,5687
NRBP	Nuclear receptor-binding protein	0,001	-8,2016
Rab-13	Ras-related protein Rab-12	0,004	-8,9666
Cytoskeletal proteins and integrin signalling:			
Af-6	Afadin (Protein Af-6)	0,038	7,4751
NEXN	Nexilin (F-actin-binding protein)	0,042	1,4674
PARD-3	Partitioning defective 3 homolog	0,025	-5,4818
MAP-1A	Microtubule-associated protein 1A	0,011	-5,9843
EMAP-3	Echinoderm microtubule-associated protein-like 3	0,039	-6,2769
TP alpha/zeta	Lamina-associated polypeptide 2, isoforms alpha/zeta	0,037	-6,7251
Af-6	Afadin	0,011	-7,2745
VINC	Vinculin (Metavinculin)	0,033	-7,5807
4.1B	Band 4.1-like protein 3 (4.1B)	0,005	-7,7485
Chromatin and transcriptional regulators:			
MBB1A	Myb-binding protein 1A	0,014	9,136
BAF170	SWI/SNF complex subunit SMARCC2 (BRG1-associated factor 170)	0,027	7,008
HMGA1	High mobility group protein HMG-I/HMG-Y	0,04	1,9479
ZFH-3	Zinc finger homeobox protein 3	0,007	-5,7724
HMGA2	High mobility group protein HMGI-C	0,008	-6,2206
mH2A1	Core histone macro-H2A.1	0,01	-6,4486
UBP2L	Ubiquitin-associated protein 2-like	0,009	-6,5338
TFE3	Transcription factor E3	0,004	-7,4519
TFIIF-alpha	General transcription factor IIF subunit 1 (Transcription initiation factor IIF subunit alpha) (TFIIF-alpha)	0,014	-8,4643
Hic-5	Transforming growth factor beta-1-induced transcript 1	0,021	-9,9962

RNA metabolism:			
PRRC2A	Protein PRRC2A (HLA-B-associated transcript 2)	0,032	9,1005
mDEAD2	ATP-dependent RNA helicase DDX3Y	0,039	6,8106
PUM2	Pumilio homolog 2	0,047	6,5932
Acinus	Apoptotic chromatin condensation inducer in the nucleus	0,031	4,1264
SFR19	Splicing factor, arginine/serine-rich 19	0,027	1,984
PRC2A	Protein PRRC2A (HLA-B-associated transcript 2)	0,023	-6,1066
SRRM2	Serine/arginine repetitive matrix protein 2	0,022	-7,5814
PAI-RBP1	Plasminogen activator inhibitor 1 RNA-binding protein	0,019	-7,9061
SNIP1	Smad nuclear-interacting protein 1	0,018	-9,0542
TCOF	Treacle protein (Treacher Collins syndrome protein homolog)	0,022	-9,6466
Cell cycle and DNA repair:			
CHAP1	Chromosome alignment-maintaining phosphoprotein 1	0,018	10,0078
PDS5B	Sister chromatid cohesion protein PDS5 homolog B	0,033	7,0366
NIPBL	Nipped-B-like protein (Delangin homolog) (SCC2 homolog)	0,023	6,2155
SFR1	Swi5-dependent recombination DNA repair protein 1	0,004	2,2461
TERF2	Telomeric repeat-binding factor 2	0,015	-1,4899
CtIP	DNA endonuclease RBBP8	0,003	-8,0982
mNIPA	Nuclear-interacting partner of ALK	0,037	-8,5767
Other:			
TOM70	Mitochondrial import receptor subunit TOM70	0,009	0,7757
JC7	Nuclear ubiquitous casein and cyclin-dependent kinase	0,036	-4,438
FAM122A	Protein FAM122A	0,021	-7,1194
MYADM	Myeloid-associated differentiation marker	0,036	-7,138
SAMD1	Atherin (Sterile alpha motif domain-containing protein 1)	0,014	-7,5364

Table 2. Searching for new Cyclin O phosphorylation targets using phoshphoproteomics. List of phosphorylated proteins with increased (red) or decreased (green) abundance. The threshold is set to $-0,5 > \log_2$ fold change $< 0,5$.

3 Characterization of Cyclin O knockout mice

Evidence collected in our group using mainly cell culture based methods showed that Cyclin O is involved in the DDR and ER stress responses. However, an important question for us is what role those cellular events play in the more systemic context of a whole organism. Therefore, the characterization of the Cyclin O knockout mice is of great interest to us. The Cyclin O gene was targeted by homologous recombination (HR) in ES cells by the KOMP (Knock-Out Mouse Project). The Cyclin O ORF (including introns 1 and 2) was replaced by the *LacZ* coding sequence preserving the Cyclin O regulatory elements of the promoter (Figure 17). The neomycin resistance cassette in the insert is flanked by loxP sequences allowing for its removal by interbreeding with transgenic mice expressing the Cre recombinase. We worked mainly with the mice containing the *Neo* cassette in the targeted locus. However, we also confirmed some of the phenotypes using mice carrying the *Neo*-deleted allele.

3.1 Cyclin O knockout mice die of hydrocephalus within the first month of postnatal life

Cyclin O KO mice are viable and born at the predicted Mendelian frequencies (data not shown), indicating that the complete loss of Cyclin O does not lead to embryonic lethality. However, Cyclin O KO females were sterile and the males subfertile (producing only 0-3 pups per litter) with evidences of hypogonadism and defects in gametogenesis (data not shown). Cyclin O KO mice were maintained on a C57Bl/6J genetic background. In addition, the

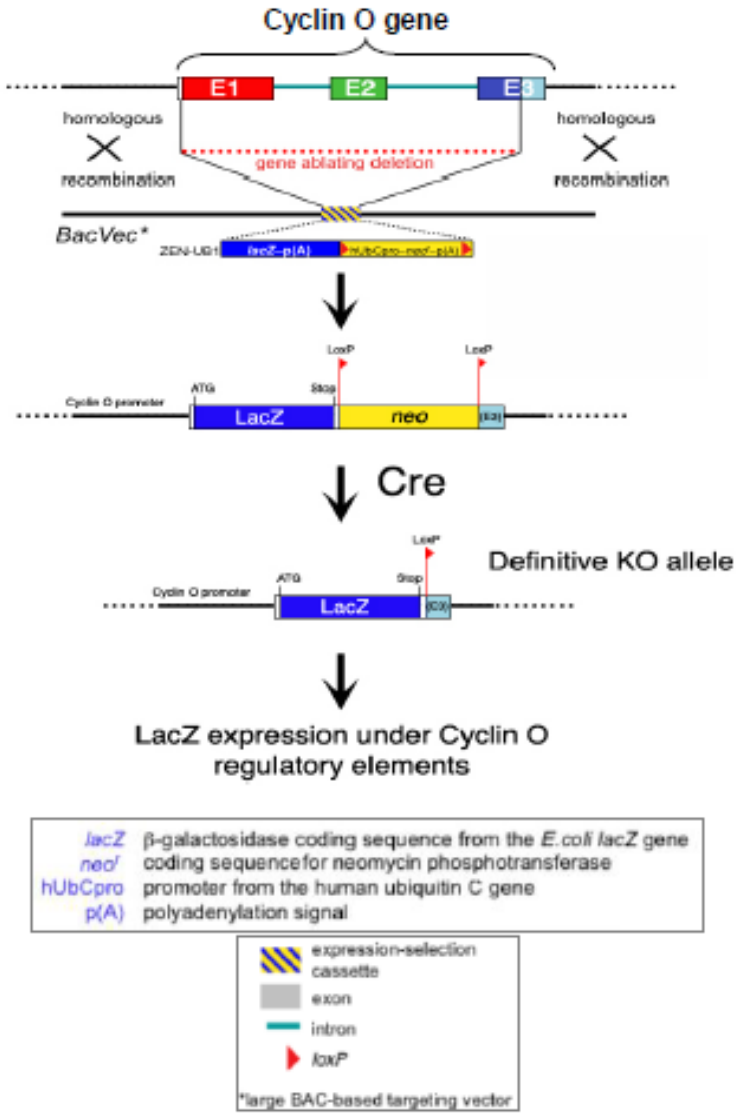

Figure 17. Targeting strategy of the Cyclin O gene in ES cells. Most of the 1st, the 2nd and part of the 3rd exons of the Cyclin O gene were replaced by a *LacZ*-neomycin cassette by HR in ES cells. The targeted gene preserves the ATG and promoter of the Cyclin O gene permitting the expression of *LacZ* under the regulatory elements of the Cyclin O promoter. The floxed neomycin cassette contains a promoter that allows to the constitutive expression of the selectable marker

hydrocephalus phenotype has been confirmed using outbreed mice (CD1 x C57Bl/6J) to rule out any effect due to the genetic background used. The C57Bl/6J genetic background develops spontaneously hydrocephalus at a frequency of 0.029% (according to JAX® NOTES Issue 490, Summer 2003- Hydrocephalus in Laboratory mice).

Around 80% of Cyclin O KO mice die or become moribund because of the development of hydrocephalus within the first month of postnatal life (Figure 18). We also observed the progressive dead of Cyclin O heterozygous (HET) mice during the first year of life because of an increased incidence of ulcerative idiopathic dermatitis most likely as a consequence of an autoimmune reaction. The C57Bl/6J genetic background develops spontaneous dermatitis at a lower frequency than observed in Cyclin O HET mice (Csiza CK, 1976). Cyclin O HET mice seem to have a shorter half life than the WT controls, although it did not reach statistical significance.

3.2 Hematological analysis

Preliminary results from analyzing blood samples of Cyclin O knockout mice indicated that there are differences in blood composition. Therefore, we set out to characterize the erythropoietic compartment of our mice. Freshly obtained blood was analysed in regard to its content of white cells, red cells, and platelets. We tentatively grouped all mice in two age categories: young (less than 300 days old) and old (more than 300 days old). Cell counts of total white blood cells, lymphocytes, granulocytes, and monocytes did not show any statistically significant difference (data not shown).

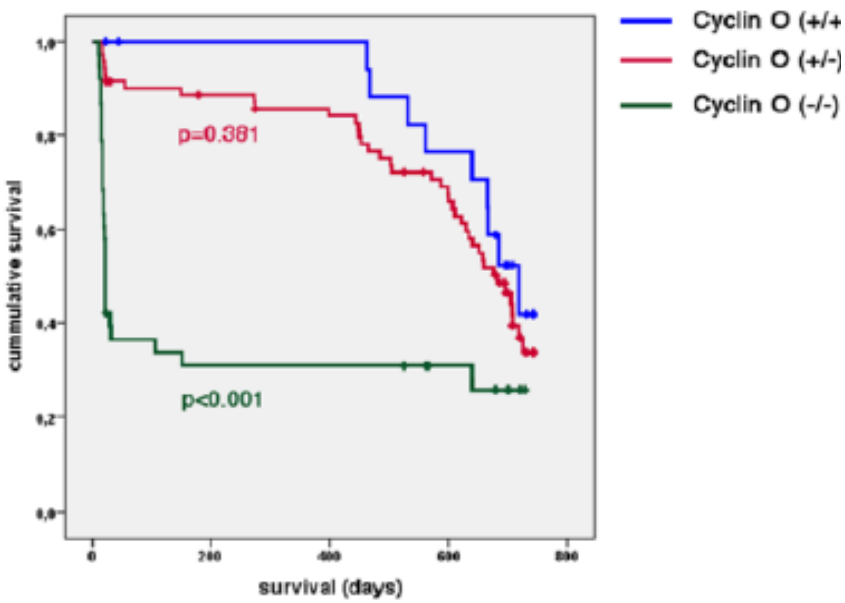

Figure 18. – Kaplan-Meier survival curve of Cyclin O WT (+/+), HET (+/-) and KO (-/-) mice.

Analysis of platelets revealed no defect as numbers, volume and shape of platelets were similar in all mice. We also performed FACS analysis to measure the percentage of proplatelets (precursors of platelets) in the blood without detecting any difference between genotypes (data not shown).

3.3 Cyclin O knockout mice are anemic

The number of RBC was lower in young homozygous mice (Figure 19). In addition, the reduction in hemoglobin concentration and hematocrit (fraction of whole blood volume that consists of RBC) in these mice was statistically significant. The parameters which describe the RBC were within normal range in all genotypes and

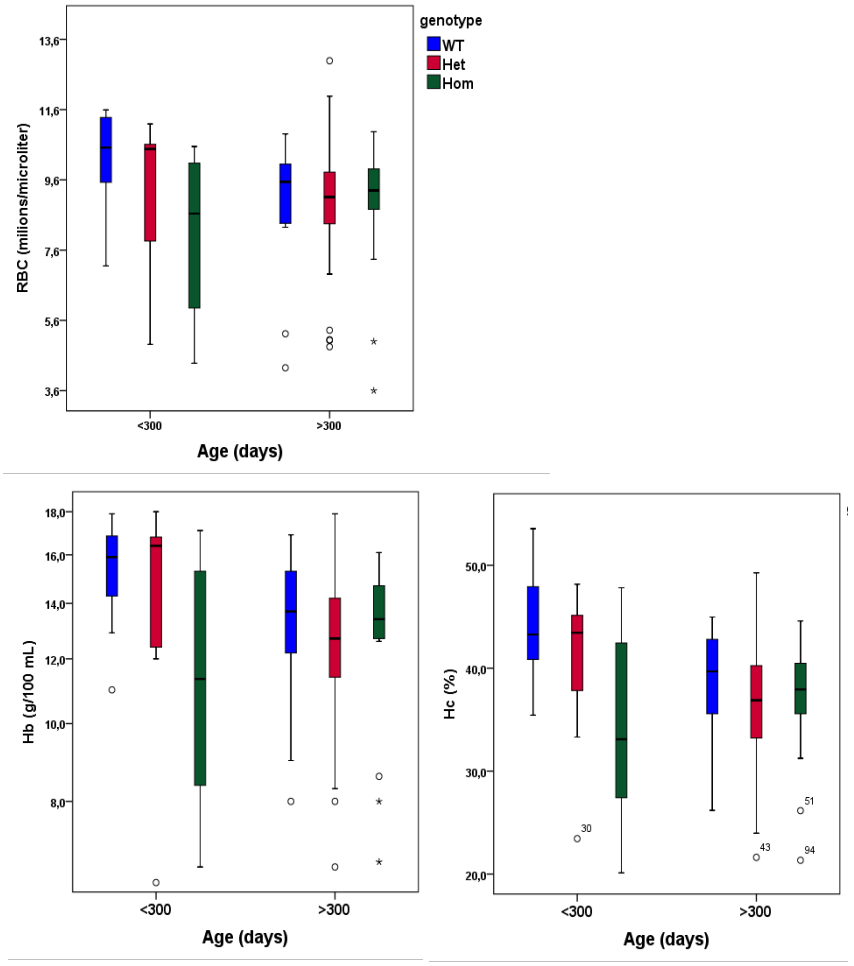

Figure 19. Young homozygous Cyclin O knockout mice suffer from anemia. Analysis of RBC was carried out by cytometric analysis of blood samples taken from wild type, heterozygous, and homozygous Cyclin O knockout mice. Depicted are total erythrocyte count (RBC), hemoglobin concentration (Hb), and Hematocrit (Hc).

age groups: no difference in amount and concentration of hemoglobin per cell was detectable, and the mean volume of the RBC was in the normal range (data not shown). Therefore, the anemic phenotype, evident by reduced hemoglobin concentration and hematocrit, is most likely due to the reduced numbers of RBC.

As a first approach to explain the anemic phenotype, under the assumption that erythropoiesis might be defective, we measured the frequency of reticulocytes as percentage of total RBC in the blood using FACS analysis in combination with the dye thiazole orange (Figure 20). No difference in the occurrence of reticulocytes and

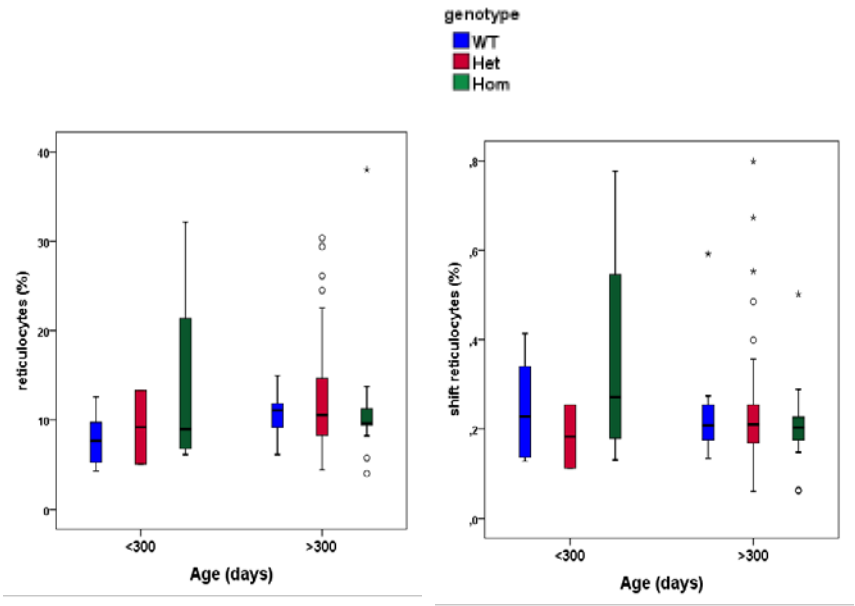

Figure 20. Abundance of reticulocytes and shift cells is unaltered in Cyclin O knockout mice. FACS analysis of thiazole orange stained RBC revealed the frequencies of reticulocytes and shift cells (reticulocytes that are 1-3 days old).

shift cells (reticulocytes that are 1-3 days old) was evident. We concluded that if erythropoiesis is aberrant, then the defect must take place at earlier stages of RBC development which requires further analysis of the erythropoiesis. Subsequently, we isolated bone marrow cells from femur and tibia to perform FACS analysis using development markers for the erythropoietic lineage. As a

general marker for RBC precursors we used Ter119 which is expressed already at early stages in proerythroblasts and remains present throughout the whole development until the terminally differentiated erythrocytes. As a second marker we used CD71 which is expressed early and progressively decreases during erythroblast development and vanishes once enucleation occurs[125]. There are four stages of erythropoiesis that can be distinguished with the Ter119/CD71 double staining[126]: stage I proerythroblast ($Ter119^{low}$ $CD71^{high}$), stage II basophilic erythroblasts ($Ter119^{high}$ $CD71^{high}$), stage III late basophilic and polychromatophilic erythroblasts ($Ter119^{high}$ $CD71^{low}$), and stage IV orthochromatophilic erythroblasts ($Ter119^{high}$ $CD71^{-}$). The percentage of $Ter119^{+}$ cells was reduced in the bone marrow of heterozygous knockout mice and to a greater degree in homozygous mice (Figure 21). A closer look at the differentiation stages revealed that early stages I and II were unaffected whereas stage III and to a larger extend stage IV showed a reduced percentage of $Ter119^{high}$ $CD71^{low}$ cells and $Ter119^{high}$ $CD71^{-}$ cells respectively. This defect in erythropoiesis may explain in part the anemic phenotype but the differences are rather small compared to other anemic mouse models. A feature commonly observed with anemia is that the organism tries to compensate the lack of RBC in the blood by inducing erythropoietic development outside of the bone marrow[127]ref?. This phenomena is called extramedullary erythropoiesis and it happens to a small extend under normal conditions as progenitors can escape at low numbers from the bone marrow. Extramedullary erythropoiesis is typically observed in

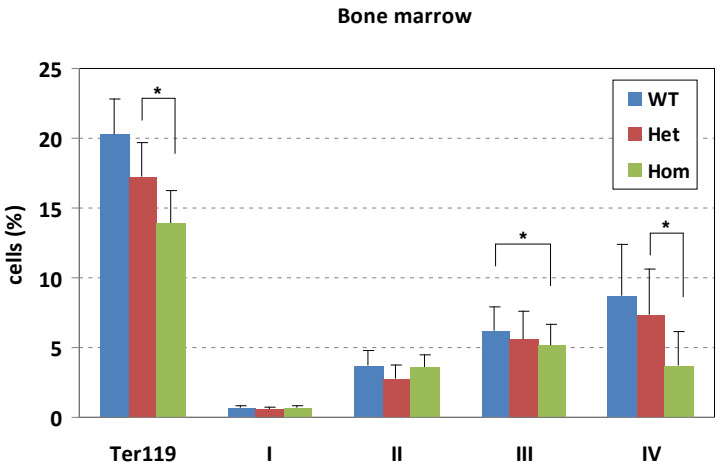

Figure 21. Erythropoiesis is reduced at late stages of erythroblast development in the bone marrow of Cyclin O knockout mice. Bone marrow cells of wild type and Cyclin O knockout mice were stained with antibodies against Ter119 and CD71 prior to analysis by FACS. Shown are, as percentage of total bone marrow cells, $Ter119^{+}$ cells and development stages I-IV. Stage I: proerythroblast $Ter119^{low}$ $CD71^{high}$, stage II: basophilic erythroblasts $Ter119^{high}$ $CD71^{high}$, stage III: late basophilic and polychromatophilic erythroblasts $Ter119^{high}$ $CD71^{low}$, stage IV: orthochromatophilic erythroblasts $Ter119^{high}$ $CD71^{-}$.

spleen and/or liver. Our analysis of splenocytes using Ter119/CD71 double staining shows an increase of $Ter119^{+}$ cells in general and specifically at development stage II (Figure 22). To confirm the FACS analysis we looked at histological sections of spleens from mice injected with BrdU. Sections were stained with antibodies against Ter119 and BrdU to detect proliferating erythrocyte precursors (Figure 23). Homozygous knockout mice showed an increased abundance of proliferating $Ter119^{+}$ cells which is in accordance with the FACS data.

A

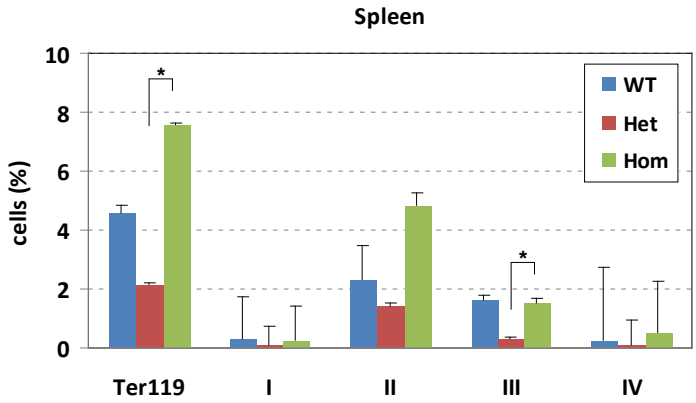

B

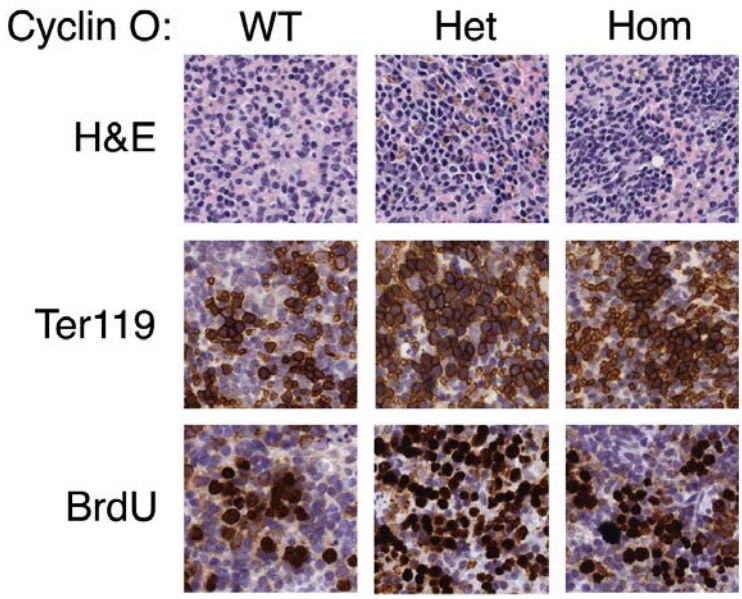

Figure 22. Extramedullary erythropoiesis in the spleen of Cyclin O knockout mice. **A** FACS analysis of splenocytes taken from wild type and Cyclin O knockout mice and stained with antibodies for Ter119 and CD71. **B** Mice were injected with BrdU 2h prior to necropsy. Sections of spleens were stained with hematoxilin/eosin (H&E) and antibodies against Ter119 and BrdU.

DISCUSSION

DISCUSSION

1. ER stress-induced apoptosis in dividing and quiescent cells depends on Cyclin O

Cyclin O has been demonstrated to be required for irradiation- or glucocorticoid-induced apoptosis in lymphoid cells[108]. It was therefore an obvious question for us to find out whether Cyclin O is also required for apoptosis induced by ER stress. Using two different cell types, immortalized fibroblasts and thymocytes, both deriving from knockout mice, we were able to show a clear reduction of apoptosis associated with Cyclin O deficiency. An important difference between the two cell types used is that the fibroblasts are cells actively dividing whereas thymocytes are a (naturally occurring) synchronized population of quiescent cells. The main problem in studying Cdks in apoptosis is their high activity present in dividing cells due to their role in the cell cycle which makes it difficult to distinguish Cdk activity related to the cell cycle from additional activation as a consequence of apoptosis signalling. For that reason, thymocytes resting in G0 are typically used to study the role of Cdks in apoptosis with the advantage that no Cdk activity is present in quiescent cells and any activation of Cdk induced by an apoptotic stimulus must therefore be part of apoptotic signalling. Several independent laboratories reported that Cdk2 is activated during apoptosis of quiescent cells[106,128]. Our experiments indicate that Cyclin O is necessary for apoptosis in dividing and in resting cells (results Figure 1). Futhermore we showed in dividing cells that Cyclin O acts in concert with Cdks.

Although we did not prove directly in resting thymocytes that Cyclin O exerts its function through Cdks we carried out kinase assays in a thymocyte derived cell linage (results Figure 2) which suggests that the same mechanism could occur in quiescent cells. Future experiments might involve a kinase assay carried out with freshly isolated thymocytes incubated with thapsigargin.

2. Biochemical positioning and signalling function of Cyclin O

We know that that Cyclin O is involved in two different apoptotic pathways: in the DNA damage[108] and in the ER stress pathway. The CHOP gene was initially identified in a search for genes induced by genotoxic stress, such as UV light, γ-radiation and alkylating agents such as methyl methanesulfonate (MMS)[129]. Induction of CHOP was reduced in Cyclin O deficient cells after treatment with γ-radiation as well as with thapsigargin. The induction of CHOP with both types of stimuli is consistent with the literature. CHOP, originally discovered in response to DNA damage, turned out to play a pivotal role as proapoptotic factor in the integrated stress response. From our experiments we can conclude that CHOP is a common target gene of Cyclin O in both DNA damage and ER stress pathways. Previous findings in our group positioned Cyclin O upstream of PERK in ER stress signalling. However, when we used cell lines deficient in signalling downstream of PERK, eIF2α S51A knockin and CHOP knockout fibroblasts, we saw a reduction in Cyclin O expression. We conclude that there is a positive feedback loop inducing Cyclin O expression downstream of CHOP (Figure 1). The

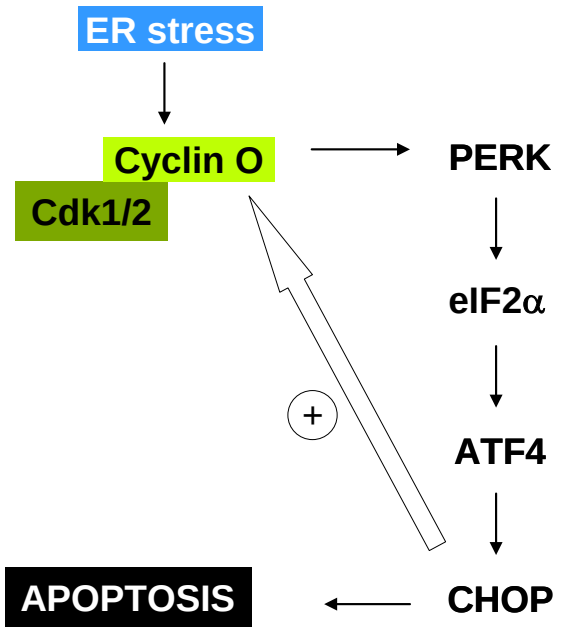

Figure 1. Positive feedback loop in Cyclin O signalling. Cyclin O activates the PERK/eIF2α/ATF4 axis leading to the expression of CHOP, which in turn increases the expression if Cyclin O.

PERK/eIF2α/ATF4 axis is the main ER stress pathway of the different UPR branches in terms of inducing apoptosis[13,130] and previous findings in our group showed that Cyclin O is not involved in neither ATF6 signalling nor IRE1α-mediated processing of XBP1 - both processes intend to restore homeostasis rather than to induce cell death. All these facts point towards Cyclin O having the function of inducing apoptosis rather than facilitating damage control or even survival in the UPR, and the aforementioned positive feedback loop might therefore be part of the cell's terminal commitment to die. Cyclin O knockout cells were clearly reduced in their capacity to undergo cell death which supports strongly the proapototic role of Cyclin O. Furthermore, we demonstrated clearly

that Cyclin O is responsible, in addition to IRE1α, for activation of p38. Phosphorylation of p38 has been described to be proapoptotic since phosphorylation of CHOP by p38 maximizes cell death[77,78]. Moreover, phosphorylation of JNK depends on Cyclin O too and JNK has extensively been described in regard to its proapoptotic role[61,65,66]. JNK2 on the other hand appears at least in one report[69] as a prosurvival protein. In our experiment (results Figure 10) JNK2p54 is phosphorylated in dependence of Cyclin O with the same kinetics as JNK1p46. A possible explanation is that at these time points the cell might not yet be fully commited to undergo cell death and still keeps prosurvival options open to allow for adaptation. If this was the case we could say that Cyclin O is not exclusively a proapoptotic factor as the phosphorylation of JNK2p54 depends on Cyclin O.

As mentioned in the introduction (chapter 4.2) ATF4 together with CHOP induce apoptosis by activating protein synthesis which leads to ROS production and subsequently to cell death (introduction Figure 11). A key step to allow resumption of protein synthesis is the dephosphorylation of eIF2α by GADD34. What is not taken into account with this model is that sustained PERK phosphorylation promotes apoptosis[13,14]. Phosphorylated PERK would counteract the GADD34 mediated dephosphorylation of eIF2α and it is not clear how sustained PERK phosphorylation and concurring dephosphorylation of eIF2α are connected with each other. One explanation may be that the Cyclin O mediated action of PERK changes during time. At the beginning Cyclin O activates PERK to

exert its immediate early response, phosphorylation of eIF2α and Nrf2, which aims towards survival rather than apoptosis (Figure 2). At later time points phosphorylated PERK does not activate the survival pathways anymore but apoptotic pathways instead. The later phase may involve substrates for PERK that have not been discovered yet. Future experiments to address this question might involve immunoprecipitation of PERK and subsequent MS analysis from thapsigargin treated cells at late time points.

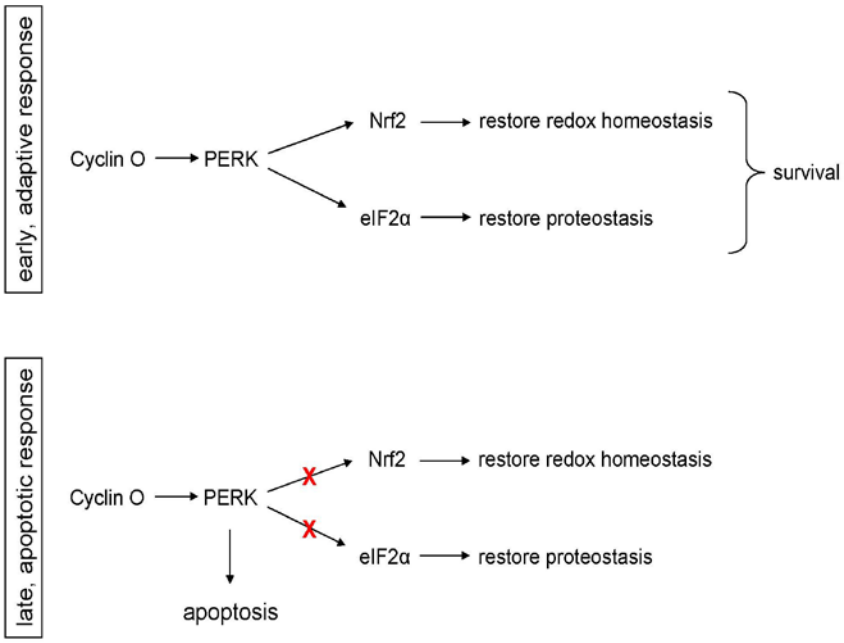

Figure 2. Early and late response. Change of actions downstream of Cyclin O and PERK. See text for details.

An open question that remains to be answered is what downstream events in Cyclin O dependent apoptosis signalling will finally lead to executioner caspase activation. Although we did not directly address this question we can hypothesize, based on the literature

and on our findings that Cyclin O is responsible for activation of JNK, p38 and CHOP, that several pathways are possible. As our experiments showed, ER stress leads to Cyclin O-mediated activation of CHOP through the PERK/eIF2α/ATF4 axis and induces MAPK signalling via MEKK4 leading to activation of p38 and JNK (Figure 3). It is reasonable to assume that at the apoptotic phase of ER stress CHOP-induced expression of GADD34 leads to dephosporylation of eIF2α although proteostasis has not been resumed yet, which results in the production of ROS[104] (see introduction chapter 4.2 and introduction Figure 11). ROS is known to activate ASK1 and subsequently JNK[81] which may constitute in our model an amplification of JNK activation in addition to the Cyclin O/MEKK4-mediated pathway. Another well known target gene of CHOP that is most likely induced is ERO1α[131] which is known to induce Ca^{2+} release from the ER by activating the inositol 1,4,5-triphosphate receptor (IP3R), which in return activates CaMKII. Sustained CaMKII activation has been described to promote JNK signalling by activating ASK1[81] and cold thus represent in our model an additional amplification of JNK activation. Furthermore, ROS induces MAPK signalling leading to activation of p38 which in turn phosphorylates CHOP to increase its activity and we have proven that CHOP induces expression of Cyclin O. Taken together, we hypothesize that Cyclin O-mediated actions lead to amplification of CHOP-dependent signalling which results in increased ROS production and sustained activation of JNK, p38 and CHOP. If the stress is unresolved the cell eventually

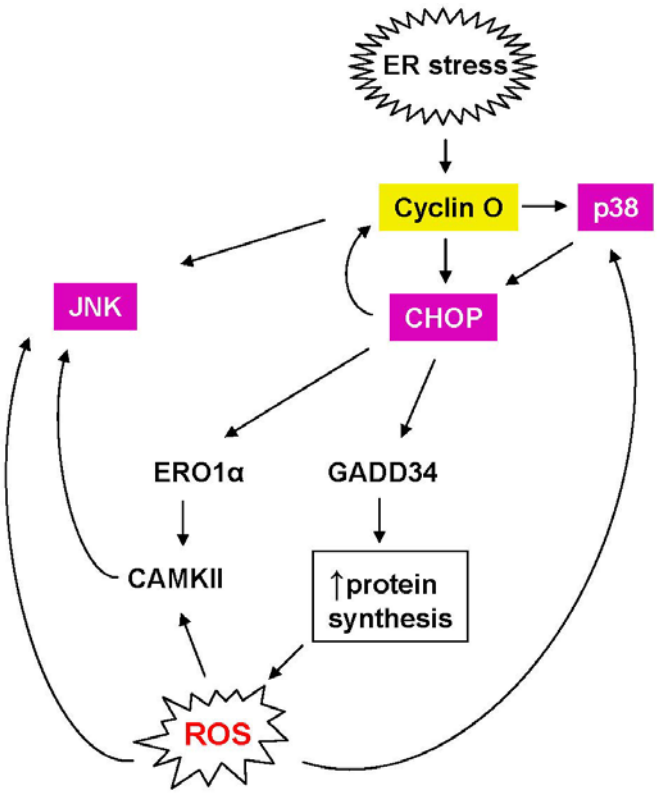

Figure 3. Amplification of Cyclin O-downstream signalling through ROS. Cyclin O-mediated activation of JNK, CHOP, and p38 leads to increased ROS production, which in turn further activates p38 and JNK.

undergoes the final stage in apoptotic signalling to activate caspases (Figure 4). A described phosphorylation substrate of JNK in ER stress is the proapoptotic BH3-only protein Bim[132] which, once activated, inhibits the antiapoptotic actions of Bcl-2. Other proapoptotic BH3-only proteins like DP5 and PUMA have been described to be upregulated in a JNK-dependent fashion[133]. CHOP downregulates the expression of Bcl-2, sensitizing cells to apoptosis[134], and induces expression of proapoptotic BAX[135]. In addition p38 phosporylates BAX directly leading to its

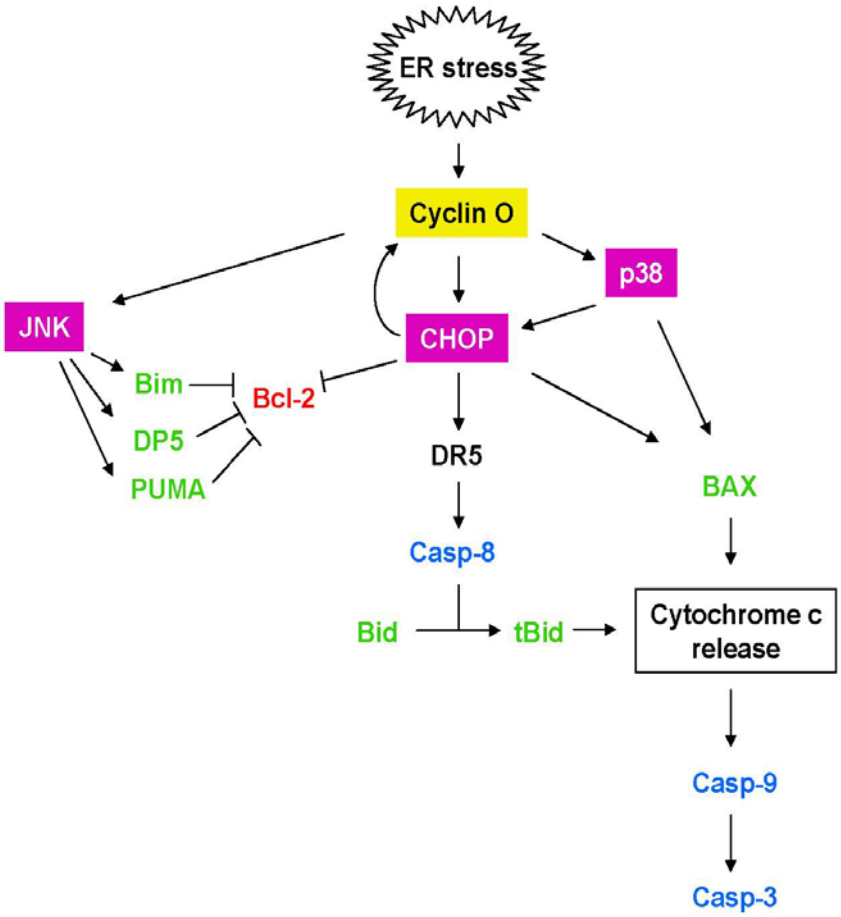

Figure 4. Cyclin O-mediated activation of caspases. At late apoptotic events JNK activates proapoptotic BH3-only proteins to inhibit Bcl-2. CHOP supresses Bcl-2 expression and induces DR5 and subsequently Casp-8-mediated cleavage of Bid. In addition, CHOP induces expression of BAX. p38 phosphorylates CHOP to enhance its activity and activates BAX. tBid and BAX translocate to the mitochondrion causing Cytochrome c release and apoptosome formation which finally leads to activation of Casp-9 and Casp-3.

translocation to the mitochondrial outer membrane[136], which is a crucial step in MOMP (see introduction chapter 4.1). CHOP-induced expression of DR5 leads to activation of Caspase-8 which in return cleaves Bid resulting in translocation of tBid to the mitochondrial outer membrane. Finally, MOMP releases

Cytochrome c and subsequent apoptosome formation activates Caspase-9 and executioner Caspase-3.

Our knockdown experiments in IRE1α-/- cells showed that Cyclin O contributes to MAPK activation independently of the well described IRE1α/TRAF2/ASK1 axis[60,61,63]. We concluded that Cyclin O is part of an additional pathway that involves Cyclin O mediated phosphorylation of MEKK4 through Cdk1 and Cdk2 (Figure 5). So far, MEKK4 has not been described to be activated in response to ER stress in mammalian cells. In *Drosophila* however, MEKK4 (D-MEKK1 in *Drosophila*) is phosphorylated by Cdk5 to induce JNK signalling in conditions of ER stress[122]. We proofed that MEKK4 is activated by ER stress in a Cyclin O-dependent manner by showing kinase activity towards its substrate MEK6. Moreover, the kinases responsible for phosphorylation of MEKK4 turned out to be Cdk1 and Cdk2, whereas Cdk5 could be ruled out in our experimental system. We identified threonine 112 as the residue that is phosphorylated by Cyclin O complexes. Typically, MEKK4 is activated by binding of regulators like GADD45, TRAF4, or AXIN which induces homodimerization and subsequent autophosphorylation of MEKK4 (Figure 6A). Thus our results may represent a novel mechanism of activation, which involves phosphorylation of MEKK4 by a kinase (Cdk1 and Cdk2). Abell *et al.* reported that phosphohorylation of MEKK4 Thr112 by GSK3β occurs *in vitro* but the biological function of this remains a mystery[137]. GSK3β is an inhibitor of MEKK4 that exerts its inhibitory function through binding to the kinase domain of

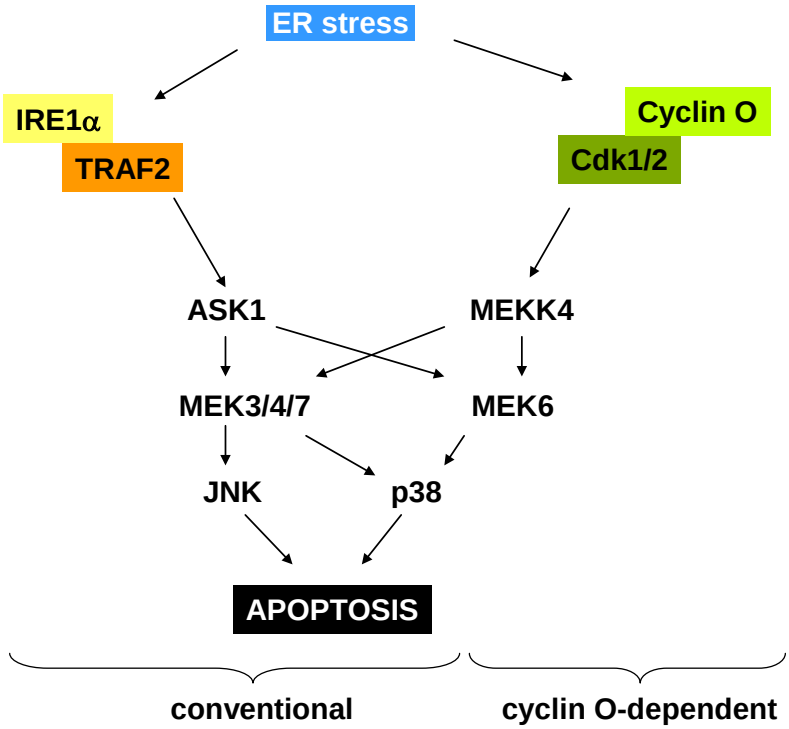

Figure 5. Cyclin O is part of an alternative pathway that induces MAPK signalling. In addition to the IRE1α/TRAF2/ASK1 axis, Cyclin O activates through Cdk1 and Cdk2 the MAP3K MEKK4, which in turn leads to activation of MEK6 and possibly other MAP2Ks. Eventually JNK and p38 are activated and induce apoptosis signalling.

MEKK4. Mutation of threonine 112 into alanine had no measurable effect on controlling MEKK4 inhibition by GSK3β. However, it might be possible that phosphorylation of Thr112 controls the interaction of MEKK4 with other regulators. A possible scenario would be that phosphorylation of Thr112 provides a sharp switch from inhibition to activation by increasing the affinity for activators so that when GSK3β dissociates from MEKK4, once its inhibitory action is not required anymore, activation of MEKK4 can occur more efficiently. An interesting detail in the context of GSK3β is

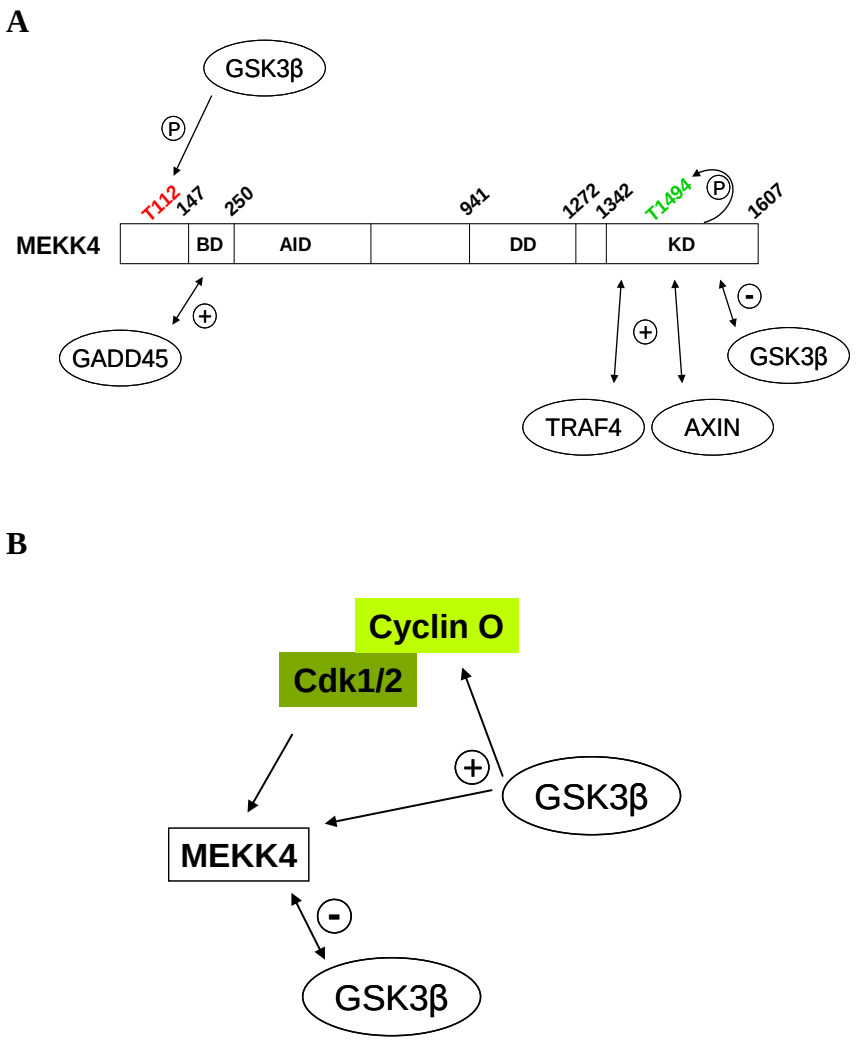

Figure 6. (A) Schematic representation of mouse MEKK4. *BD* binding domain, *AID* autoinhibitory domain, *DD* dimerization domain, *KD* kinase domain. T1494 is phosphorylated through the canonical activation of MEKK4 which involves binding of a positive regulator leading to homodimerization and autophosphorylation. **(B)** Putative mechansim in which kinase activity of GSK3β provides positive regulation of Cyclin O and MEKK4 whereas binding of GSK3β to the kinase domain of MEKK4 has an inhibitory effect.

that Cyclin O harbors a GSK3β phosphorylation site in its N-term. It is possible that the GSK3β kinase activity provides positive regulation not only by phosphorylating MEKK4 Thr112 directly but also through phosphorylation and activation of Cyclin O which in turn increases phosphorylation of MEKK4 Thr112 through Cdk1/2 (Figure 6B).

Since we knew that Cyclin O is involved in both radiation- and ER stress-induced apoptosis we used cells deficient in eIF2α signalling to assess whether those two pathways are linked together. In our system Caspase-8 is only activated by radiation and not by ER stress and therefore Caspase-8 does not contribute to ER stress signalling (Figure 7). Caspase-8 has been described to be activated in other cell lines like Jurkat[92], multiple myeloma, and carcinoma cells[93] upon ER stress. However, in our fibroblasts this does not seem to be the case. eIF2α–dependent induction of CHOP on the other hand occurs in both conditions and contributes thus to both signalling pathways. Although we did not proof directly the involvement of Cyclin O in these experiments previous results from our group positioned Cyclin O upstream of PERK in ER stress signalling and upstream of Caspase-8 in DNA damage response signalling. As depicted in figure 7, it seems that Cyclin O bifurcates into two possible signalling pathways both of which are activated in response to radiation but in conditions of ER stress only the PERK axis is induced. However, to be completely sure that Caspase-8 is not activated in response to thapsigargin it might make sense to check at much later time points than the ones we chose as in some

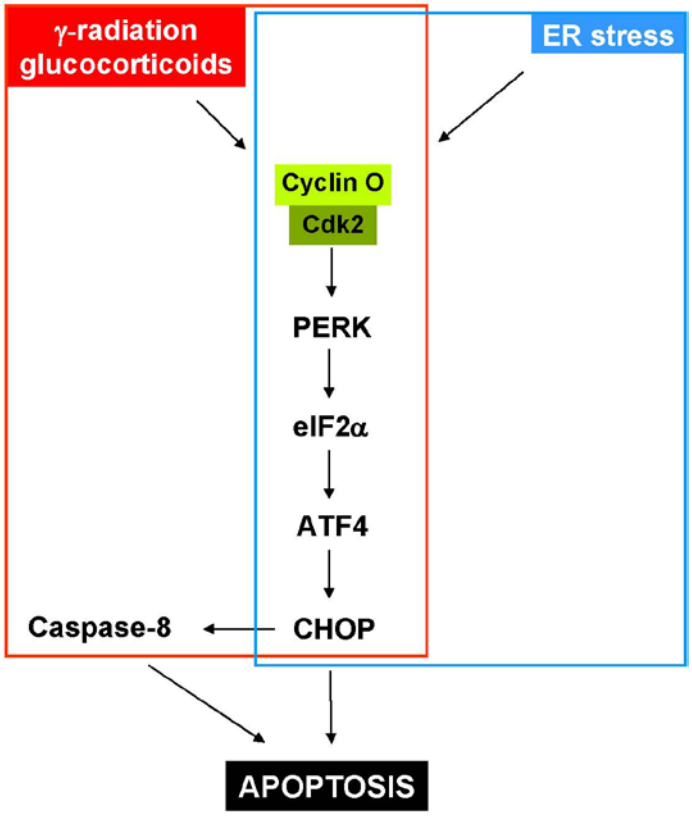

Figure 7. Crosstalk between the ER stress pathway and DDR. ER-stress and γ-radiation induces Cyclin O-mediated expression of CHOP in an eIF2α-dependent fashion. But, only γ-radiation leads to Caspase-8 activation.

cell lines incubation up to 24 hours is necessary to detect Caspase-8 activation[93].

3. Mechanism of PERK activation by Cyclin O

Our pull-down experiments demonstrate that Cyclin O binds to PERK either directly or they are both part of the same complex. We know that Cyclin O forms complexes with Cdk1/2 in unstressed cells[108] and previous results from our group showed that in unstressed and ER stressed cells there is direct or indirect

interaction between Cyclin O and p58, a known inhibitor of PERK that exerts its function by binding to the kinase domain of PERK. Taken all those facts together, we can postulate a probable mechanism as depicted in figure 8. Under normal conditions PERK is bound and inhibited by p58 together with Cyclin O and Cdk1/2. ER stress induces the release of p58, Cyclin O, and Cdk1/2 from PERK. Subsequently, PERK is now free to phosphorylate itself and eIF2α while Cdk1/2 phosphorylates MEKK4. The question remains how exactly does Cyclin O activate PERK? Earlier experiments that led to positioning of Cyclin O upstream of PERK showed that overexpression of Cyclin O induced autophosphorylation of PERK so Cyclin O must have some direct or indirect influence on PERK. It is possible that Cyclin O derepresses PERK by facilitating dissociation of p58 from PERK. This mechanism could occur simply by physical interaction of Cyclin O with PERK and/or p58 but we cannot exclude that Cdk1/2 may participate in Cyclin O-mediated activation of PERK either by phosphorylating p58 and thus enhancing dissociation or by phosphorylating and activating PERK directly.

4. Anemic phenotype of Cyclin O knockout mice

We detected a reduced number of RBC, low hemoglobin concentration, and diminished hematocrit values in the blood of Cyclin O knockout mice. In an attempt to understand why this anemic phenotype occurs we analyzed the bone marrow in terms of RBC development. The literature is not consistent in regard to the percentage of cells in the different development stages when the

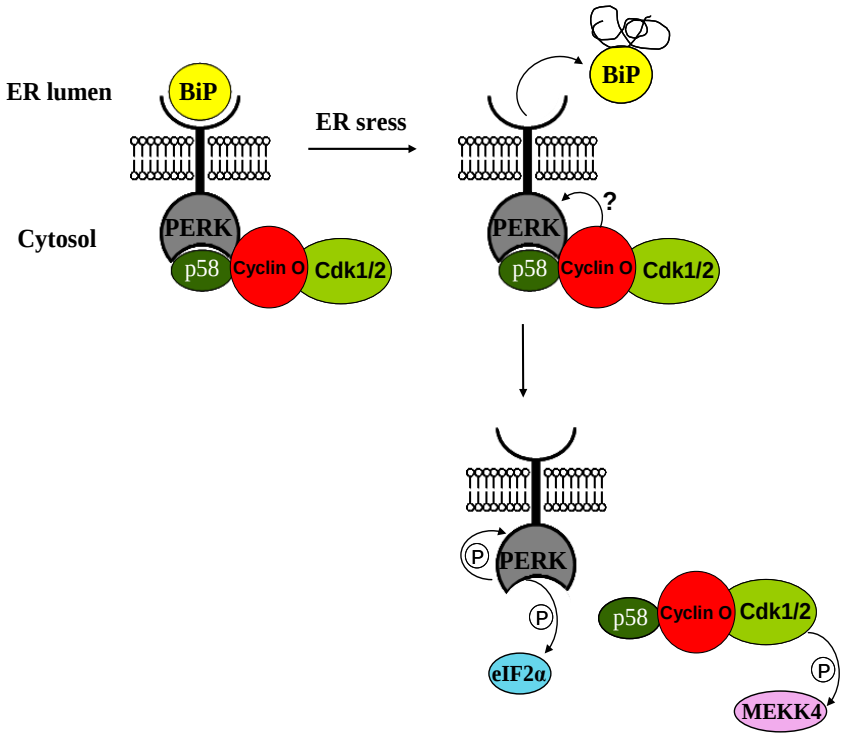

Figure 8. Putative mechanism of Cyclin O-mediated activation of PERK. Upon ER stress Cyclin O allows autophosphorylation of PERK possibly by mediating dissociation of p58. Activated PERK is now free to phosphorylate eIF2α.

Ter119/CD71 staining procedure is employed. For example, basophilic erythroblasts in wild type mice have been reported to be as low as 5 percent[127] and as high as 30 percent[138]. However, standard deviation and reproducibility of our experiments seem to be acceptable and the results indicate that late basophilic, polychromatophilic, and orthochromatophilic erythroblasts were reduced in knockout mice compared to their wild type counterparts.

CONCLUSIONS

1. Apoptosis induced by ER stress depends on Cyclin O.
2. ER stress induces Cyclin O-associated Cdk activity.
3. ER stress induced expression of Cyclin O depends on eIF2α and CHOP.
4. ER-stress and γ-radiation induce expression of CHOP in an eIF2α-dependent fashion. But, only with γ-radiation is Caspase-8 activated.
5. Cyclin O binds to PERK and PKR *in vitro*.
6. MEKK4 is activated by Cyclin O-Cdk1/2 complexes via phosphorylation at threonine 112.
7. Activation of p38 and JNK depends on Cyclin O and occurs independently of IRE1α.
8. Cyclin O knockout mice suffer from anemia and show extramedullary erythropoiesis in the spleen.

BIBLIOGRAPHY

BIBLIOGRAPHY

1. Jackson, R. J., Hellen, C. U. T. & Pestova, T. V. The mechanism of eukaryotic translation initiation and principles of its regulation. *Nat. Rev. Mol. Cell Biol.* **11,** 113–27 (2010).

2. Naveau, M., Lazennec-Schurdevin, C., Panvert, M., Mechulam, Y. & Schmitt, E. tRNA binding properties of eukaryotic translation initiation factor 2 from Encephalitozoon cuniculi. *Biochemistry* **49,** 8680–8 (2010).

3. Krishnamoorthy, T., Pavitt, G. D., Zhang, F., Dever, T. E. & Hinnebusch, A. G. Tight binding of the phosphorylated alpha subunit of initiation factor 2 (eIF2alpha) to the regulatory subunits of guanine nucleotide exchange factor eIF2B is required for inhibition of translation initiation. *Mol. Cell. Biol.* **21,** 5018–30 (2001).

4. Lu, P. D., Harding, H. P. & Ron, D. Translation reinitiation at alternative open reading frames regulates gene expression in an integrated stress response. *J. Cell Biol.* **167,** 27–33 (2004).

5. McCullough, K. D., Martindale, J. L., Klotz, L. O., Aw, T. Y. & Holbrook, N. J. Gadd153 sensitizes cells to endoplasmic reticulum stress by down-regulating Bcl2 and perturbing the cellular redox state. *Mol. Cell. Biol.* **21,** 1249–59 (2001).

6. Ghosh, A. P., Klocke, B. J., Ballestas, M. E. & Roth, K. A. CHOP potentially co-operates with FOXO3a in neuronal cells to regulate PUMA and BIM expression in response to ER stress. *PLoS One* **7,** e39586 (2012).

7. Puthalakath, H. *et al.* ER Stress Triggers Apoptosis by Activating BH3-Only Protein Bim. *Cell* **129,** 1337–1349 (2007).

8. Novoa, I. *et al.* Stress-induced gene expression requires programmed recovery from translational repression. *EMBO J.* **22,** 1180–7 (2003).

9. Harding, H. P. *et al.* An Integrated Stress Response Regulates Amino Acid Metabolism and Resistance to Oxidative Stress. *Mol. Cell* **11,** 619–633 (2003).

10. Harding, H. P., Zhang, Y. & Ron, D. Protein translation and folding are coupled by an endoplasmic-reticulum-resident kinase. *Nature* **397,** 271–274 (1999).

11. Bertolotti, a, Zhang, Y., Hendershot, L. M., Harding, H. P. & Ron, D. Dynamic interaction of BiP and ER stress transducers in the unfolded-protein response. *Nat. Cell Biol.* **2,** 326–32 (2000).

12. Cullinan, S. B. & Diehl, J. A. Coordination of ER and oxidative stress signaling: the PERK/Nrf2 signaling pathway. *Int. J. Biochem. Cell Biol.* **38,** 317–32 (2006).

13. Lin, J. H., Li, H., Zhang, Y., Ron, D. & Walter, P. Divergent effects of PERK and IRE1 signaling on cell viability. *PLoS One* **4,** e4170 (2009).

14. Lin, J. H. *et al.* IRE1 signaling affects cell fate during the unfolded protein response. *Science* **318,** 944–9 (2007).

15. Ito, T., Yang, M., Stratford, W. & May, W. S. RAX , a Cellular Activator for Double-stranded RNA-dependent Protein Kinase during Stress Signaling. *J. Biol. Chem.* **274,** 15427–15432 (1999).

16. Nakamura, T. *et al.* Double-stranded RNA-dependent protein kinase links pathogen sensing with stress and metabolic homeostasis. *Cell* **140,** 338–48 (2010).

17. Onuki, R. *et al.* An RNA-dependent protein kinase is involved in tunicamycin-induced apoptosis and Alzheimer's disease. *EMBO J.* **23,** 959–68 (2004).

18. Vattem, K. M., Staschke, K. a & Wek, R. C. Mechanism of activation of the double-stranded-RNA-dependent protein kinase, PKR: role of dimerization and cellular localization in the stimulation of PKR phosphorylation of eukaryotic initiation factor-2 (eIF2). *Eur. J. Biochem.* **268,** 3674–84 (2001).

19. Singh, M., Fowlkes, V., Handy, I., Patel, C. V & Patel, R. C. Essential role of PACT-mediated PKR activation in tunicamycin-induced apoptosis. *J. Mol. Biol.* **385,** 457–68 (2009).

20. Li, G., Scull, C., Ozcan, L. & Tabas, I. NADPH oxidase links endoplasmic reticulum stress, oxidative stress, and PKR activation to induce apoptosis. *J. Cell Biol.* **191,** 1113–25 (2010).

21. D'Acquisto, F. & Ghosh, S. PACT and PKR: turning on NF-kappa B in the absence of virus. *Sci. STKE* **2001,** re1 (2001).

22. Deval, C. *et al.* Amino acid limitation regulates the expression of genes involved in several specific biological processes through GCN2-dependent and GCN2-independent pathways. *FEBS J.* **276,** 707–18 (2009).

23. Zhu, S. & Wek, R. C. Ribosome-binding domain of eukaryotic initiation factor-2 kinase GCN2 facilitates translation control. *J. Biol. Chem.* **273,** 1808–14 (1998).

24. Dong, J., Qiu, H., Garcia-Barrio, M., Anderson, J. & Hinnebusch, A. G. Uncharged tRNA Activates GCN2 by Displacing the Protein Kinase Moiety from a Bipartite tRNA-Binding Domain. *Mol. Cell* **6,** 269–279 (2000).

25. Berlanga, J. J. *et al.* Antiviral effect of the mammalian translation initiation factor 2alpha kinase GCN2 against RNA viruses. *EMBO J.* **25,** 1730–40 (2006).

26. Ye, J. *et al.* The GCN2-ATF4 pathway is critical for tumour cell survival and proliferation in response to nutrient deprivation. *EMBO J.* **29,** 2082–96 (2010).

27. Liu, Y. *et al.* Regulation of G(1) arrest and apoptosis in hypoxia by PERK and GCN2-mediated eIF2alpha phosphorylation. *Neoplasia* **12,** 61–8 (2010).

28. Grallert, B. & Boye, E. The Gcn2 Kinase as a Cell Cycle Regulator. *Cell Cycle* **6,** 2768–2772 (2007).

29. Bauer, B. N., Rafie-Kolpin, M., Lu, L., Han, A. & Chen, J.-J. Multiple Autophosphorylation Is Essential for the Formation of the Active and Stable Homodimer of Heme-Regulated eIF2α Kinase †. *Biochemistry* **40,** 11543–11551 (2001).

30. Rafie-Kolpin, M., Han, A.-P. & Chen, J.-J. Autophosphorylation of threonine 485 in the activation loop is essential for attaining eIF2alpha kinase activity of HRI. *Biochemistry* **42,** 6536–44 (2003).

31. Lu, L., Han, A. P. & Chen, J. J. Translation initiation control by heme-regulated eukaryotic initiation factor 2alpha kinase in erythroid cells under cytoplasmic stresses. *Mol. Cell. Biol.* **21,** 7971–80 (2001).

32. Acharya, P., Chen, J.-J. & Correia, M. A. Hepatic heme-regulated inhibitor (HRI) eukaryotic initiation factor 2alpha kinase: a protagonist of heme-mediated translational control of CYP2B enzymes and a modulator of basal endoplasmic reticulum stress tone. *Mol. Pharmacol.* **77,** 575–92 (2010).

33. Bertolotti, A. *et al.* Increased sensitivity to dextran sodium sulfate colitis in IRE1beta-deficient mice. *J. Clin. Invest.* **107,** 585–93 (2001).

34. Iwawaki, T. *et al.* Translational control by the ER transmembrane kinase/ribonuclease IRE1 under ER stress. *Nat. Cell Biol.* **3,** 158–64 (2001).

35. Yoshida, H., Matsui, T., Yamamoto, A., Okada, T. & Mori, K. XBP1 mRNA Is Induced by ATF6 and Spliced by IRE1 in Response to ER Stress to Produce a Highly Active Transcription Factor. *Cell* **107,** 881–891 (2001).

36. Acosta-Alvear, D. *et al.* XBP1 controls diverse cell type- and condition-specific transcriptional regulatory networks. *Mol. Cell* **27,** 53–66 (2007).

37. Lee, A.-H., Iwakoshi, N. N. & Glimcher, L. H. XBP-1 regulates a subset of endoplasmic reticulum resident chaperone genes in the unfolded protein response. *Mol. Cell. Biol.* **23,** 7448–59 (2003).

38. Yoshida, H., Oku, M., Suzuki, M. & Mori, K. pXBP1(U) encoded in XBP1 pre-mRNA negatively regulates unfolded protein response activator pXBP1(S) in mammalian ER stress response. *J. Cell Biol.* **172,** 565–75 (2006).

39. Hollien, J. & Weissman, J. S. Decay of endoplasmic reticulum-localized mRNAs during the unfolded protein response. *Science* **313,** 104–7 (2006).

40. Oikawa, D., Tokuda, M., Hosoda, A. & Iwawaki, T. Identification of a consensus element recognized and cleaved by IRE1 alpha. *Nucleic Acids Res.* **38,** 6265–73 (2010).

41. Tirasophon, W., Lee, K., Callaghan, B., Welihinda, A. & Kaufman, R. J. The endoribonuclease activity of mammalian IRE1 autoregulates its mRNA and is required for the unfolded protein response. *Genes Dev.* **14,** 2725–36 (2000).

42. Hetz, C. *et al.* Proapoptotic BAX and BAK modulate the unfolded protein response by a direct interaction with IRE1alpha. *Science* **312,** 572–6 (2006).

43. Hu, P. *et al.* Autocrine Tumor Necrosis Factor Alpha Links Endoplasmic Reticulum Stress to the Membrane Death Receptor Pathway through IRE1 α -Mediated NF- κ B Activation and Down-Regulation of TRAF2 Expression

Autocrine Tumor Necrosis Factor Alpha Links Endoplasmic Ret. (2006). doi:10.1128/MCB.26.8.3071

44. Shen, J. & Prywes, R. Dependence of site-2 protease cleavage of ATF6 on prior site-1 protease digestion is determined by the size of the luminal domain of ATF6. *J. Biol. Chem.* **279,** 43046–51 (2004).

45. Yamamoto, K., Yoshida, H., Kokame, K., Kaufman, R. J. & Mori, K. Differential contributions of ATF6 and XBP1 to the activation of endoplasmic reticulum stress-responsive cis-acting elements ERSE, UPRE and ERSE-II. *J. Biochem.* **136,** 343–50 (2004).

46. Ma, Y., Brewer, J. W., Diehl, J. A. & Hendershot, L. M. Two distinct stress signaling pathways converge upon the CHOP promoter during the mammalian unfolded protein response. *J. Mol. Biol.* **318,** 1351–65 (2002).

47. Yoshida, H., Matsui, T., Yamamoto, A., Okada, T. & Mori, K. XBP1 mRNA is induced by ATF6 and spliced by IRE1 in response to ER stress to produce a highly active transcription factor. *Cell* **107,** 881–91 (2001).

48. Thuerauf, D. J., Morrison, L. & Glembotski, C. C. Opposing roles for ATF6alpha and ATF6beta in endoplasmic reticulum stress response gene induction. *J. Biol. Chem.* **279,** 21078–84 (2004).

49. Thuerauf, D. J., Morrison, L. E., Hoover, H. & Glembotski, C. C. Coordination of ATF6-mediated transcription and ATF6 degradation by a domain that is shared with the viral transcription factor, VP16. *J. Biol. Chem.* **277,** 20734–9 (2002).

50. Asada, R., Kanemoto, S., Kondo, S., Saito, A. & Imaizumi, K. The signalling from endoplasmic reticulum-resident bZIP transcription factors involved in diverse cellular physiology. *J. Biochem.* **149,** 507–18 (2011).

51. Kondo, S. *et al.* OASIS, a CREB/ATF-family member, modulates UPR signalling in astrocytes. *Nat. Cell Biol.* **7,** 186–94 (2005).

52. Zhang, K. *et al.* Endoplasmic reticulum stress activates cleavage of CREBH to induce a systemic inflammatory response. *Cell* **124,** 587–99 (2006).

53. Yoshida, H., Uemura, A. & Mori, K. pXBP1(U), a negative regulator of the unfolded protein response activator pXBP1(S), targets ATF6 but not ATF4 in proteasome-mediated degradation. *Cell Struct. Funct.* **34,** 1–10 (2009).

54. Yamamoto, K. *et al.* Transcriptional induction of mammalian ER quality control proteins is mediated by single or combined action of ATF6alpha and XBP1. *Dev. Cell* **13,** 365–76 (2007).

55. Yamaguchi, Y. *et al.* Endoplasmic reticulum (ER) chaperone regulation and survival of cells compensating for deficiency in the ER stress response kinase, PERK. *J. Biol. Chem.* **283,** 17020–9 (2008).

56. Teske, B. F. *et al.* The eIF2 kinase PERK and the integrated stress response facilitate activation of ATF6 during endoplasmic reticulum stress. *Mol. Biol. Cell* **22,** 4390–405 (2011).

57. Cargnello, M. & Roux, P. P. Activation and function of the MAPKs and their substrates, the MAPK-activated protein kinases. *Microbiol. Mol. Biol. Rev.* **75,** 50–83 (2011).

58. Hung, J.-H. *et al.* Endoplasmic reticulum stress stimulates the expression of cyclooxygenase-2 through activation of NF-kappaB and pp38 mitogen-activated protein kinase. *J. Biol. Chem.* **279,** 46384–92 (2004).

59. Li, J. & Holbrook, N. J. Elevated gadd153/chop expression and enhanced c-Jun N-terminal protein kinase activation

sensitizes aged cells to ER stress. *Exp. Gerontol.* **39,** 735–44 (2004).

60. Urano, F. *et al.* Coupling of stress in the ER to activation of JNK protein kinases by transmembrane protein kinase IRE1. *Science* **287,** 664–6 (2000).

61. Nishitoh, H. *et al.* ASK1 is essential for endoplasmic reticulum stress-induced neuronal cell death triggered by expanded polyglutamine repeats. *Genes Dev.* **16,** 1345–55 (2002).

62. Gotoh, Y. & Cooper, J. A. Reactive oxygen species- and dimerization-induced activation of apoptosis signal-regulating kinase 1 in tumor necrosis factor-alpha signal transduction. *J. Biol. Chem.* **273,** 17477–82 (1998).

63. Ichijo, H. *et al.* Induction of apoptosis by ASK1, a mammalian MAPKKK that activates SAPK/JNK and p38 signaling pathways. *Science* **275,** 90–4 (1997).

64. Matsuzawa, A. & Ichijo, H. Redox control of cell fate by MAP kinase: physiological roles of ASK1-MAP kinase pathway in stress signaling. *Biochim. Biophys. Acta* **1780,** 1325–36 (2008).

65. Gu, J. J., Wang, Z., Reeves, R. & Magnuson, N. S. PIM1 phosphorylates and negatively regulates ASK1-mediated apoptosis. *Oncogene* **28,** 4261–71 (2009).

66. Kim, A. H., Khursigara, G., Sun, X., Franke, T. F. & Chao, M. V. Akt phosphorylates and negatively regulates apoptosis signal-regulating kinase 1. *Mol. Cell. Biol.* **21,** 893–901 (2001).

67. Morita, K. *et al.* Negative feedback regulation of ASK1 by protein phosphatase 5 (PP5) in response to oxidative stress. *EMBO J.* **20,** 6028–36 (2001).

68. Goldman, E. H., Chen, L. & Fu, H. Activation of apoptosis signal-regulating kinase 1 by reactive oxygen species through dephosphorylation at serine 967 and 14-3-3 dissociation. *J. Biol. Chem.* **279,** 10442–9 (2004).

69. Raciti, M., Lotti, L. V, Valia, S., Pulcinelli, F. M. & Di Renzo, L. JNK2 is activated during ER stress and promotes cell survival. *Cell Death Dis.* **3,** e429 (2012).

70. Hibi, M., Lin, A., Smeal, T., Minden, A. & Karin, M. Identification of an oncoprotein- and UV-responsive protein kinase that binds and potentiates the c-Jun activation domain. *Genes Dev.* **7,** 2135–48 (1993).

71. Zhao, P. *et al.* c-Jun inhibits thapsigargin-induced ER stress through up-regulation of DSCR1/Adapt78. *Exp. Biol. Med. (Maywood).* **233,** 1289–300 (2008).

72. Nakagawa, T. *et al.* Caspase-12 mediates endoplasmic-reticulum-specific apoptosis and cytotoxicity by amyloid-beta. *Nature* **403,** 98–103 (2000).

73. Hitomi, J. *et al.* Involvement of caspase-4 in endoplasmic reticulum stress-induced apoptosis and Abeta-induced cell death. *J. Cell Biol.* **165,** 347–56 (2004).

74. Mukerjee, N., McGinnis, K. M., Park, Y. H., Gnegy, M. E. & Wang, K. K. Caspase-mediated proteolytic activation of calcineurin in thapsigargin-mediated apoptosis in SH-SY5Y neuroblastoma cells. *Arch. Biochem. Biophys.* **379,** 337–43 (2000).

75. Nguyên, D. T. *et al.* Nck-dependent activation of extracellular signal-regulated kinase-1 and regulation of cell survival during endoplasmic reticulum stress. *Mol. Biol. Cell* **15,** 4248–60 (2004).

76. Zhang, L. J. *et al.* Inhibition of MEK blocks GRP78 up-regulation and enhances apoptosis induced by ER stress in gastric cancer cells. *Cancer Lett.* **274,** 40–6 (2009).

77. Wang, X. Z. & Ron, D. Stress-induced phosphorylation and activation of the transcription factor CHOP (GADD153) by p38 MAP Kinase. *Science* **272,** 1347–9 (1996).

78. Maytin, E. V, Ubeda, M., Lin, J. C. & Habener, J. F. Stress-inducible transcription factor CHOP/gadd153 induces apoptosis in mammalian cells via p38 kinase-dependent and -independent mechanisms. *Exp. Cell Res.* **267,** 193–204 (2001).

79. Timmins, J. M. *et al.* Calcium/calmodulin-dependent protein kinase II links ER stress with Fas and mitochondrial apoptosis pathways. *J. Clin. Invest.* **119,** 2925–41 (2009).

80. Erickson, J. R. *et al.* A dynamic pathway for calcium-independent activation of CaMKII by methionine oxidation. *Cell* **133,** 462–74 (2008).

81. Kashiwase, K. *et al.* CaMKII activates ASK1 and NF-kappaB to induce cardiomyocyte hypertrophy. *Biochem. Biophys. Res. Commun.* **327,** 136–42 (2005).

82. Thuerauf, D. J. *et al.* p38 Mitogen-activated protein kinase mediates the transcriptional induction of the atrial natriuretic factor gene through a serum response element. A potential role for the transcription factor ATF6. *J. Biol. Chem.* **273,** 20636–43 (1998).

83. Luo, S. & Lee, A. S. Requirement of the p38 mitogen-activated protein kinase signalling pathway for the induction of the 78 kDa glucose-regulated protein/immunoglobulin heavy-chain binding protein by azetidine stress: activating transcription factor 6 as a target for stress-i. *Biochem. J.* **366,** 787–95 (2002).

84. Chen, L. *et al.* Differential targeting of prosurvival Bcl-2 proteins by their BH3-only ligands allows complementary apoptotic function. *Mol. Cell* **17,** 393–403 (2005).

85. Willis, S. N. *et al.* Apoptosis initiated when BH3 ligands engage multiple Bcl-2 homologs, not Bax or Bak. *Science* **315,** 856–9 (2007).

86. Willis, S. N. *et al.* Proapoptotic Bak is sequestered by Mcl-1 and Bcl-xL, but not Bcl-2, until displaced by BH3-only proteins. *Genes Dev.* **19,** 1294–305 (2005).

87. Letai, A. *et al.* Distinct BH3 domains either sensitize or activate mitochondrial apoptosis, serving as prototype cancer therapeutics. *Cancer Cell* **2,** 183–92 (2002).

88. Gavathiotis, E. *et al.* BAX activation is initiated at a novel interaction site. *Nature* **455,** 1076–81 (2008).

89. Kim, H. *et al.* Hierarchical regulation of mitochondrion-dependent apoptosis by BCL-2 subfamilies. *Nat. Cell Biol.* **8,** 1348–58 (2006).

90. Certo, M. *et al.* Mitochondria primed by death signals determine cellular addiction to antiapoptotic BCL-2 family members. *Cancer Cell* **9,** 351–65 (2006).

91. Tenev, T. *et al.* The Ripoptosome, a signaling platform that assembles in response to genotoxic stress and loss of IAPs. *Mol. Cell* **43,** 432–48 (2011).

92. Mishra, R. & Karande, A. A. Endoplasmic Reticulum Stress-Mediated Activation of p38 MAPK, Caspase-2 and Caspase-8 Leads to Abrin-Induced Apoptosis. *PLoS One* **9,** e92586 (2014).

93. Lu, M. *et al.* Opposing unfolded-protein-response signals converge on death receptor 5 to control apoptosis. *Science* **345,** 98–101 (2014).

94. Han, D. *et al.* IRE1alpha kinase activation modes control alternate endoribonuclease outputs to determine divergent cell fates. *Cell* **138,** 562–75 (2009).

95. Klee, M., Pallauf, K., Alcalá, S., Fleischer, A. & Pimentel-Muiños, F. X. Mitochondrial apoptosis induced by BH3-only molecules in the exclusive presence of endoplasmic reticular Bak. *EMBO J.* **28,** 1757–68 (2009).

96. Bruhat, A. *et al.* Amino Acids Control Mammalian Gene Transcription□: Activating Transcription Factor 2 Is Essential for the Amino Acid Responsiveness of the CHOP Promoter Amino Acids Control Mammalian Gene Transcription □: Activating Transcriptio Essential for . (2000). doi:10.1128/MCB.20.19.7192-7204.2000.Updated

97. Chiribau, C.-B., Gaccioli, F., Huang, C. C., Yuan, C. L. & Hatzoglou, M. Molecular symbiosis of CHOP and C/EBP beta isoform LIP contributes to endoplasmic reticulum stress-induced apoptosis. *Mol. Cell. Biol.* **30,** 3722–31 (2010).

98. Fu, H. Y. *et al.* Ablation of C/EBP homologous protein attenuates endoplasmic reticulum-mediated apoptosis and cardiac dysfunction induced by pressure overload. *Circulation* **122,** 361–9 (2010).

99. Cazanave, S. C. *et al.* CHOP and AP-1 cooperatively mediate PUMA expression during lipoapoptosis. *Am. J. Physiol. Gastrointest. Liver Physiol.* **299,** G236–43 (2010).

100. Tsukano, H. *et al.* The endoplasmic reticulum stress-C/EBP homologous protein pathway-mediated apoptosis in macrophages contributes to the instability of atherosclerotic plaques. *Arterioscler. Thromb. Vasc. Biol.* **30,** 1925–32 (2010).

101. Ohoka, N., Yoshii, S., Hattori, T., Onozaki, K. & Hayashi, H. TRB3, a novel ER stress-inducible gene, is induced via ATF4-CHOP pathway and is involved in cell death. *EMBO J.* **24,** 1243–55 (2005).

102. Jousse, C. *et al.* TRB3 inhibits the transcriptional activation of stress-regulated genes by a negative feedback on the ATF4 pathway. *J. Biol. Chem.* **282,** 15851–61 (2007).

103. Wilson, N. S., Dixit, V. & Ashkenazi, A. Death receptor signal transducers: nodes of coordination in immune signaling networks. *Nat. Immunol.* **10,** 348–55 (2009).

104. Han, J. *et al.* ER-stress-induced transcriptional regulation increases protein synthesis leading to cell death. *Nat. Cell Biol.* **15,** 481–90 (2013).

105. Williams, O., Gil-Gómez, G., Norton, T., Kioussis, D. & Brady, H. J. Activation of Cdk2 is a requirement for antigen-mediated thymic negative selection. *Eur. J. Immunol.* **30,** 709–13 (2000).

106. Gil-Gómez, G., Berns, a & Brady, H. J. A link between cell cycle and cell death: Bax and Bcl-2 modulate Cdk2 activation during thymocyte apoptosis. *EMBO J.* **17,** 7209–7218 (1998).

107. Granés, F., Roig, M. B., Brady, H. J. M. & Gil-Gómez, G. Cdk2 activation acts upstream of the mitochondrion during glucocorticoid induced thymocyte apoptosis. *Eur. J. Immunol.* **34,** 2781–2790 (2004).

108. Roig, M. B. *et al.* Identification of a novel cyclin required for the intrinsic apoptosis pathway in lymphoid cells. *Cell Death Differ.* **16,** 230–43 (2009).

109. Ortet Cortada, L. Signalling of Cyclin O complexes through eIF2alpha phosphorylation. *PhD thesis* (2010).

110. Chasis, J. A. & Mohandas, N. Erythroblastic islands: niches for erythropoiesis. *Blood* **112,** 470–8 (2008).

111. Geiduschek, J. B. & Singer, S. J. Molecular changes in the membranes of mouse erythroid cells accompanying differentiation. *Cell* **16,** 149–63 (1979).

112. Lee, J. C.-M. *et al.* Mechanism of protein sorting during erythroblast enucleation: role of cytoskeletal connectivity. *Blood* **103,** 1912–9 (2004).

113. Liu, J., Mohandas, N. & An, X. Membrane assembly during erythropoiesis. *Curr. Opin. Hematol.* **18,** 133–8 (2011).

114. McGrath, K. E., Bushnell, T. P. & Palis, J. Multispectral imaging of hematopoietic cells: where flow meets morphology. *J. Immunol. Methods* **336,** 91–7 (2008).

115. Yoshida, H. *et al.* Phosphatidylserine-dependent engulfment by macrophages of nuclei from erythroid precursor cells. *Nature* **437,** 754–8 (2005).

116. Johnstone, R. M. The Jeanne Manery-Fisher Memorial Lecture 1991. Maturation of reticulocytes: formation of exosomes as a mechanism for shedding membrane proteins. *Biochem. Cell Biol.* **70,** 179–90

117. Waugh, R. E., Mantalaris, A., Bauserman, R. G., Hwang, W. C. & Wu, J. H. Membrane instability in late-stage erythropoiesis. *Blood* **97,** 1869–75 (2001).

118. Griffiths, R. E. *et al.* The ins and outs of human reticulocyte maturation: autophagy and the endosome/exosome pathway. *Autophagy* **8,** 1150–1 (2012).

119. Low, P. S., Waugh, S. M., Zinke, K. & Drenckhahn, D. The role of hemoglobin denaturation and band 3 clustering in red blood cell aging. *Science* **227,** 531–3 (1985).

120. *The Proteomics Protocols Handbook*. (Humana Press, 2005). doi:10.1385/1592598900

121. Sibley, C. H. & Tomkins, G. M. Isolation of lymphoma cell variants resistant to killing by glucocorticoids. *Cell* **2,** 213–20 (1974).

122. Kang, M.-J., Chung, J. & Ryoo, H. D. CDK5 and MEKK1 mediate pro-apoptotic signalling following endoplasmic reticulum stress in an autosomal dominant retinitis pigmentosa model. *Nat. Cell Biol.* **14,** 409–415 (2012).

123. Roset i Huguet, R. STUDY OF THE REGULATION AND SIGNALLING OF CDK2-CYCLIN O COMPLEXES DURING APOPTOSIS Doctoral thesis. *PhD thesis* (2008).

124. Miyake, Z., Takekawa, M., Ge, Q. & Saito, H. Activation of MTK1/MEKK4 by GADD45 through induced N-C dissociation and dimerization-mediated trans autophosphorylation of the MTK1 kinase domain. *Mol. Cell. Biol.* **27,** 2765–76 (2007).

125. Chen, K. *et al.* Resolving the distinct stages in erythroid differentiation based on dynamic changes in membrane protein expression during erythropoiesis. *Proc. Natl. Acad. Sci. U. S. A.* **106,** 17413–8 (2009).

126. Socolovsky, M. *et al.* Ineffective erythropoiesis in Stat5a(-/-)5b(-/-) mice due to decreased survival of early erythroblasts. *Blood* **98,** 3261–73 (2001).

127. Slavova-Azmanova, N. S. *et al.* Gain-of-function Lyn induces anemia: appropriate Lyn activity is essential for normal erythropoiesis and Epo receptor signaling. *Blood* **122,** 262–71 (2013).

128. Hakem, A., Sasaki, T., Kozieradzki, I. & Penninger, J. M. The cyclin-dependent kinase Cdk2 regulates thymocyte apoptosis. *J. Exp. Med.* **189,** 957–68 (1999).

129. Fornace, A. J., Alamo, I. & Hollander, M. C. DNA damage-inducible transcripts in mammalian cells. *Proc. Natl. Acad. Sci. U. S. A.* **85,** 8800–4 (1988).

130. Lin, J. H. *et al.* IRE1 signaling affects cell fate during the unfolded protein response. *Science* **318,** 944–9 (2007).

131. Li, G. *et al.* Role of ERO1-alpha-mediated stimulation of inositol 1,4,5-triphosphate receptor activity in endoplasmic reticulum stress-induced apoptosis. *J. Cell Biol.* **186,** 783–92 (2009).

132. Lei, K. & Davis, R. J. JNK phosphorylation of Bim-related members of the Bcl2 family induces Bax-dependent apoptosis. *Proc. Natl. Acad. Sci. U. S. A.* **100,** 2432–7 (2003).

133. Smith, M. I. & Deshmukh, M. Endoplasmic reticulum stress-induced apoptosis requires bax for commitment and Apaf-1 for execution in primary neurons. *Cell Death Differ.* **14,** 1011–9 (2007).

134. Wang, X. Z. *et al.* Identification of novel stress-induced genes downstream of chop. *EMBO J.* **17,** 3619–30 (1998).

135. Mccullough, K. D., Martindale, J. L., Aw, T. & Holbrook, N. J. Gadd153 Sensitizes Cells to Endoplasmic Reticulum Stress by Down-Regulating Bcl2 and Perturbing the Cellular Redox State Gadd153 Sensitizes Cells to Endoplasmic Reticulum Stress by Down-Regulating Bcl2 and Perturbing the Cellular Redox State. (2001). doi:10.1128/MCB.21.4.1249

136. Park, G. Bin *et al.* Reactive oxygen species and p38 MAPK regulate Bax translocation and calcium redistribution in salubrinal-induced apoptosis of EBV-transformed B cells. *Cancer Lett.* **313,** 235–48 (2011).

137. Abell, A. N., Granger, D. a & Johnson, G. L. MEKK4 stimulation of p38 and JNK activity is negatively regulated by GSK3beta. *J. Biol. Chem.* **282,** 30476–84 (2007).

138. Boles, N. C., Peddibhotla, S., Chen, A. J., Goodell, M. a & Rosen, J. M. Chk1 haploinsufficiency results in anemia and defective erythropoiesis. *PLoS One* **5,** e8581 (2010).